Establishment of 293 based AAV packaging cell lines using shRNA-mediated *rep* silencing

Joana Filipa Gaspar Diogo

Thesis to obtain the Master of Science Degree in

Biotechnology

Supervisors: Ana Sofia Coroadinha, PhD
Prof. Gabriel António Amaro Monteiro, PhD

Examination Committee

Chairperson: Prof. Arsénio do Carmo Sales Mendes Fialho, PhD

Supervisor: Ana Sofia Coroadinha, PhD

Members of the Committee: Nuno Filipe Santos Bernardes, PhD

December 2020

Preface

The work presented in this thesis was performed at Instituto de Biologia Experimental e Tecnológica (iBET)/ Instituto de Tecnologia Química e Biológica António Xavier (ITQB) of Universidade Nova de Lisboa, Oeiras, Portugal during the period September 2019-December 2020, under the supervision of Ana Sofia Coroadinha, PhD, iBET/ITQB, UNL and Ana Sofia Fernandes, PhD, iBET, and within the frame of an internal iBET project. The thesis was co-supervised at Instituto Superior Técnico by Prof. Gabriel António Amaro Monteiro, PhD.

Declaration

I declare that this document is an original work of my own authorship and that it fulfils all the requirements of the Code of Conduct and Good Practices of the Universidade de Lisboa.

Acknowledgments

This thesis symbolizes the end of a journey with as many victories as failures but also with many lessons learned and knowledge acquired. It made me grow as a person and as a professional and I am sure it will help me conquer all challenges ahead. To all who have helped and supported me along this year, I want to express my deepest gratitude.

To my supervisor, Dr. Ana Sofia Coroadinha for believing in my potential and giving me the opportunity to work in the Cell Line Development & Molecular Virology group. For all the guidance and help provided.

A very special acknowledgment to Sofia Fernandes for allowing me to work on this project. For all the dedication, patience and guidance provided. For all the theoretical and practical knowledge transmitted. For all the advice and sharing of ideas. Thank you for being there for me and helping me grow.

To Professor Gabriel Monteiro for accepting to be my internal supervisor and for always being available to help me.

To the Cell Line Development & Molecular Virology group, Ana Sofia Coroadinha, Ana Filipa Rodrigues, Ana Isabel Almeida, Ana Raquel Fernandes, Catarina Silva, Elisa Cabral, Maria Fonseca, Maria João Carreiro, Mariana Ferreira, Miguel Guerreiro, Rodrigo Nogueira, Sofia Fernandes and Tiago Vaz for all your help, advice and great work environment. For always making me feel as I was part of the team.

To the flowers, Catarina Silva, Elisa Cabral, Maria Fonseca, Mariana Ferreira, Rodrigo Nogueira and Tiago Vaz for receiving me with open arms and always being available to discuss ideas and solve problems.

To my master's degree colleagues, Ana Raquel Fernandes and Maria João Carreiro. I could not have asked for better people to go through this journey with. Thank you for all the laughter, tears, and ideas we shared during our coffee breaks and for all your constant support.

Para a minha família (pais, avós, tios e primos) e amigos: Obrigada por sempre acreditarem em mim, por todo o carinho e pelo apoio incondicional durante os bons e os maus momentos. Sem vocês não seria possível.

Para o meu namorado, Ricardo, por estar sempre ao meu lado, por me ouvir desabafar, por me conseguir animar, pelo carinho, pelo amor incondicional. Sem ti não teria conseguido.

Resumo

O principal objetivo deste trabalho foi instituir os pilares para estabelecer linhas celulares de empacotamento de AAV baseadas em 293 contendo um mecanismo para controlar a citotoxicidade da Rep, através do silenciamento por shRNA e do sistema Cre/loxP.

Quatro shRNAs direcionados para a *rep* foram desenhados e clonados individualmente entre sequências loxP. Na sua presença, a expressão de *rep* será silenciada. Após infeção com um adenovírus que expresse Cre (AdV-Cre), a sequência de shRNA deverá ser excisada, reconstituindo a expressão de *rep*.

Este sistema foi testado em expressão transiente e estável e neste último por infeção com adenovírus. Em transiente, os níveis de *rep* foram semelhantes, independentemente da presença de shRNA. Na presença de *rep*, a expressão de *cap* foi 5 vezes superior. As populações estáveis apresentaram entre 0 e 1 cópia dos elementos genéticos do plasmídeo de empacotamento. A expressão de *cap* foi inferior à transiente. Após infeção com AdV-Cre, ocorreu amplificação de *rep-cap* na população controlo que expressa *rep-cap* (sem shRNA). No entanto, nas populações que expressam shRNA, os níveis de *rep* permaneceram baixos antes e após infeção. Assim, não foi possível validar a eficiência dos shRNAs. Neste trabalho conclui-se que será necessário integrar o *rep* em múltiplas cópias ou num locus de elevada expressão. Globalmente, esta tese contribuiu para estabelecer métodos essenciais, assim como para gerar conhecimento que serão utilizados no desenvolvimento de linhas produtoras de AAVs de elevadas produtividades, nomeadamente, através do aperfeiçoamento do desenho, seleção e entrega das cassetes de expressão de shRNAs e *rep-cap*.

Palavras-chave: vírus adeno-associado, linha celular de empacotamento de AAV, células 293, citotoxicidade da Rep, shRNA, sistema Cre/loxP

Abstract

The main goal of this work was to settle the pillars for establishing stable AAV packaging 293 based cell lines harbouring a mechanism to control Rep induced cytotoxicity, based on shRNA-mediated silencing and the Cre/loxP system.

Four different *rep*-silencing shRNAs were successfully designed and cloned separately between loxP sites. In their presence, *rep* expression should be silenced. Infection with an adenovirus expressing Cre (AdV-Cre) will excise the shRNA-coding sequence reconstituting *rep* expression.

The system was tested in transient and stable expression and in the latter challenged through AdV infection. In transient, *rep* mRNA levels showed to be similar in all transfected cells, regardless of shRNA presence. In the presence of *rep*, *cap* expression was 5-fold higher than *rep.* The selected stable populations had integrated copies of packaging plasmid components ranging from 0 to 1 and *cap* expression was lower, when compared to transient. After AdV-Cre infection of the stable control population harbouring *rep* and *cap* without shRNA, we observed an increase in *rep-cap* levels. However, in the *rep*-silenced populations, *rep* mRNA levels remained low before and after infection. Thus, it was not possible to validate the silencing effect of each shRNA. In this work we conclude that either multiple copies or high expressing locus should be pursued to express *rep*. Overall this work contributed to establish important methods and generated knowledge that will be used to establish high producer AAV cell lines, namely through the further improvement of the design, selection and delivery of the shRNAs and *rep-cap* expression cassettes.

Keywords: adeno-associated virus, AAV packaging cell line, 293 cells, Rep-induced cytotoxicity, shRNA interference, Cre/loxP system.

Contents

List of tables

List of figures

List of abbreviations

293	Human Embryonic Kidney 293 cells
293T	Human Embryonic Kidney 293 cells
AAP	Assembly-activated protein
AAV	Adeno-associated virus
AAV2	Adeno-associated virus serotype 2
AAVR	Adeno-associated virus receptor
AAVS1	Adeno-associated virus integration site 1
AdV	Adenovirus
AdV5	Adenovirus serotype 5
AdV-Control	Adenovirus not expressing Cre recombinase
AdV-Cre	Adenovirus expressing Cre recombinase
ALB	Human albumin gene
Amp	Ampicillin
BEVS	Baculovirus expression vector system
BHK	Baby hamster kidney cells
bp	Base pairs
BSA	Bovine serum albumin
BSD	Blasticidin S Deaminase
cDNA	Complementary DNA
cHS4	Chicken hypersensitivity site 4 insulator
CMV	Cytomegalovirus
CNS	Central nervous system
CsCl	Caesium chloride
C_T	Crossing threshold
dPCR	Digital polymerase chain reaction
ds oligo	Double-stranded oligonucleotide
dsDNA	Double-stranded DNA
E	PCR efficiency
E. coli	*Escherichia coli*
ELISA	Enzyme-linked immunosorbent assay
EMA	European Medicines Agency
FBS	Fetal bovine serum
FC	Flow cytometry
GAL-SIA	Terminal N-linked galactose of sialic acid
gDNA	Genomic DNA
GFP	Green fluorescent protein
hPGK	Human PGK promoter
hpt	Hours post-transfection

HSPG	Heparan sulphate proteoglycans
HSV	Herpes Simplex Virus
IAC	Immune-affinity chromatography
iCre	Codon optimized Cre recombinase
IEC	Ion-exchange chromatography
IP	Infectious particles
ITRs	Inverted terminal repeats
kb	Kilobases
kDa	Kilodalton
LPLD	Lipoprotein lipase deficiency
m	Slope
MAAP	Membrane-associated accessory protein
MCB	Master cell bank
MCM	Minichromossome C
miRNA	Micro RNA
MOI	Multiplicity of infection
M-PER	Mammalian protein extraction reagent
mRNA	Messenger RNA
N.D.	Not determined
NPC	Nuclear pore complex
NRT	No reverse transcriptase control
nt	Nucleotide
NTC	Non-template control
ORF	Open reading frame
P2A	Self-cleaving 2A peptide from porcine teschovirus-1
PCNA	Proliferating cell nuclear antigen
PEI	Polyethylenimine
pF	Primer forward
pI	Isoelectric point
PLA2	Phospholipase A2
pR	Primer reverse
pRC	pJGD-RC-ΔshRNA
pRC-sh1	pJGD-RC-shRNA1
pRC-sh2	pJGD-RC-shRNA2
pRC-sh3	pJGD-RC-shRNA3
pRC-sh4	pJGD-RC-shRNA4
pRC-shscr	pJGD-RC-shRNAscr
pΔRepC	pJGD-C-ΔshRNAΔRep
qPCR	Quantitative polymerase chain reaction
r^2	Coefficient of determination

rAAV	Recombinant AAV
RBS	*rep*-binding site
rBV	Recombinant baculovirus
RC	*rep-cap*
RG	Reference gene
rHSV	Recombinant herpes simplex virus vectors
RNAi	RNA interference
RPC	Replication factor C
RPE	Retinal pigment epithelium
RT-qPCR	Reverse transcription polymerase chain reaction
scAAV	Self-complementary adeno-associated virus
SD	Standard deviation
SEAP	Secreted embryonic alkaline phosphatase
shRNA	Short hairpin RNA
shRNA1-4	*rep*-silencing shRNAs
shRNAscr	Scrambled shRNA
SIA	α2-3 and α2–6 N-linked sialic acid
SMA1	Spinal Muscular Atrophy type 1
ssDNA	Single-stranded DNA
$TCID_{50}$	Median tissue culture infectious dose
TOP1	DNA topoisomerase 1 gene
TP	Total particles
Trs	Terminal resolution site
TU	Transducing units
UBC	Polyubiquitin c gene
VA RNA	Viral associated RNA
VG	Viral genome
VR	Variable region
WPRE	Woodchuck Hepatitis Virus Posttranscriptional Regulatory Element
wt	Wild-type

1 Introduction

1.1 Fundamentals of adeno-associated virus biology

1.1.1 Discovery and classification

In 1965, Atchinson and colleagues reported the existence of small virus-like particles in preparations of simian adenovirus. These were shown to be antigenically different from adenovirus (AdV) and replication-defective, since particle production, as well as cell escape, relied on AdV co-infection. Hence, these particles were named adeno-associated virus (AAV) [1]. Two years later, AAV was also found in human isolates [2].

AAV belongs to the *Parvoviridae* family that is divided into two subfamilies: *Parvovirinae*, which infects vertebrates, and *Densovirinae*, which infects only invertebrates [2]. The subfamily *Parvovirinae* contains 8 genera: *Amdoparvovirus*, *Aveparvovirus*, *Bocaparvovirus*, *Copinaparvovirus*, *Dependoparvovirus*, *Erythroparvovirus*, *Protoparvovirus* and *Tetraparvovirus* [3]. AAVs belong to the genus *Dependoparvovirus* and only replicate in the presence of a helper virus, such as AdV, herpes simplex virus (HSV) or cytomegalovirus (CMV) [4].

1.1.2 AAV infection

AAV is generally considered non-pathogenic since it has not been unequivocally associated with any human pathology [5]. AAV persistence requires latency in specialized cells in order to evade the host immune system until viral spread becomes possible. Reactivation can be induced by different stimuli, such as infection with a helper virus or cellular stress [6], [7]. *In vivo*, wild-type (wt) AAV2 has been detected in 5% of human tissue samples, mainly in circular episomal (extrachromosomal) form, in a head-to-tail array with deletions and rearrangements in the viral inverted terminal repeats (ITRs). Additionally, one integration event was shown in chromosome 1 [8].

In cell culture, wt AAV2 displays a biphasic life cycle: a latent phase and a lytic phase. AAV can establish latency by integration in chromosome 19 (q13.4) in a specific site termed adeno-associated virus integration site 1 (AAVS1) [9] in a tandem head-to-tail conformation, mediated by the AAV ITRs and the non-structural viral Rep proteins [10]. The lytic phase begins when cells containing AAV are co-infected with a helper virus. After the excision of the provirus from the host genome, AAV DNA replication, viral gene expression, protein production and packaging occur. Finally, the assembled virion is released by helper virus-induced lysis [11].

As discussed in more detail in section 1.2, recombinant AAV (rAAV) vectors, used in gene therapies, do not code for Rep proteins (required for integration), so genome integration is greatly reduced. Therefore, rAAV are predominantly maintained episomally [12], [13]. However, vector integration can still occur through homologous and non-homologous recombination [14].

1.1.3 AAV genome

AAV is an icosahedral nonenveloped virus (18 – 26 nm) with a single-stranded DNA (ssDNA) genome of 4.7 kilobases (kb), which can encapsidate the sense or antisense strand. The viral genome **(Figure 1.1)** is flanked by ITRs of 145 base pairs (bp) [5]. These structures are composed of a 125 bp palindromic sequence [11] that forms a T-shaped hairpin by complementarity and contain *cis*-elements, such as the *rep*-binding site (RBS) and terminal resolution site (trs), necessary for replication and packaging [4]. The remaining 20 nucleotides are named the D-sequence [11] **(Figure 1.2)**.

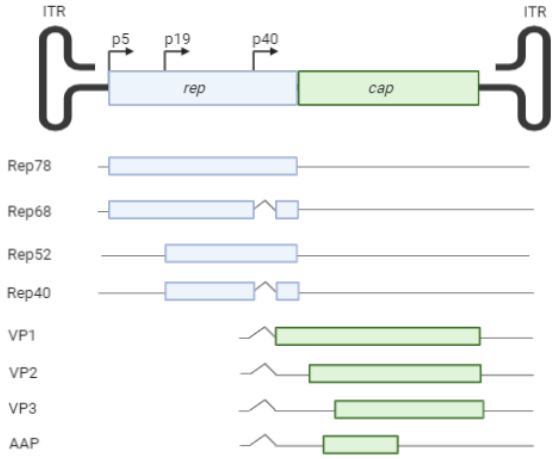

Figure 1.1: Schematic representation of the wt AAV2 genome (created with BioRender). wt AAV2 genome is flanked by ITRs and contains three promoters (p5, p19 and p40) and two genes (*rep* and *cap*). p5 controls the expression of variants Rep78/68 while p19 promotes the expression of Rep52/40. The p40 promoter initiates *cap* gene expression where VP1, VP2 and VP3 are originated from alternative splicing and leaky scanning. VP2 is expressed from a non-canonical start codon (ACG). An alternate open reading frame (ORF) in the *cap* gene codes for *AAP*.

There are three promoters, named after their map position in the genome: p5, p19 and p40, the first two regulate *rep* gene expression and the latter *cap* and *AAP* (assembly-activating protein) gene expression [5] **(Figure 1.1)**.

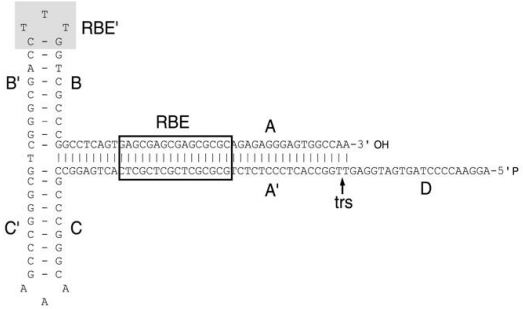

Figure 1.2: ITR illustrative scheme [15]. ITRs are T-shaped palindromic sequences with 145 bp containing several key elements for AAV replication and packaging: RBE/RBS and trs. The last 20 nucleotides are known as the D-sequence (D).

The *rep* gene encodes four non-structural replication proteins, the Rep proteins, designated by their molecular weight. The major, Rep78 and Rep68, are expressed from promoter p5 whereas p19 activates the transcription of the smaller Rep proteins, Rep52 and Rep40 [11]. Unspliced mRNAs will encode for Rep78 and Rep52 while spliced ones will originate Rep68 and Rep40 [4]. Rep78/68 possess helicase and ATPase activity, as well as a site-specific endonuclease activity, which plays a crucial role

in DNA replication and site-specific integration into the host genome [15]. These proteins are required for fundamentally every phase of the AAV replication phase, including DNA replication [16], [17], site-specific integration [7], integrated genome excision [18] and regulation of cellular and viral promoters [19]. Rep52/40 mediate the accumulation and packaging of the ssDNA genome into the capsid, thus exhibiting helicase (3' – 5') and ATPase activity [20], [21].

In the absence of helper virus, it has been documented that Rep proteins repress p5, p19 and other heterologous promoters [22]–[25]. This repression is mostly achieved through the binding of Rep78/68 to p5 and other cellular proteins, such as YY1 and MLTF [19], [26]. In the presence of AdV co-infection, Rep can transactivate the transcription of all three AAV promoters, acting as both a repressor and an activator [19], [27], [28]. This feedback loop regulation can aid in controlling Rep-induced cytotoxicity since it has been reported that Rep78 expression induces cell apoptosis mediated by caspase-3 and an accumulation of cells in the G_1 phase [29], [30].

The p40 promoter controls the expression of the *cap* gene, coding for the three viral proteins present in the icosahedral capsid: VP1, VP2 and VP3. Alternative splicing generates major and minor spliced products. VP1 is transcribed from minor spliced mRNA and major spliced products originate VP2 and VP3. The VP2 is initiated with a non-canonical start codon (ACG). This mechanism is related to their abundance in the mature virion (VP1:VP2:VP3 – 1:1:10) [31], [32]

The N-termini of VP1 possesses phospholipase A2 activity (PLA2), which is required for infectivity and endosomal escape [33], [34]. As for VP2, it was demonstrated to be nonessential for assembly and infectivity [35] but necessary for nuclear transport [36]. The VP3 capsid protein is composed of conserved β-Barrel motifs with antiparallel β-sheets, where the intra-strand loops are variable among serotypes [37]. This will determine receptor usage and serology [4].

Sonntag *et al.* (2010) showed the existence of an alternative ORF in the *cap* gene, which from a non-conventional translation start site (CTG), coded for a 23 kilodalton (kDa) protein named AAP. It locates in the host cell nucleus and targets newly synthesized capsid proteins to this organelle, also participating in the assembly reaction and capsid stability [38], [39].

In 1999, at the far end (3929-4393 nucleotides) of the AAV genome, a gene named X was identified as well as a possible new promoter, the p81 [40], [41]. It has been suggested that it might have a role in AAV replication [42]. Additionally, in 2019 was detected a frameshift gene in the VP1 region coding for a protein named MAAP (membrane-associated accessory protein) which is hypothesized to have a role in viral production [43]. Further studies are still warranted to confirm the importance of these two proteins in the AAV life cycle.

1.1.4 AAV virion and serotypes

The AAV2 icosahedral capsid is composed of 60 subunits of VP1, VP2 and VP3 in a 1:1:10 molar ratio [4]. The function of the capsid is to protect the virion genome, serve as an intermediate for cell surface receptor binding as well as to facilitate intracellular viral trafficking [11].

The structural topology of the capsid contains pores at each 5-fold axis, depressions at each 2-fold axis and three protrusions that surround each 3-fold axis [44]. The pores serve as an exchange intermediate between the interior and the outside, such as for ssDNA packaging mediated by Rep

proteins [45]. Additionally, each VP has a core region that contains variable regions (VR), which determine serotype and are thought to control cellular tropism and transduction efficiency [11]. Currently, 13 AAV serotypes have been isolated [46]. **Table 1.1** shows data regarding each serotype, divided by their origin, primary receptors, and tropism. The existence of serotypes is of great importance for gene therapy since it allows the selective transduction of specific cell types.

Table 1.1: AAV Serotypes – origin, primary receptors and tropism.

Serotype	**Origin** [11], [47]	**Primary receptor** [46]	**Tropism** [11], [48]–[51]
AAV1	Non-human primate	SIA	CNS, heart, RPE, Skeletal muscle, intestine
AAV2	Human	HSPG	CNS, kidney, photoreceptor cells, RPE
AAV3	Non-human	HSPG	Inner ear
AAV4	Non-human	SIA	CNS, lung, RPE
AAV5	Human	SIA	CNS, lung, photoreceptor cells, RPE, intestine
AAV6	Human	HSPG; SIA	Lung, skeletal muscle, bone marrow
AAV7	Non-human primate	N.D.	Liver, lung
AAV8	Non-human primate	N.D.	CNS, heart, liver, pancreas, photoreceptor cells, RPE, skeletal muscle
AAV9	Human	GAL-SIA	CNS, heart, liver, lung, skeletal muscle, brain, fat
AAV10	Non-human primate	N.D.	RPE
AAV11	Non-human primate	N.D.	N.D.
AAV12	Non-human primate	N.D.	N.D.
AAV13	Non-human primate	HSPG	N.D.

SIA, α2-3 and α2–6 N-linked sialic acid; HSPG, Heparan sulfate proteoglycans; GAL-SIA, Terminal N-linked galactose of sialic acid; CNS, central nervous system; RPE, Retinal Pigment Epithelium; N.D., not determined.

Cell entry of non-enveloped viruses involves the interaction of the capsid with cell surface glycosaminoglycan receptors. Interactions with secondary co-receptors appear to dictate intracellular trafficking [48]. In 2019, a new transmembrane protein, termed AAV receptor (AAVR) was reported to serve as a critical host factor for all serotypes tested (AAV1, 2, 3B, 5, 6, 8 and 9). This indicated AAVR as a universal receptor for AAV infection [52].

Classically, AAV is accepted as a non-pathogenic virus, however, it can elicit immune responses (extensively reviewed in [53]). Epidemiological studies have shown that 40 – 80% of the human population is seropositive for antibodies against AAV [54]. Despite the existent immunity, the most used

rAAV serotypes are the ones isolated from natural sources without any artificial modification due to their promising clinical features. However, to aid in immune system evasion, generate specific tropism and increase stability, different strategies of AAV capsid engineering can be applied [15], [55].

1.1.5 AAV cell entry and replication

AAV infection consists of a dynamic set of processes that can be divided into attachment to the cell surface, internalization, endosomal trafficking, nuclear import and gene expression/replication [11]. In this section, AAV2 cell entry and replication will be described since it is the most well-known and studied serotype.

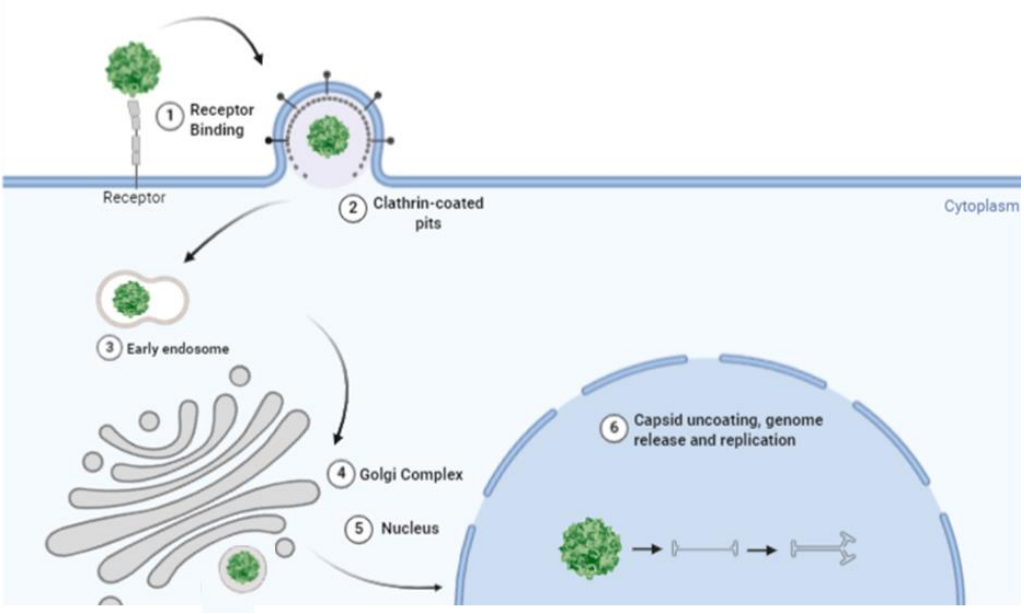

Figure 1.3: Illustrative scheme of AAV cell entry and transduction (created with BioRender). (1) Cell attachment of the virion through receptor binding; (2) AAV internalization mediated by clathrin-coated pits; (3) AAV trafficking through early endosomes; (4) AAV trafficking through the Golgi complex; (5) AAV nuclear entry; (6) AAV capsid uncoating, genome release and replication in the nucleus.

The first step in viral entry is the attachment of the viral capsid to the target cell's receptors **(Figure 1.3 – (1))**. When it comes to cellular receptors, glycan conjugates are the primary sources. O- and N-linked sugars, as well as proteins, serve as co-receptors [11]. AAVs are rapidly internalized through receptor-mediated endocytosis from clathrin-coated pits associated with dynamin **(Figure 1.3 – (2))** [56]. Then, they transverse to the cytoplasmic space through early endosomes **(Figure 1.3 – (3))** [57] in which the acidic pH (6.0 - 5.5) induces conformational changes in the VP1/VP2 capsid region, exposing the PLA2 domain required for endosomal escape and the nuclear localization signal [58]. Afterwards, the virions can circulate through the Golgi complex **(Figure 1.3 – (4))** [59] and lysosome [57]. Then, the intact AAV virion enters the nucleus through the nuclear pore complex (NPC) **(Figure 1.3 – (5))** by the action of nuclear localization signals in the N-termini of AAV VP1 and VP2 [36]. It is suggested that this mechanism involves components of the canonical nuclear import pathway, such as the NPC and importins [60] or even host cell caspases, involved in nuclear envelope breakdown during apoptosis [60]. Often, AAVs are sequestered by autophagosomes or are degraded in proteasomes [61].

AAV genome replication consists in unidirectional strand-displacement replication and can be divided into unidirectional DNA synthesis and terminal resolution, as exemplified in **Figure 1.4**. The ITRs form a double hairpin structure that provides a base-paired 3'-hydroxyl group (replication primer), from which unidirectional DNA synthesis can occur **(Figure 1.4 – (1))**. It is believed that helper viruses and/or cellular machinery mediate this step [11], [62]. It is suggested that replication factor C (RFC), proliferating cell nuclear antigen (PCNA), DNA polymerase δ [63] and minichromosome maintenance (MCM) complex play an important role in viral replication [64]. It was demonstrated that Rep proteins interact with several cellular proteins, such as the MCM complex (DNA replication), RCN1 (membrane transport), SMC2 (chromatin dynamics), EDD1 (ubiquitin ligase), IRS4 (signal transduction), and FUS (splicing) [65]. Once the AAV double-stranded DNA (dsDNA) is synthesized, terminal resolution occurs. The large Rep78/68 proteins specifically bind to the RBS and generate a strand-specific nick at the trs, which originates another 3'-hydroxyl primer **(Figure 1.4 – (2))**. Then, the ITR is unwound also by Rep78/68 and is replicated **(Figure 1.4 – (3))**. Afterwards, the ITR is reconfigured to its hairpin structure **(Figure 1.4 – (4))** and the 3'-OH primer will lead strand displacement synthesis using cellular complexes [66]–[68] **(Figure 1.4 – (5))**. The replication process can generate either a double or single-stranded AAV genome. The first one would serve as a replication template whereas the last would be for genome packaging [11].

Capsid assembly consists of two steps, first, the empty capsids are rapidly formed and then become slowly packaged with AAV ssDNA [69]. Both sense or antisense strands are packaged with the same frequency and efficiency through the five-fold axis capsid pore by a Rep-mediated process [11], [70].

As previously mentioned, for a productive AAV infection helper functions are needed to induce changes in the cellular environment. However, it has been reported that AAV replication can occur independently in specific cells, such as keratinocytes [71]. Additionally, it was shown that purified nuclei from HEK 293 (293) and NIH3T3 cells contain all the machinery necessary for uncoating and viral second-strand DNA synthesis, even in the absence of a helper virus [72].

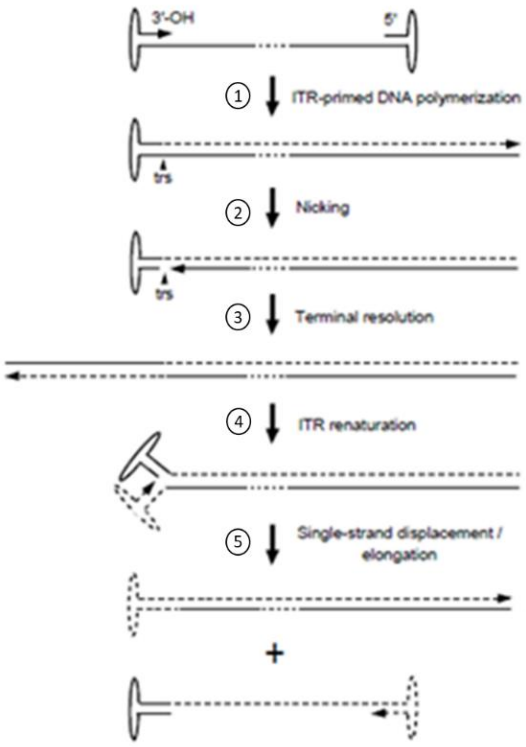

Figure 1.4: Model of AAV DNA replication by unidirectional strand-displacement (Adapted from [73]**).** (1) The ITRs provide a base-paired hydroxyl group from which unidirectional DNA synthesis occurs. (2) Rep-specific nicking on the trs forms a new free 3'-hydroxyl group (3) from which the ITRs are replicated in a process mediated by Rep78/68, named terminal resolution. (4) After ITR renaturation, the AAV genome is elongated by single-strand displacement and the newly synthesized ITR is renatured into a terminal hairpin (5).

1.1.6 Viral helper functions

1.1.6.1 Adenovirus

The genes from AdV that provide helper functions have been identified: *E1a*, *E1b*, *E2* and *E4* together with viral associated RNA (VA RNA) [4]. *E1a* is the first gene expressed during AdV infection and will transcriptionally activate other AdV early genes [74]. In AAV replication, *E1a* gene products bind to a cellular transcriptional repressor (YY1) [26] to control viral p5 and p19 promoters [74], [75], relieving its repression which leads to the expression of non-structural Rep proteins. It has been shown that E1b together with E4 are required for efficient and timely accumulation of AAV DNA, mRNA and proteins [76]. Additionally, these proteins also degrade the MRN complex, composed of DNA repair proteins, capable of limiting AAV transduction [77]. The *E2a* gene codes for a ssDNA binding protein present in replication centres that recruits AAV genome into the nucleus [78]. As for VA RNA, it inhibits the phosphorylation of interferon-inducible eLF-2 protein kinase, a cellular anti-viral mechanism that blocks viral protein translation, stimulating the expression of AAV proteins [79], [80].

1.1.6.2 Herpes Simplex Virus

Initially, a group of proteins was identified as being able to induce AAV replication: the helicase/primase complex (UL5/8/52) and the ssDNA-Binding Protein, ICP8 [81]. It was shown that ICP8 forms a complex with AAV Rep78 and AAV DNA to recruit them to subnuclear HSV replication

compartments [82]. Furthermore, it was demonstrated that HSV primase activity (UL52) is not necessary for AAV DNA replication, whereas the presence of a functional UL5 helicase increases replication efficiency [83]. It was also shown that immediate-early ICP0 protein, a known activator of viral gene expression, could promote *rep* gene transcription in latently infected cells with wt AAV2 [84]. Alazard-Dany *et al*. (2009) [85] later demonstrated that HSV proteins ICP4 and ICP22 showed to have a synergistic effect with ICP0 and that the HSV-1 DNA polymerase complex (UL30/UL42) also contributes to enhancing AAV DNA replication.

1.2 Recombinant AAV as a viral vector in gene therapy

Gene therapy can be generally defined as the transference of genetic material, with the purpose of regulating, repairing, replacing, adding or deleting a genetic sequence to provide therapeutic or prophylactic effects [86]. Amid the available systems for gene delivery, AAV has been gaining increased attention due to its non-pathogenic nature, low immune and inflammatory responses, reduced toxicity [87], [88] and capability of long-term transgene expression in humans [89], [90]. Additionally, this virus can transduce dividing and non-dividing cells and the existence of several serotypes allows for tissue specificity and different infectivity efficiencies [91], [92]. Nevertheless, this vector also presents some challenges such as its small packaging capacity (< 5 kb) [93], potential pre-existing patient adaptive immune response [54] and possible risks of insertional mutagenesis [94].

Historically, in 1982 Samulski *et al.* cloned the AAV2 genome in a pBR322 plasmid and were able to produce AAV particles when transfecting human cells and using AdV type 5 (AdV5) as a helper virus [95]. Additional studies demonstrated that was possible to delete AAV *rep* and *cap* sequences while keeping the ITRs to ensure genome replication and packaging. AAV genes could be complemented in *trans*, preventing the packaging of wt AAV [96], [97]. Thus, vectors containing only the ITRs became the standard approach for AAV-mediated gene therapy [98] **(Figure 1.5)**.

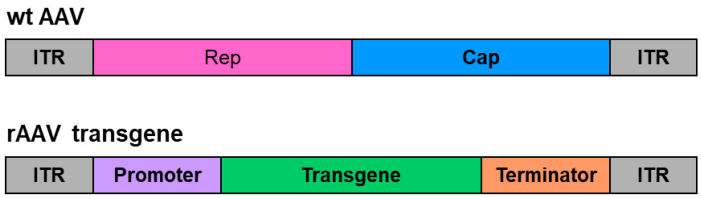

Figure 1.5: wt AAV versus AAV vector - genome comparison. In AAV vectors, the *rep* and *cap* genes are replaced by a transgene expression cassette and their functions are provided in *trans*.

AAV vectors can be used in different gene therapy strategies, namely gene addition, editing and silencing. Gene addition consists in gene delivery to compensate for a loss of function caused by a genetic mutation. It is suitable for targeting monogenic diseases [99] and was successfully used in gene therapy treatments performed with Glybera and Luxturna, which will be further described in this section. For AAV vector-mediated gene editing, homologous recombination is performed through a transgene donor sequence with homology arms. To enhance efficiency and specificity, AAV vectors can be coupled with targeted nucleases (reviewed in [100]). As for gene silencing, the use of rAAV combined with RNA interference (RNAi) approaches, either short hairpin RNA (shRNA) or micro RNA (miRNA), can tackle diseases resulting from both loss-of-function or toxic gain-of-function [101], such as in Huntington's

disease [102]. Furthermore, several strategies have been developed to overcome some of the inherent limitations of rAAV. Expanding AAV vector packaging capacity can be performed through the use of two rAAV coupled with homologous recombination (overlapping dual vectors), *trans*-splicing (*trans*-splicing dual vectors) or both (hybrid dual vectors) – reviewed in [103]. To overcome the limiting step that is dsDNA synthesis [104], self-complementary AAVs (scAAV), in which the uncoated DNA folds into a double strand, were also generated (reviewed in [105]).

The therapeutic success of AAV vectors correlates with the increase of approved clinical trials in the last years, in a variety of pathologies, such as Parkinson's disease [106], retinal disorders [107], Alzheimer's disease [108] and Duchenne's muscular dystrophy [109]. One important hallmark was the approval of the first gene therapy product, Glybera (alipogene tiparvovec), a rAAV1 carrying the lipoprotein lipase gene for the treatment of lipoprotein lipase deficiency (LPLD) by the European Medicines Agency (EMA) [110]. From there on, several AAV based gene therapy products have also been approved, such as Luxturna (voretigene neparovec-rzyl) an AAV2 containing a normal *rpe65* gene for the treatment of Leber congenital amaurosis (LCA) [111] and Zolgensma (onasemnogene abeparvovec-xioi) a self-complementary AAV9 (scAAV9) based therapy to deliver a healthy *smn* gene to patients with spinal muscular atrophy type 1 (SMA1) [112].

1.3 rAAV manufacturing platforms

In a clinical setting, the application of rAAV should be supported by the creation of production and purification systems capable of generating a final product at acceptable costs that consistently presents high purity and potency. *In vivo*, viral vector dose requirements can reach the $1x10^{15}$ to $1x10^{16}$ viral genome (VG) range [113]. For example, in an AAV-FIX based gene therapy study (NCT00979238) doses of $2x10^{11}$, $6x10^{11}$ and $10x10^{12}$ VG/kg were implemented [114]. The manufacture of such amounts, while being feasible remains a challenge for the currently available production methods [113]. Currently, rAAV vectors can be produced in insect cells using a baculovirus expression vector system (BEVS) or, in mammalian cells either using transient transfection protocols, rHSV infection (harbouring AAV components) or through packaging or producer cell lines followed by AdV infection **(Figure 1.6)**.

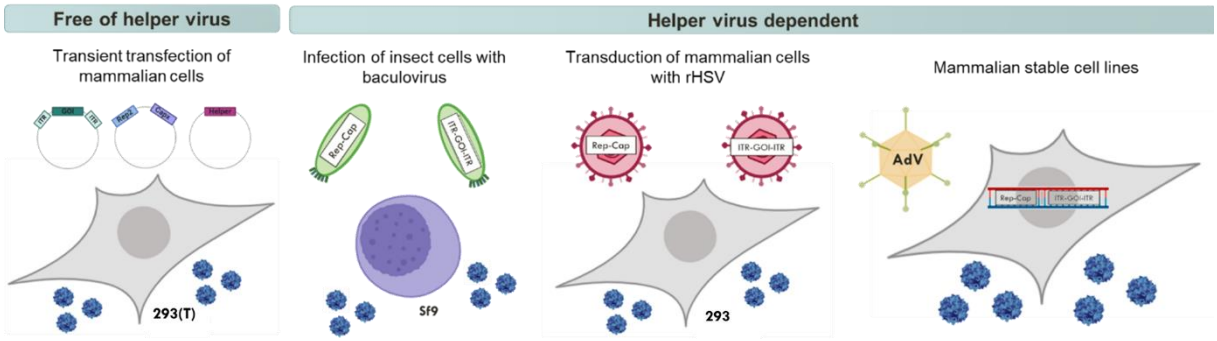

Figure 1.6: Representative scheme of the available rAAV manufacturing systems (created with BioRender). AAV vectors can be produced without helper viruses, using transient transfection protocols or with the use of helper viruses, namely with insect cells infected with baculovirus through BEVS, rHSV infection of mammalian cells or by the establishment of packaging/producer mammalian stable cell lines.

1.3.1 Transient transfection of mammalian cells

One of the most used methods for rAAV production is the plasmid transient transfection of 293 or 293T mammalian cells, which constitutively express AdV *E1a* and *E1b* genes. This system, devoid of helper virus, requires three main components: (a) the transgene vector, with the gene of interest (GOI) and its regulatory elements (promoter, polyA, introns, etc) flanked by AAV ITRs; (b) the AAV *rep* and *cap* genes and (c) additional helper functions provided by other AdV helper genes, such as *E2a*, *E4* and VA RNA [115].

Most often, rAAVs are produced by a triple transfection approach using one vector plasmid with the GOI and two helper plasmids containing AAV *rep-cap* genes or AdV genes. This approach has evolved to a double transfection where only one helper plasmid (containing *rep*, *cap* and AdV-helper genes) is used [25]. The plasmid DNA is typically delivered to cells by calcium phosphate precipitation or by a cationic polymer, polyethylenimine (PEI) [115]. The main advantages of this approach are the absence of infectious AdV and a greatly reduced risk of replication-competent AAV presence in viral preparations, combined with great flexibility and simplicity of implementation, especially in the early stages of product development [116], [117].

In addition, 293 cells have been adapted to suspension, which can facilitate the scale-up of the process [118], [119]. Blessing *et al.* (2019) [119] developed a scalable AAV production bioprocess using orbitally shaken bioreactors and HEKExpress suspension-adapted cells. From the cleared cell lysates, rAAV yields reached $1.14x10^{11}$ and $1.07x10^{11}$ VG/Batch, for AAV2 and 8, respectively. Also, it was shown that these rAAVs are bioequivalent and might display higher potency than the ones created with adherent 293 cells. Nevertheless, scale-up ultimately requires laborious and expensive preparation of large quantities of plasmid DNA [120], resulting in variability in transfection efficiency and a reduced batch to batch reproducibility, that can limit clinical needs [121], [122].

1.3.2 Establishment of mammalian stable cell lines

To overcome transient transfection drawbacks, the establishment of AAV vector stable cell lines is a key strategy, since these can be easily characterized and allow for easy scale-up for commercial manufacture and can generate relatively high vector titers [121], [123] with increased reproducibility. In contrast to transient transfection methods, which only produce rAAV in the first 72 to 96 hours post-transfection, stable cell lines can be productive for more prolonged periods [121].

There are two types of stable cell lines: packaging and producer. A stable packaging cell line has AAV *rep* and *cap* genes integrated into the chromosome. So, rAAV vectors can be produced by delivering the vector genome by transfection and helper virus infection [120]. In a rAAV producer cell line, the vector transgene is also stably integrated into the host cell and viral vector production only requires the infection with the helper virus. Again, these cell lines can be adapted to grow in animal serum-free suspension conditions, reducing the costs and increasing the safety of the overall process [120], [124]. Despite the advantages, the selection process of a high-producer clone is laborious and requires the confirmation of certain key characteristics, such as the stable maintenance of the *rep-cap* and GOI sequences throughout culture time; the silencing of the AAV promoters during cell sub-culturing

and expansion; and the induction and amplification of *rep-cap* gene expression when co-infected with a helper virus [115]. Also, each vector and serotype combination requires the establishment of a cell line, which is complex and costly [113]. Nevertheless, if a variety of rAAVs are needed, a packaging cell line only containing the *rep-cap* sequence is particularly useful since it allows flexibility for transgene usage [120].

Mammalian stable cell lines can be established in many different cell lines, namely HeLa, A549 and 293 cells. Genetic characterization of some of these stable cell lines showed *rep-cap* sequences in a head-to-tail tandem configuration with varying copy numbers, from 2 to 60 [124]–[129]. One crucial observation that has been documented across plenty of studies is the relation between *rep-cap* amplification upon AdV infection and high rAAV productivities [123], [127], [129], [130]. It seems that stable cell lines mimic wt AAV lytic life cycle (post-adenoviral co-infection) by amplifying *rep* and *cap* genes [130]. However, it appears that genome integrated *rep-cap* copy number is not clearly related to rAAV productivity [123]. Nevertheless, it has been referred that increased productivity levels might also be attributed to a higher number of integrated copies [129]. In Liu *et al.* (2000) [130], HeLa cells with 4-5 integrated copies and AAV vector productivity of $2x10^4$ VG/cell reached lower yields than the ones described in Martin *et. al (2013)* [129], which produced $2x10^5$ VG/cell in cell lines with 10-50 integrated copies of *rep-cap*. Another key point in AAV vector production is AdV multiplicity of infection (MOI) [130]. In general, 293 cell lines require a lower MOI value when compared to HeLa and A549 [123]–[129], [131]. In **table 1.2** is an overview of some of the cell lines discussed below, regarding clone screening and *rep* integrated copies as well as its amplification.

Table 1.2: Summary of established mammalian stable cell lines for the manufacturing of rAAV. Clones screened and integrated *rep* copy number as well as its amplification upon AdV infection are specified.

Cell line	Clones screened	High producer clones	Integrated copies	*rep* amplification	Reference
HeLa (B50)	708	7	5	100-fold	Gao *et al.* (1998) [126]
HeLa (HeRC32)	N.I.	N.I.	1-2	100-fold	Chadeuf *et al.* (2000) [131]
HeLa S3	409	25	12-50	600-fold	Martin *et al.* (2013) [129]
A549 (SY69)	1296	1	8-10	300-fold	Farson *et al.* (2004) [128]
A549 (K209)	800	3	2.7	1000-fold	Gao *et al.* (2002) [127]
293 (293-GFP-145)	N.I.	N.I.	50	10-fold	Qiao *et al.* (2002) [124]
293	48	10	10-50	10 to 20-fold	Yuan *et al.* (2011) [123]

N.I. – not indicated

1.3.2.1 HeLa based stable cell lines

Clark *et al.* (1995) [125] were the first group to develop a producer HeLa based stable cell line with *rep-cap* genes and the transgene vector integrated into the genome. It paved the work for further improvements in the generation of cell lines able to provide high titer preparations of rAAV.

Inoue *et al.* (1998) [132] generated a HeLa-derived packaging cell line where AAV *rep-cap* sequences and the transgene expression cassette are under the dependence of a doxycycline-inducible

promoter. In the presence of the inductor and with posterior AdV infection, rAAV production occurs with a yield of approximately 10^4 viral particles/cell. Furthermore, copy numbers of the integrated AAV helper and vector constructs increased up to 10-fold after doxycycline induction, reaching 25 to 100 copies per cell. In the same year, Gao and colleagues [126] developed a stable cell line containing integrated copies of *rep-cap*. Helper virus functions were then provided by infection with an AdV defective in *E2b* and the transgene was provided by subsequent infection with an AdV-AAV hybrid vector. Out of the 708 isolated clones, 8 of them were able to trans-complement *rep-cap*. The best producer clone, B50, possessed 5 copies of the *rep-cap* plasmids arranged in a head-to-tail conformation and yielded $5.9x10^5$ total genome copies/cell.

Chadeuf *et al.* (2000) [131] developed a clone derived from HeLa cells (HeRC32) with two integrated copies of *rep-cap* genes. After transient transfection with the transgene vector, adenoviral helper activities were delivered either by wt AdV or an adenoviral plasmid. Results showed that efficient rAAV yields correlated with a 100-fold amplification of *rep-cap* genes when infection with wt AdV occurred, yielding $1.4x10^{11}$ total particles (using 20x15 cm plates). However, rAAV yields significantly decreased when the adenoviral infection was replaced by a helper plasmid delivery (≤10^8 total particles using 20x15 cm plates). This cell line is routinely used for some rAAV characterization tests, namely infection/replication assays (see section 1.4.2).

The first scalable upstream process for clinical-grade rAAV production was based on a HeLa producer stable cell line [133]. This process uses a suspension adapted HeLa subclone (HeLa S3) at the 250 L scale for rAAV1 production in animal components-free medium with high productivity (> $1x10^5$VG/cell) [129], [134]. In 2013, a new HeLa S3 based suspension producer cell line was designed by the transfection of a plasmid containing the wt AAV2 *rep-cap* genes and the vector transgene (expressing the secreted embryonic alkaline phosphatase (SEAP) gene and a cell selection marker) (**Figure 1.7**). These cells were then infected with wt AdV using a MOI of 100. Out of 409 screened clones, only 25 of them were high producers. Upon infection with AdV, *rep-cap* was amplified 100-fold with rAAV yields reaching up to $2x10^5$ VG/cell. Productivity remained stable over 60 population doublings [129].

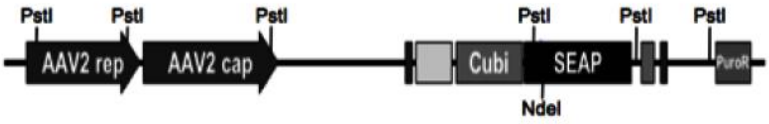

Figure 1.7: Schematic representation of the plasmid used to develop the HeLaS3 producer cells in Martin *et al.* (2013) [129]**.** The plasmid is composed of AAV2 *rep* and *cap* genes controlled by their native promoters and a SEAP gene, controlled by a constitutive CMV-Ub hybrid promoter (Cubi). A puromycin drug resistance selection marker is also present (PuroR).

Establishment of stable cell lines in HeLa cells ultimately results in a low frequency of high producer clones and raises safety concerns, since for rAAV production a step with replication-competent AdV is required, thus demanding further purification protocols and might result in the presence of pathogenic AdV in the final clinical product [120].

1.3.2.2 A549 based stable cell lines

In 2002, Gao *et al.* [127] designed an approach to establish an A549 based stable cell line through the transfection of cells with a construct containing the *rep-cap* genes from AAV2. From the 800 clones screened, the best producer, K209, had 2.7 *rep-cap* integrated copies that, after AdV infection, were amplified to 5240. 72 hours post-transfection and infection with AdV (MOI of 10), rAAV-CMVGFP yields reached 262 TU/cell. Two years after, a suspension stable cell line was established by transfecting the cells with two plasmids: one carrying the *rep-cap* genes (with a mutated start codon following p5 promoter). Out of 1296 clones, only one (clone 10) was found to be positive for *rep-cap*. Genetic characterization showed 8 to 10 copies of *rep-cap* in the genome and after AdV infection, the number increased 300-fold. Clone SY69 that carried an *EF1α-GFP* transgene demonstrated high yields of $2.1x10^5$ viral particles/cell and clone SP53.26 containing a *CMV-GFP* transgene provided $3.5x10^4$ viral particles/cell.

Similarly to HeLa based cell lines, AAV vector production requires the infection with wt AdV and the frequency of finding a high producer clone is lower when compared to 293 cells. On the other hand, this cell line has already a broad clinical application in the manufacturing of vectors to be used in clinical trials and for AdV production [135].

1.3.2.3 293 based stable cell lines

As indicated above, the presence of adenoviral *E1a/E1b* genes in 293 based cell lines allows the use of a non-pathogenic replication-defective AdV for helper functions. These types of AdV have been widely applied in gene therapy and have shown an overall safe profile [123].

Nevertheless, for a successful rAAV production in these cells, *rep* expression must be tightly controlled and engineered, since the AdV5 *E1* gene can trigger the production of Rep proteins, known to exert cytostatic and cytotoxic effects, if constitutively expressed [136]–[138]. For instance, Chadeuf *et al.* (2000) [131] tried to develop a packaging cell line based on 293 (293RC21) similarly to HeRC32 cells, however, the obtained rAAV titters were lower than the ones obtained with the HeLa based cell line and after 1 month of passages, rAAV productivity decreased more than 10-fold.

Several attempts have been made to overcome Rep-induced cytotoxicity. Okada *et al.* (2001) [139] and Qiao *et al.* (2002) [124] developed two different strategies based on *rep* coding region disruption. In the first study, a cell line (293CR) was genetically engineered to constitutively express an antisense *rep-cap* mRNA, whose expression was driven by a *loxP*-flanked CMV promoter. In the absence of Cre recombinase (recognizes loxP sites), this antisense orientation silenced the expression of *rep-cap*. After infection with an AdV-Cre, the CMV promoter is excised and *rep* and *cap* gene expression occurs through their endogenous promoters (**Figure 1.8**). With this, titers of up to $1x10^9$ vector particles per 3.5 cm dish were obtained after infection with AdV-Cre (MOI of 1) [139]. In the other study, a control mechanism named “dual splicing switch” was developed, in which the *rep* gene was disrupted through the insertion of a DNA sequence flanked by *loxP* sites downstream of the AAV p19 promoter (**Figure 1.9**). Rep expression was then restored after infection with an AdV-Cre. One cell line (293-GFP-145) achieved high yields of $8.6x10^9$ transducing units (TU) per 10 cm plate with an AdV-Cre

MOI of 5. The *rep-cap* gene sequence was amplified from 50 (integrated) copies to more than 500 per cell. Despite the good AAV productivity in the first screenings, a decrease in rAAV production was also observed over cell passages, possibly due to the cell line instability.

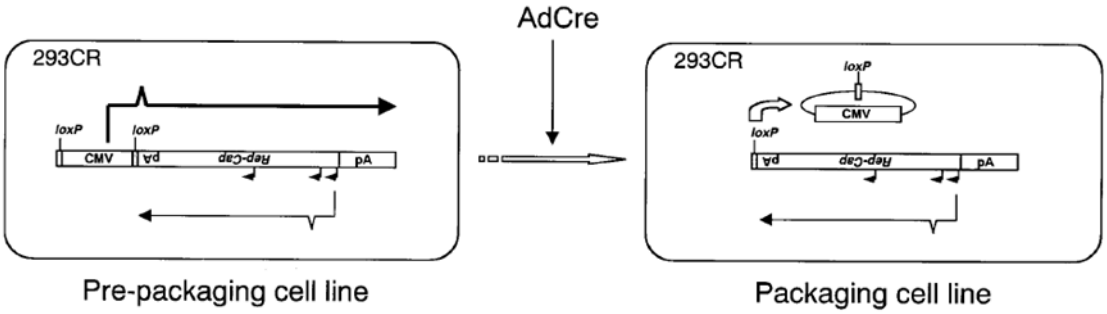

Figure 1.8: Schematic representation of the *rep*-control mechanism developed in Okada *et al.* (2001) [139] (adapted from [139])**.** The pre-packaging cell line constitutively expresses the antisense *rep-cap* driven by a loxP-flanked CMV promoter. Upon infection with AdV-Cre, the CMV promoter sequence is excised, and *rep-cap* expression occurs through their endogenous promoters (packaging cell line).

In 2011, the strategy developed by Qiao *et al.* (2002) [124] was simplified and optimized (**Figure 1.9**), resulting in a packaging cell line with a normal growth rate and morphology after multiple passages. Out of the 48 clones screened, 10 of them were considered to be high producers. Integrated *rep-cap* copies per cell varied from 10 to 50 and, after AdV-Cre infection (MOI of 5), were amplified 10-20 times. As for yields, it reached up to $2.8x10^{13}$ VG per 20x15 cm plates. Additionally, this methodology was successfully applied in the production of ssAAV and scAAV vectors as well as AAV2, AAV8 and AAV9 [123]. Mizukami *et al.* improved the methodology present in Okada *et al.* (2001) [139] by also controlling *cap* gene expression by using Cre/loxP technology. After transfection with a LacZ plasmid vector and infection with AdV-Cre (MOI of 1), a packaging titer of $2.1x10^{10}$ VG/10 cm plate was achieved. This study highlights the importance of controlling separately *cap* expression for successful AAV vector production [140].

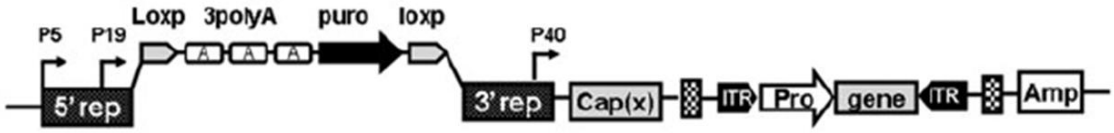

Figure 1.9: Schematic representation of the *rep*-control mechanism developed in Qiao *et al.* (2002) [124] **and simplified by *Yuan et al.* (2011)** [123] (Adapted from [123])**.** The AAV *rep* gene sequence is disrupted by a DNA sequence flanked by loxP sites. Upon AdV-Cre infection, this DNA sequence is excised, and *rep* expression is restored.

Despite the reported instability and Rep-induced cytotoxicity, the use of 293 cell lines displays some significant advantages when comparing to HeLa or A549. The use of replication-defective AdV provides a better safety profile when compared to wt AdV [123]. Moreover, the frequency of finding a high producer clone is higher than for HeLa based cell lines, as it is shown by the previously mentioned studies (**Table 1.2**).

1.3.3 Infection of insect cells with recombinant baculovirus

As an alternative to mammalian cells, rAAVs can be produced in Sf9 insect cells by the baculovirus expression vector system (BEVS). Insect cells can grow in suspension at high cell densities and perform post-translational modifications [113]. However, as AAV introns and promoters do not function properly in these cells [141], most of the strategies were developed to overcome these constraints.

The first approach was performed in 2002 by Urabe *et al.* [142] where suspension Sf9 cells were infected with three recombinant baculoviruses (rBV): one containing the *cap* gene (Bac-VP), the other the *rep*78/52 gene (Bac-Rep), and the last with the GOI flanked by AAV ITRs. Despite obtaining good yields ($5x10^4$ VG/cell), the Bac-Rep vector revealed genetic instability through serial passages. Further improvements were performed, such as the genetic engineering of *rep-cap* sequences to correct VP stoichiometry, increase AAV vector potency and increase Rep protein stability [143], [144]. In other approaches, the number of rBV used was reduced to two (one expressing Rep and Cap proteins and the other the GOI) [143].

Stable packaging cell lines were also established. In 2009, a Sf9 packaging cell line with integrated copies of *rep-cap* was established, yielding $1.4x10^5$ VG/cell [145]. A production system named OneBac was also developed, which consists of a plethora of Sf9 cell lines harbouring silent copies of *rep* and *cap* genes from AAV1-12 [146]. Five years after, it was upgraded to provide serotype and GOI versatility through the generation of rBV carrying both a *cap* gene and the rAAV transgene and the creation of a Sf9 stable cell line, coding for the AAV2 *rep* gene. rAAV2, 8 and 9 yields exceeded 10^5 VG/cell and had similar properties to the ones produced in 293 [147].

The Baculovirus-Sf9 cell line approach has several advantages when compared to the ones previously discussed: the use of animal serum-free media and the absence of a pathogenic helper virus, since baculoviruses do not actively replicate in mammalian cells [115]. As disadvantages, are the reported AAV cassette instability when expansion at an high titer is performed, the assembly of rAAV particles with an incorrect ratio of capsid proteins and the decreased potency of produced rAAV [113], [148]. Moreover, clinical applications demand more extensive research on baculovirus-derived contaminants (infectious baculovirus particles, residual DNA and proteins) [115].

1.3.4 Infection of mammalian cells with recombinant HSV vectors

The use of HSV to produce rAAV is based on its role as a helper virus on wt AAV life cycle. For safety concerns and yield optimization, recombinant HSV vectors (rHSV) are based on the d27.1 replication-deficient HSV variant, that lacks ICP27 expression, thus, these viral stocks are produced in V27 cells [113]. This method, designed by Conway *et al.* in 1999 relies on two rHSV, one carrying the GOI flanked by AAV ITRs and another with the *rep* and *cap* genes, which are used to transduce 293 derived cells [149]. rHSV transduction can also be done in baby hamster kidney (BHK) cells that can be adapted to suspension culture and achieve yields as high as $2.4x10^{14}$ VG/L [150]. Additionally, Adamson-Small and colleagues described a rAAV9 production and purification method using rHSV/293 capable of reaching yields of more than $1x10^5$ VG/cell with increased vector infectivity [151].

Nevertheless, the removal of animal-derived components use during production and efficient scale-up remain challenges for this method [152]. Also, infection with rHSV only generates about 8% of viral particles containing genome while in other systems can go up to 30% [115].

1.4 Purification and characterization of rAAV

1.4.1 Downstream processing of rAAV

For clinical manufacturing, the implemented purification methods should be scalable and reproducible in order to obtain a safe final product with high purity and potency. The rAAV purification steps are mostly based on vector physicochemical parameters such as size, density and charge [153]. rAAV vectors are highly resistant to extreme conditions of temperature (from 4°C to 55°C), pH (from 3 to 8.5) and detergent use [154]. Downstream processing of AAV vectors comprises harvest, clarification, capture chromatography, polishing, concentration and formulation, sterile filtration and finish [155].

rAAV particles are usually harvested from the supernatant after cell lysis, which can be performed through freeze-thaw, homogenization, osmotic shock [115], [155] or with detergents, such as Triton X-100 [156]. After cell disruption, a nuclease treatment using benzonase is typically performed to eliminate free nucleic acids. Other insoluble cell components are removed through clarification by centrifugation or filtration, for example [115].

In most research laboratories, rAAV vectors are routinely purified by density gradient ultracentrifugation with caesium chloride (CsCl) isopycnic gradients [157] or iodixanol step gradients [158]. Despite presenting similar recovery yields, the CsCl method ensures that the final product has less than 1% of empty particles, comparing to 20% when using iodixanol [159]. However, CsCl is toxic for humans and its elimination requires additional steps [115]. rAAV can also be purified by chromatographic processes, such as ion-exchange chromatography (IEC) or immune affinity chromatography (IAC). IEC relies on rAAV net surface charge alteration, depending on the isoelectric point (pI) and the pH [155]. This chromatography can be optimized to separate full and empty capsids [160], despite their small difference in pI (5.9 and 6.3, respectively [161]). Nevertheless, it lacks selectivity, since many impurities can display a similar pI to rAAV [155] and specific conditions must be defined for each AAV serotype [153]. Alternatively, IAC is an extremely specific capture step that can also be used to purify different rAAV serotypes. An example of a broad affinity column is the POROS™ Capture Select™ AAVX by Termofisher that can purify rAAV1-9, AAVrh10 and synthetic serotypes. IAC has the advantage of binding very few impurities due to high avidity and stringent washing conditions, allowing for a high yield after one step of purification [155].

Several techniques, such as heating above 50ºC [155], high hydrostatic pressure [162] and the use of Triton X-100 detergent [152], [163] are frequently used to eliminate helper viruses (AdV, Baculovirus or HSV). This is a mandatory step to reduce or abolish the potential immunoreactivity and pathogenicity for the patients in the final clinical product [155].

1.4.2 Characterization of rAAV production

Before reaching any research or clinical applications, rAAV are usually characterized in terms of total particles (TP), VG and infectious particles (IP). In this section, an overview of characterization parameters and techniques will be provided.

rAAV productivity in TP can be determined using an enzyme-linked immunosorbent assay (ELISA). This assay is based on a monoclonal antibody that detects a conformational epitope, not present on unassembled capsid proteins [164]. For example, the A20 antibody recognizes a surface epitope of assembled AAV2 capsids [165] and is currently used in ELISA [164].

One important criterion for AAV vector characterization is vector genome titer quantification, expressed in VG, which indicates the presence of full particles in the final product [166]. There are several quantification techniques available, such as UV spectrophotometry [167], dot-blot hybridization [168] and quantitative real-time PCR (qPCR) [169]. Currently, the latter is the most widely accepted and used for rAAV quantification as is simple and robust [166]. Recently, a new technology named digital PCR (dPCR) has emerged to overcome some limitations of qPCR, such as the need for a standard curve and the sensitivity to reaction-derived inhibitors [166], [170]. One important detail is that these systems will not indicate whether the virus is infectious or if the transgene cassette is functional. To determine the integrity of the packaged genome, the contained DNA should be extracted and analysed, for example by alkaline electrophoresis to determine its size and integrity [171] or by analytical ultracentrifugation (AUC) [172]. By using ELISA and qPCR quantification, empty-to-full capsid ratios can be indirectly estimated [169], [173]. Still, there are a few direct methods to directly achieve this ratio, such as sedimentation velocity AUC or electron microscopy [166], [171], [173], [174].

Infectivity of the produced viral rAAV particles must be assessed. It is mostly based on two categories: transduction/expression assays or infection/replication assays [175]. Transduction/expression assays evaluate vector quality through transduction levels and rely on two main approaches: the transduction of cells with serial dilutions of rAAV stocks of unknown titer [176] or the transduction of cells with a defined quantity of VG [142]. Infection/replication assays analyse vector quality by determining whether the gene was trafficked into the nucleus [175]. They rely on HeLa *rep-cap-trans*-complementing cells, such as C12 or HeLaRC32 [173], [177] and on the supply of AdV helper functions so that rAAV can replicate [175]. Then, vector genomes can be detected, usually by qPCR [178]. The latter is the most reliable method for assaying rAAV functionality, however, a universal titrating cell line should be made available for use [175].

Perceptibly, the purification protocols are not completely effective in removing all impurities, therefore contaminants should also be assessed. Illegitimate packaging of DNA sequences, such as *rep-cap*, plasmid fragments (as antibiotic resistance genes), portions of host cellular genome and oncogenes (e.g. SV40 large-T antigen and *E1a*) have been reported in final rAAV preparations [179]. Total DNA quantification can be performed with qPCR using primers to detect these specific target sequences. Also, host cell proteins and impurities derived from production and purification processes (such as raw materials, detergents, antibiotic resistance genes, etc) can be assayed by qPCR, ELISA or mass spectrometry [173].

2 Aim and Strategy

The main goal of this work is to establish the pillar methodologies to develop stable AAV packaging 293 based cell lines harbouring a control mechanism for viral *rep* gene expression. Thus, a Cre dependent shRNA-mediated *rep* silencing system strategy was designed **(Figure 2.1)**. In the presence of a *rep*-specific shRNA (flanked by loxP sites) and absence of Cre recombinase, the AAV Rep protein expression is expected to be silenced. After infection with a non-replicative AdV expressing Cre (AdV-Cre), the recombinase should catalyse the excision of the loxP-shRNA site, restoring Rep expression. Through this strategy, we aim for the translational control of Rep proteins, therefore managing their cytotoxic effects in 293 cells.

The first objective of this thesis comprised the construction and testing of different packaging plasmids, coding for *rep*-specific shRNA sequences. For that, we also optimized PEI-mediated transfection to improve transfection efficiency and cell survival. The second and last objective was to characterize the established stable populations regarding plasmid copy number integration, *rep-cap* gene expression and Rep protein production, before and after AdV-Cre infection. Genomic DNA, RNA and protein values were assessed by qPCR, RT-qPCR and western blot, respectively.

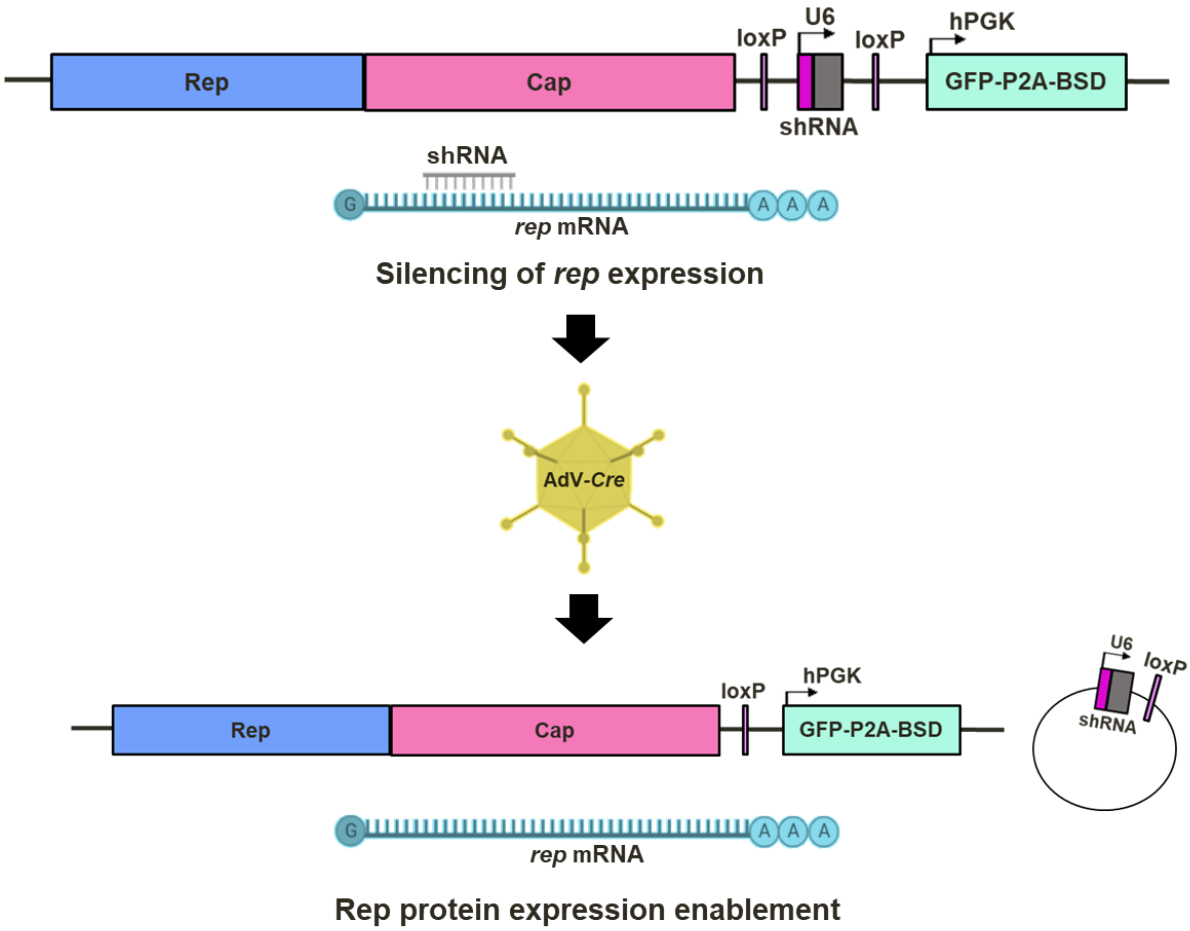

Figure 2.1: Schematic illustration of the *rep* gene expression control mechanism (created with BioRender). This strategy is based on the action of shRNA and on the Cre/loxP system. In the presence of a *rep*-silencing shRNA, *rep* gene expression is silenced through the binding of the shRNA to the *rep* mRNA. However, when the helper AdV-Cre is provided, Cre recombinase cleaves the loxP sites and excises the shRNA-coding sequence, therefore enabling Rep protein expression.

3 Materials and Methods

3.1 Bacterial strains, plasmids, and culture conditions

In this work two cloning strains of *Escherichia coli* (*E. coli*) were used: NEB® Stable Competent *E. coli* (New England Biolabs®, *Massachusetts, USA*) and Stellar™ Competent Cells (Takara Bio, California, USA). The *E. coli* strains harboring the recombinant plasmids were selected and grown in agar or in liquid cultures in the presence of Ampicillin (Amp), using Fast Media Amp LB (InvivoGen, Toulouse, France), following the manufacturer's instructions, at 37 ºC with aeration.

Table 3.1 describes the vectors and recombinant plasmids used in this work.

Table 3.1: Plasmids used and constructed in the scope of this work and their main properties.

Plasmid	Relevant characteristics	Reference
pSF-RC-loxPU6	pUC19-derived plasmid with AAV2 *rep-cap* genes and *lox*P sites flanking the U6 promoter	This study (Genscript, New Jersey, USA)
pFIN-EF1A-GFP-WPRE	Chicken β-globin HS4 core sequence (cHS4 insulator)	Addgene Plasmid # 44352 [180]
pSF-RC-loxPU6-cHS4	pSF-RC-loxPU6-derived with cHS4 insulator	This study
pJGD-RC-ΔshRNA (pRC)	pSF-RC-loxPU6-cHS4-derived with eGFP-P2A-BSD fusion gene expression under the control of hPGK promoter	This study
pJGD-C-ΔshRNAΔRep (pΔRepC)	pJGD-RC-ΔshRNA–derived deleted for the *rep* gene	This study
pJGD-RC-shRNA1 (pRC-sh1)	pJGD-RC-ΔshRNA–derived expressing *shRNA1* under the control of promoter U6	This study
pJGD-RC-shRNA2 (pRC-sh2)	pJGD-RC-ΔshRNA–derived expressing *shRNA2* under the control of promoter U6	This study
pJGD-RC-shRNA3 (pRC-sh3)	pJGD-RC-ΔshRNA–derived expressing *shRNA3* under the control of promoter U6	This study
pJGD-RC-shRNA4 (pRC-sh4)	pJGD-RC-ΔshRNA–derived expressing *shRNA4* under the control of promoter U6	This study
pJGD-RC-shRNAscr (pRC-shscr)	pJGD-RC-ΔshRNA–derived expressing a scrambled RNA under the control of promoter U6	This study
pSTD	Plasmid used as the standard curve for qPCR, containing AAV2 *rep* and *cap genes, GFP* and partial human *ALB genes.*	This study

RC, *rep-cap*; WPRE, Woodchuck Hepatitis Virus Posttranscriptional Regulatory Element; cHS4, chicken hypersensitivity site 4 insulator; hPGK, human PGK promoter; GFP, green fluorescent protein; P2A, Self-cleaving 2A peptide from porcine teschovirus-1; BSD, blasticidin S deaminase protein; shRNA, short-hairpin RNA; ALB, human albumin gene; Between parentheses are the shorter versions of the used plasmids name.

3.2 General methods and techniques of molecular biology in bacteria

3.2.1 DNA synthesis, PCR amplification and cloning

The generation of recombinant plasmids was performed using gene synthesis services provided by GenScript (New Jersey, USA) and IDT (Integrated DNA Technologies, Iowa, USA) or through PCR DNA amplification using Phusion High-Fidelity DNA Polymerase (Thermo Fisher Scientific,

Massachusetts, USA), in a Biometra T3 thermocycler (Analytik Jena, Germany). The PCR conditions were defined based on primers annealing temperature, size of product amplification and the specifications of DNA polymerase. When needed, vectors and recombinant plasmids were cleaved with restriction enzymes (New England Biolabs, NEB®, Massachusetts, USA).

The PCR products and restriction fragments were resolved in 0.7% (w/v) agarose gel (NZYTech, Lisbon, Portugal), prepared in 1x Tris-Acetate-EDTA (TAE) buffer (Fisher Bioreagents, Massachusetts, USA) with 0.05 µL/mL RedSafe Nucleic Acid Staining Solution (INtRON Biotechnology, Hong Kong, China). The DNA was visualized in GelDoc XR+ system (BioRad, California, USA) and purified with NucleoSpin Gel and PCR Clean-up kit (Macherey-Nagel, Düren, Germany). DNA concentration and quality were determined by a Nanodrop 2000C Spectrophotometer (Thermo Fisher Scientific, Massachusetts, USA). Purity was measured through absorbance ratios at 260/280 nm and 260/230 nm.

The obtained DNA fragments were cloned using In-Fusion HD Cloning Kit (Takara Bio, California, USA) following manufacturer's instructions and cloned into *E. coli* NEB stable or Stellar. Stocks of transformed bacteria were prepared in 15% glycerol and stored at -80ºC.

Sections 3.4 and 3.5 describe the specific steps employed in the generation of the different recombinant plasmids used in this work.

3.2.2 Plasmid purification and quality control

Small scale plasmid recovery was performed using GeneJET Plasmid Miniprep Kit (Thermo Fisher Scientific, Massachusetts, USA), and resuspended in MiliQ water (HyClone HyPure Water – GE life sciences, Pennsylvania, USA). For mammalian cells transfection, high-pure grade DNA was purified using the large scale Genopure Plasmid Maxi Kit (Roche Applied Science, Penzberg, Germany) and resuspended in TE buffer (VWR, Pennsylvania, USA). Only plasmid DNA with a A260/A280 ratio of 1.8 ± 0.2 was considered acceptable and used. The sequence of resulting recombinant plasmids was screened by restriction enzymes digestion and DNA sequence analysis (Eurofins Genomics, Val Fleuri, Luxembourg).

3.3 shRNA design and ssDNA annealing

The design of four shRNA sequences targeting the AAV2 *rep* gene (shRNA1 – 4) and the non-target scrambled control (shRNAscr) was based on results delivered by three different bioinformatics tools, namely BLOCK-iT™ RNAi Designer (Thermo Fisher Scientific, Maryland, USA), GPP Web Portal [181] (Broad Institute; Massachusetts, USA) and GenScript siRNA Target Finder [182] (GenScript, New Jersey, USA). Complementary single-stranded oligonucleotides (ss oligo) were synthesized (IDT, Iowa, USA), containing i) at least 15 bp extensions that are complementary to the ends of *Sbf*I and *Mlu*I linearized plasmid pRC; ii) 21 nt of designed shRNA; iii) TCAAGAG hairpin and iv) U6 terminator TTTTT (**table 3.2**). To generate the double-stranded oligonucleotides (ds oligo), 30 µM of each ss oligo was mixed in 1X CutSmart® Buffer (New England Biolabs, Massachusetts, USA*),* in a final volume of 40 µL. The annealing reaction was conducted for 4 minutes at 95ºC followed by 25 minutes at 25ºC. The integrity of each ds oligo was verified in a 3% (w/v) agarose gel.

Table 3.2: Sequences of the synthesized DNA oligonucleotides coding for the *rep*-specific and scrambled shRNAs.

shRNA		Oligonucleotide sequence (5'- 3')
shRNA1	Oligo 1	aggacgaaaccctgcaggGTTAGCTTAAACCGCATAGTTTCAAGAGAACTATGCGGTTTAAGCTA ACttttt acgcgtcaattctcgac
	Oligo 2	gtcgagaattgacgcgtaaaaaGTTAGCTTAAACCGCATAGTTCTCTTGAAACTATGCGGTTTAA GCTAACcctgcagggtttcgtcct
shRNA2	Oligo 1	aggacgaaaccctgcaggAACTGGTTCGCGGTCACAAAGTCAAGAGCTTTGTGACCGCGAACCA GTTttttt acgcgtcaattctcgac
	Oligo 2	gtcgagaattgacgcgtaaaaaAACTGGTTCGCGGTCACAAAGCTCTTGACTTTGTGACCGCGA ACCAGTTcctgcagggtttcgtcct
shRNA3	Oligo 1	aggacgaaaccctgcaggGGACAATGCGGGAAAGATTATTCAAGAGATAATCTTTCCCGCATTG TCCttttt acgcgtcaattctcgac
	Oligo 2	gtcgagaattgacgcgtaaaaaGGACAATGCGGGAAAGATTATCTCTTGAATAATCTTTCCCGC ATTGTCCcctgcagggtttcgtcct
shRNA4	Oligo 1	aggacgaaaccctgcaggAATATGCGGCTTCCGTCTTTCTCAAGAGGAAAGACGGAAGCCGCAT ATTttttt acgcgtcaattctcgac
	Oligo 2	gtcgagaattgacgcgtaaaaaAATATGCGGCTTCCGTCTTTCCTCTTGAGAAAGACGGAAGCC GCATATTcctgcagggtttcgtcct
shRNA scr	Oligo 1	aggacgaaaccctgcaggGTTAGCTTAAACCGCATAGTTTCAAGAGAACTATGCGGTTTAAGCT AACttttt acgcgtcaattctcgac
	Oligo 2	gtcgagaattgacgcgtaaaaaGTTAGCTTAAACCGCATAGTTCTCTTGAAACTATGCGGTTTA AGCTAACcctgcagggtttcgtcct

Black, homology arms for In-Fusion cloning; blue, shRNA coding sequence.

3.4 Construction of *rep*-specific shRNA expressing constructs and plasmid controls

To obtain the plasmid backbone (pRC) used for shRNA sequences cloning, several steps were performed. First, the generation of a pUC19-derived recombinant plasmid (pSF-RC-loxPU6) through synthetic synthesis (Genscript, New Jersey, USA), which contains i) AAV2 *rep-cap* genes (Genbank NC_001401.2, nt 190 – 4469); ii) wt *loxP* sequences flanking human U6 promoter and *Sbf*I/*Mlu*I restriction sites (U6 as in pLKO.1, Sigma-Aldrich, Missouri, USA) and iii) a SV40 polyA. For cloning purposes, the *Bmr*I, *Bsr*DI and *Hpa*I sites were included downstream *loxP*-flanking sequences. Then, this vector was digested with *Bmr*I and *Bsr*DI to allow the insertion of a 764-bp fragment containing chicken β-globin HS4 core sequence (Addgene #44352 [180]) by In-Fusion cloning (Takara Bio, California, USA). The resulting plasmid was named pSF-RC-loxPU6-cHS4. Third, an oligonucleotide containing the region P2A (porcine teschovirus 2A [183]) and BSD gene [184] was purchased as a gBlock from IDT and inserted downstream of the GFP gene from the pRRLSIN.cPPT.PGK-GFP.WPRE plasmid (Addgene #12252, kindly provided by Dr. Didier Trono), generating an intermediate plasmid, pSF-GFP-P2A-BSD. Lastly, using pSF-GFP-P2A-BSD as template, a 2414-bp fragment, containing human PGK (hPGK) promoter and GFP-P2A-BSD fusion gene was PCR amplified with primers pF-hPGK (CTCGAATTACCGCGTTAGCTTGATATCGAATTCCCACG) and pR-WPRE (GGCGTCGTCAAAGGTTAACGTACCGAGCTCGAATTCCA) and inserted into *Hpa*I site of pSF-RC-

loxPU6-cHS4, by In-Fusion cloning. To construct the shRNA-coding plasmids (pRC-sh1-4 and pRC-shscr), 60 ng of ds oligo coding for each shRNA was used for cloning into pRC, double digested with *Sbf*I and *Mlu*I.

As a control, a plasmid without the AAV2 *rep* gene, named pΔRepC, was generated through the digestion of pRC with *Nru*I and *Swa*I to remove the *rep* gene. Afterwards, the plasmid was circularized using T4 DNA Ligase.

The resulting plasmids were then transformed into NEB stable cells and selected in the presence of Amp. Plasmid sequence was confirmed using restriction endonucleases and by sequencing using SUPREMERUN service (Eurofins Genomics, Val Fleuri, Luxembourg).

3.5 Construction of quantitative (q)PCR standard curve plasmid

For the construction of plasmid pSTD, an ALB-FH-GFP gBlock was synthesized (IDT, Iowa, USA), which contains the 16001-16640 portion of the *ALB* gene, and the complete sequence of the *GFP* gene. Plasmid pSTD-SFqPCR, used as a backbone was digested with *Eco*RV/*Nsi*I so that the gBlock could be cloned by In-Fusion (Takara Bio, California, USA). The resulting plasmid was transformed into Stellar competent cells and selected in the presence of Amp. Plasmid cloning was confirmed through the digestion of the construct with *Xba*I/*Mlu*I and by sequencing using LIGHTRUN tube (Eurofins Genomics, Val Fleuri, Luxembourg).

3.6 Cell lines and culture conditions

293 (ATCC, American Type Culture Collection, CRL-1573) is a human embryonic kidney cell line containing Adenovirus 5 E1a/b genes. This cell line was used for transient transfections and stable population establishment. Cells were grown in Dulbecco's modified Eagle's Medium (DMEM; Gibco™ – Thermo Fisher Scientific, Massachusetts, USA) supplemented with 10% (v/v) Fetal Bovine Serum (FBS; Gibco™ – Thermo Fisher Scientific, Massachusetts, USA), under adherent conditions using standard polystyrene treated cell culture flasks (Corning Life Sciences, New York, USA). For cell selection, the culture medium was supplemented with Blasticidin (InvivoGen, Toulouse, France). All cells were cultured at 37 ºC in a humidified atmosphere with 8% (v/v) CO_2.

3.7 Determination of cell concentration and viability

Cell concentration and viability were evaluated by the trypan blue exclusion method. Cells were diluted in 0.1% (v/v) trypan blue (Merck, Darmstadt, Germany) in Phosphate Buffer Saline (Gibco™ – Thermo Fisher Scientific, Massachusetts, USA) and counted manually using a Fuchs-Rosenthal hemocytometer (Marienfield-Superior, Lauda-Königshofen, Germany) on an inverted microscope (Olympus, Tokyo, Japan).

3.8 Transfection of 293 cells with PEI

3.8.1 Establishment of AAV packaging cell lines harbouring *rep*-specific shRNA

293 cells were seeded at $1x10^5$ cells/cm^2, to reach 70-80% confluency at time of transfection (24 hours post-seeding). For traceability and quality control purposes, transfection was performed using linear 25 kDa PEIpro® (Polyplus transfection, Illkirsch, France) in a 1:1 (w/w) DNA:PEI ratio. Both plasmids and PEI solutions were prepared in serum free DMEM. Next, the PEI solution was added to the plasmid mix and incubated for 15 minutes at room temperature. Lastly, the transfection mix was added to each cell sample. The culture medium was exchanged 4 to 6 hours later. Cells were analysed 48 hours post-transfection (48 hpt) by fluorescence microscopy and flow cytometry. Cell selection was performed by adding DMEM 10% (v/v) supplemented with blasticidin (InvivoGen, Toulouse, France). Cells in selection were observed every 48 hours and if necessary, passaged and/or re-splitted, into new medium with BSD. When cells reached approximately 80-90% confluence in a T75 and around 90% of them were GFP positive, master cell banks (MCB) were generated at $3x10^6$ cells/mL in CryoStor® (STEMCELL™ Technologies, Vancouver, Canada). Afterwards, gDNA, RNA and protein were extracted (as in sections 3.10.3, 3.10.1 and 3.13, respectively) from all populations (n=3). The established population names are as described in **Table 3.3**.

Table 3.3: Established stable populations based on 293 cells in this study and their main features.

Cell population	Features	Used to study
RepCap	293 based cell line harbouring pRC	Evaluate constitutive expression of *rep-cap*
∆Rep	293 based cell line harbouring p∆RepC	Control population without the *rep* gene
RC-shscr	293 based cell line harbouring pRC-shscr	Control population harbouring a scrambled shRNA.
RC-sh1	293 based cell line harbouring pRC-sh1	Evaluate *rep* knockdown mediated by shRNA1
RC-sh2	293 based cell line harbouring pRC-sh2	Evaluate *rep* knockdown mediated by shRNA2
RC-sh3	293 based cell line harbouring pRC-sh3	Evaluate *rep* knockdown mediated by shRNA3
RC-sh4	293 based cell line harbouring pRC-sh4	Evaluate *rep* knockdown mediated by shRNA4

3.8.2 Transient transfection of plasmids harbouring *rep*-specific shRNA

To increase cell survival after PEI-mediated cell transfection, a protocol optimization was performed. Several DNA concentrations of vectors pRC and a control expressing GFP fluorescent reporter (pGFP) were tested, namely 2, 3, 4 and 5 µg per 10^6 cells, using a 1:1.5 (w/w) DNA:PEI (Polysciences Inc., Hirschberg, Germany) ratio. The protocol was performed as explained in section 3.8.1. 48 hpt cell morphology and transfection efficiency were analysed by fluorescence microscopy and flow cytometry, respectively. gDNA, total RNA and protein were extracted from the best condition (as in sections 3.10.3, 3.10.1 and 3.13, respectively) (n=1).

3.9 Microscopy, flow cytometry data acquisition and analysis

Cells were analysed by fluorescence microscopy, using a Leica DMI6000 inverted microscope (Olympus). Flow cytometry was conducted in a BD FACS Celesta™ (BD Biosciences, California, USA) to quantify the percentage and fluorescence intensity of GFP-positive cells. Gates were set using untransfected 293 cells as negative control. Single cells were isolated from debris and doublets based on their SSC vs FSC characteristics. All analysed samples were diluted in DPBS (Gibco™ – Thermo Fisher Scientific, Massachusetts, USA) to reach a final concentration of 2% FBS. Data analysis was performed with FlowJo Software (BD Biosciences, California, USA).

3.10 Nucleic acid extraction from mammalian cells

3.10.1 RNA extraction

Total RNA was extracted from cell pellets using QIAamp® RNeasy Mini Kit (Qiagen, Hilden, Germany) according to manufacturer instructions and eluted in RNase-free water. Cell extracts obtained from transient transfections were treated twice with DNase to eliminate contaminant plasmid DNA. RNA yields were quantified using Nanodrop 2000C spectrophotometer (Thermo Fisher Scientific, Massachusetts, USA), and purity was accessed through the absorbance ratios at 260/280 nm and 260/230 nm. Only 260/280 nm absorbance ratios of 2.0 ± 0.2 of the RNA samples were considered to be pure. RNA was immediately used for complementary DNA (cDNA) synthesis or stored at -80 °C until further use.

3.10.2 cDNA synthesis

cDNA synthesis was performed using Transcriptor High Fidelity cDNA Synthesis Kit (Roche Applied Science, Penzberg, Germany), following manufacturer's instructions. 2 µg of total RNA and anchored-oligo(dT) primers for total mRNA reverse transcription were used. The cDNA products were either diluted in 80 µL of ultrapure water (Milli-Q®, Merck Millipore, Billerica, MA, USA) or left in the original reaction volume (20 µL) and then stored at -20°C until further use.

3.10.3 Genomic DNA extraction

Genomic DNA (gDNA) extraction was performed using DNeasy Blood & Tissue Kit (Qiagen, Hilden, Germany) following the manufacturer's instruction. Genomic DNA was eluted in 200 µL of AE buffer (provided in the kit) and stored at -20°C until further use.

3.11 Copy number determination of *rep*, *cap* and *GFP* by qPCR

3.11.1 Primers/probe set and thermal cycling

The primers and probes used in copy number determination are listed in **Table 3.4**. 5 µL of each sample (always tested in duplicate) was added to a 20 µL final volume qPCR reaction with LightCycler® 480 Probes Master Mix (Roche Life Science, Penzberg, Germany) and appropriate primers-probe sets at a final concentration of 0.5 µM and 0.25 µM, respectively. A no template DNA negative control (NTC) was included to monitor sample cross contamination. Thermal cycling was carried out in a LightCycler® 480 Real Time PCR System (Roche Applied Science, Penzberg, Germany), at 95°C for 10 minutes, followed by 45 cycles of 95°C for 10 seconds, annealing at 62°C for 30 seconds, and extension at 72°C for 1 second (single acquisition) and a cooling step at 40 °C during 10 seconds. For all analyses, technical replicates with standard deviation (SD) higher than 0.3 were not considered.

Table 3.4: Primers and probe sets for copy number determination by qPCR.

Name	Sequence 5´- 3	Reference
pF-GFP	GAACCGCATCGAGCTGAA	This study
pR-GFP	TGCTTGTCGGCCATGATATAG	
Probe-GFP (FAM[1])	TTGCCGTCCTCCTTGAAGTCGAT	
pF-Cap	CGACCCAAGAGACTCAACTTC	This study
pR-Cap	GAACCGTGCTGGTAAGGTTAT	
Probe-Cap (FAM)	AAAGAGGTCACGCAGAATGACGGT	
pF-Rep	GGCAGCCTTGATTTGGGA	Martin *et al.* (2013) [129]
pR-Rep	GACCAGGCCTCATACATCTCCTT	
Probe-Rep (FAM)	AATGCGGCCTCCAACTCGCG	
pF-ALB	GCTGTCATCTCTTGTGGGCTGT	Pasmant *et al.* (2007) [185]
pR-ALB	ACTCATGGGAGCTGCTGGTTC	
Probe-ALB (HEX[2])	CCTGTCATGCCCACACAAATCTCTCC	

[1]FAM, 6-carboxyfluorescein; [2]HEX, Hexachlorofluorescein

3.11.2 Experiment validation

Primer/probe validation of rep, cap and ALB was carried out in singleplex and multiplex qPCR using plasmid pSTD as the calibration curve using the dilution method. The C_T of pSTD 10-fold dilutions, ranging from 10^8-10^2 copies/µL were plotted against log $_{(DNA\ concentration)}$ and a linear regression was generated to determine slope and PCR efficiency (E), calculated as (1):

$$E(\%) = 10^{\left(-\frac{1}{slope}\right)-1} * 100 \quad (1)$$

Multiplex qPCR protocol was considered valid if singleplex and multiplex i) were within one C_T value for each dilution, and presented similar amplification efficiencies, between 95-100% and ii) the coefficient of determination (r^2) was greater than 0.98. qPCR for GFP was performed in a singleplex reaction and validated based on described amplification efficiency and r^2.

3.11.3 Gene copy number determination

150 ng of total cellular DNA extracted from stable populations (as in section 3.10.3) was analysed in multiplex qPCR. Integrated plasmid copy number per cell was calculated by normalizing to albumin (*ALB)* with an assumed number of 2 copies per 293 cell, using the following equation (2):

$$\text{Copies}/Cell = \frac{Copies/\mu L\ of\ rep,cap\ or\ eGFP}{Copies/\mu L\ of\ ALB} \times 2 \quad (2)$$

Cut-off values were established using non-transfected 293 cells and copies/cell values above 0.5 were rounded to 1 copy/cell.

3.12 *rep*, *cap* and GFP gene expression analysis by RT-qPCR

3.12.1 Primers/probe sets and thermal cycling

Primers and probes used in gene expression analysis are listed in **Tables 3.4** and **3.5**. The primers/probe set of reference genes (RG) *UBC* (Genbank NM_021009.7, ID 7316) and *TOP1* (Genbank NM_003286.4, ID 7150) were designed using PrimeQuest® Tool from IDT (https://www.idtdna.com/pages/tools/primerquest). qPCR programme used is as depicted in section 3.11.1. A NTC and a no reverse transcriptase (NRT) control were added. Samples were tested in duplicate and a C_T with SD higher than 0.3 were not considered in the analysis. Sample C_T values higher than 35 were not considered as gene amplification.

Table 3.5: Primers and probe sets of reference genes used in gene expression analysis.

Name	Sequence 5´- 3	Reference
pF-UBC	GATTTGGGTCGCAGTTCTTG	This study
pR-UBC	CCTTATCTTGGATCTTTGCCTTG	
Probe-UBC (HEX)	TCGATGGTGTCACTGGGCTCAAC	
pF-TOP1	CTGTAGCCCTGTACTTCATCG	This study
pR-TOP1	CTACCACATATTCCTGACCATCC	
Probe-TOP1	CCTTCCTCCTTTTCATTGCCTGCTCT	

UBC, polyubiquitin-C precursor; TOP1, DNA topoisomerase 1

3.12.2 Validation of comparative ($\Delta\Delta C_T$) method for relative expression

In an initial experiment the amplification efficiencies of target (*Rep*, *Cap* and *GFP*) and RG (*TOP1* and *UBC*) were calculated running standard curves containing each amplicon in the same sample, following the method described by Livak and Schmittgen (2001) [186]. For that, 293 cells were transfected with pRC, total RNA was extracted, and cDNA synthesized (see sections 3.10.1 and 3.10.2). The ΔC_T ($C_{T\ rep,\ cap\ or\ GFP}$ - $C_{T\ UBC\ or\ TOP1}$) was calculated for each serial 3-fold dilution, and plotted against $\log_{(cDNA\ concentration)}$ to create a semi-log regression line and respective slope. The experiment was considered valid if the absolute value of the slope of ΔC_T vs. log input was below 0.1.

3.12.3 Relative gene expression determination

5 µL of cDNA (diluted 1:5) from stable populations and transient transfections was analysed in singleplex qPCR for the detection of *rep*, *cap*, *GFP*, *TOP1* and *UBC*. mRNA transcripts were normalized to both *UBC* and *TOP1* mRNA levels within the same sample, and the results were calculated as fold change relative to control cells using the $\Delta\Delta C_T$ method [187].

3.13 Whole cell protein extraction and quantification

To assess protein expression of AVV2 Rep, whole cell protein extraction was performed from the 293 stable populations and transient transfections. Cells were harvested, counted, pelleted at 300 *g* for 10 minutes and washed with DPBS. Cell lyses was conducted using Mammalian Protein Extraction Reagent (M-PER) (Thermo Fisher Scientific™, Massachusetts, USA) with 1x cOmplete™ EDTA-free Protease Inhibitor Cocktail (Roche Applied Science, Penzberg, Germany), using 100 µl per 2 million of cells. The mixture was vortexed and placed at 4ºC for 10 minutes. Extracts clarification was done by centrifugation (14,000 *g* for 10 minutes). Samples were stored at -20ºC for short-term and -80ºC for long-term storage.

Total protein quantification was performed with BCA Protein Assay Kit (Thermo Fisher Scientific™, Massachusetts, USA) according to the manufacturer's instructions. Bovine serum albumin (BSA) (Thermo Fisher Scientific™, Massachusetts, USA) was used to establish the standard calibration curve. Samples were diluted and applied in duplicates.

3.14 Western blot

Protein levels of AAV Rep protein were evaluated by Western blot, using NuPAGE® electrophoresis system (Invitrogen-Thermo Scientific™) for protein electrophoresis separation. A normalized quantity of 30 µg of total protein per sample was prepared in denaturing conditions according to manufacturer's instructions. Reduced samples were separated in a 4–12 % (w/v) Bis-Tris NuPAGE® gel, with NuPAGE® MOP SDS Running Buffer, at 180 V for 60 minutes. SeeBlue® Plus2 Pre-Stained protein standard (Thermo Scientific™) was used as the molecular weight marker.

The protein solutions were transferred into iBlot™ 2 Transfer Stacks mini nitrocellulose membrane (Thermo Fisher Scientific, Massachusetts, USA), according to manufacturer's instructions, using an iBlot™ 2 Gel Transfer Device (Thermo Fisher Scientific, Massachusetts, USA). After transferring, membranes were blocked with a blocking solution 0.1% (w/v) Tween 20 (Sigma-Aldrich, Missouri, USA) and 5% (w/v) skim milk powder (Sigma-Aldrich, Missouri, USA) in Tris-Buffered Saline (TBS) (Sigma-Aldrich, Missouri, USA), for 1 hour at room temperature. Membranes were washed 3 times during 10 minutes with washing solution 0.1% (w/v) Tween 20 in TBS (TBST). An anti-AAV2 replicase mouse monoclonal antibody, 303.9 (American Research Products - ARP, Massachusetts, USA) and a mouse monoclonal anti-α-tubulin (Sigma-Aldrich, #T1199) antibody were diluted in 1:500 and 1:2000, respectively, using blocking solution and incubated overnight with gentle agitation, at room temperature. Membranes were washed 3 times during 10 minutes with TBST and incubated with a

horseradish peroxidase-linked ECL Anti-Mouse IgG (NA931) (GE Healthcare, Chicago, United States) secondary antibody, which was diluted 1:1000 in blocking solution, for 2 hours at room temperature. Chemiluminescence detection was performed by incubating the membranes with Amersham™ ECL™ prime western blotting detection reagent (GE Healthcare, Chicago, United States), according to manufacturer's instructions and analysed using ChemiDoc XRS System (BioRad, California, USA).

3.15 Western blot by Jess

AAV Rep protein levels were also evaluated by Western blot using JESS (Protein Simple, California, USA). First, protein extracts were diluted to have a concentration lower than 3 µg/µL. Then, they were prepared and run according to manufacturer's instructions. For Rep detection, an anti-AAV2 replicase mouse monoclonal antibody, 303.9 (American Research Products - ARP, Massachusetts, USA) was used in a 1:5 dilution.

3.16 Adenovirus production and purification

A non-pathogenic, non-replicative human AdV5 (*E1*/*E3* deleted), expressing a codon optimized Cre (iCre) under the dependence of a CMV promoter (Ad-CMV-iCre, SignaGen Laboratories, Rockville, USA) was amplified in 293 cells. This virus was used in subsequent assays, named in this work AdV-Cre.

293 cells were seeded at $1.1x10^5$ cells/cm^2, in order to reach 70-80% confluency at time of infection (24 hours post-seeding). Cells were infected in a MOI of 5 using human AdV5 expressing Cre recombinase (Ad-CMV-iCre, SignaGen Laboratories, Rockville, USA). 44 hours post-infection, 293 cells from nine 75 cm^2 tissue culture flasks were recovered and centrifuged in a Hettich ROTINA 420R centrifuge at 3000 g for 10 min at 4ºC. The supernatant was collected and filtered through a 0.45 µm filter and stored at -80ºC in 1 mL aliquots. The cell pellet was resuspended in lysis buffer (0.1% Triton X-100 10 mM Tris Buffer pH 8.0), vortexed for 5 – 15 sec and centrifuged in a Hettich ROTINA 420R centrifuge at 3000 g for 10 min at 4ºC. The resulting supernatant containing the produced AdV vector (AdV-Cre) was purified by a caesium chloride (CsCl) density gradient through ultracentrifugation. The supernatant was layered onto a gradient of CsCl 1.25 g/mL and CsCl 1.45 g/mL, afterwards, mineral oil was added on top to avoid aerosol formation. The tubes were centrifuged at 35,000 rpm for 90 min at 18ºC in a Beckman Optima LE-80K using a Beckman SW40Ti swinging bucket rotor. The lower virus band from each tube was collected using a needle and syringe. Subsequentially, a continuous gradient with CsCl 1.34 g/mL was performed. The tubes were centrifuged for 19 hours at 35,000 rpm at 18°C in a Beckman SW40Ti swinging bucket rotor. The virus band from each tube was aspirated and sent for desalting, using an AKTA system with a Hiprep 26/10 desalting column (Merck, Darmstadt, Germany), where the CsCl solution was exchanged by 10 mM Tris pH 8.0, 2 mM MgCl2 buffer. This solution was diluted by adding an equal amount of 1M Trehalose, 4 mM, MgCl2, 10 mM Tris Buffer pH 8 in order to achieve a final storage buffer of 10 mM Tris pH 8.0, 2 mM MgCl2 and 0.5 M Trehalose. Viral aliquotes of 250 µL were performed and stored at -80ºC.

3.17 AdV-Cre viral titering - $TCID_{50}$ assay

Adenoviral infectious titer was determined by TCID50, an end-point dilution method. In this assay serial dilutions of viral stock are plated in 293 cells growing in the wells of a 96-well plate to determine the dilution at which 50% of the wells are infected

293 cells at $1.1x10^5$ cells/cm^2 were seeded in a 96-well plate, in culture media until reached a confluency of 80%. Then, 10-fold viral dilutions, ranging from 10^{-1} – 10^{-15} were prepared in dilution medium (DMEM, low glucose, pyruvate, no glutamine, no phenol red supplemented with 4 mM L-Glutamine (Gibco™, Thermo Fisher Scientific, Massachusetts, USA). 50 µL of each viral dilution was added, in triplicate to 8 wells containing the 293 cell monolayer and incubated at 37ºC with 5% CO2. After 1 hour of infection, 150 µL of dilution medium supplemented with 5% FBS (Gibco™, Thermo Fisher Scientific, Massachusetts, USA) was added and incubated continued at 37ºC, 5% CO^2. Plates were examined after 7- and 9-days post-infection. Infectious titer was determined using KARBER statistical method, which from 50 µL of dilution, the titer is given by $T=10^{1+d(S-0.5)}$, where d= log 10 of the dilutions and S= sum of the rations of positive wells per row.

3.18 Infection of 293 cells with AdV-Cre and AdV-Control

To activate the expression of *rep-cap*, AAV packaging 293 stable cell populations were infected with AdV-Cre. As an infection control, the populations were also infected with another helper virus without Cre, a E1-deleted AdV serotype 5 (provided by Dr. Genevievè Libeau, CIRAD-EMVT, Montpellier, France), named AdV-Control in this work. Cells were seeded at $1.1x10^5$ cells/cm^2 in 6-well plates and infected with an MOI of 5, 24 hours post-seeding (confluency of 70-80%). 42 hours post-infection, cells were collected and total RNA and gDNA was extracted as described in sections 3.10.1 and 3.10.3, respectively.

4 Results

4.1 Design and construction of *rep*-specific shRNAs

This experimental work focuses on the post-transcriptional control of Rep expression based on shRNA-mediated knockdown. To our knowledge, there are no known sequences of shRNA for gene knockdown of AAV *rep*. The four *rep*-specific shRNAs (shRNA 1- 4) used in this work were empirically selected from a list of results obtained with three different software programs (Invitrogen, GPP Web portal and Genscript). The spliced full-length *rep78* mRNA was used as the template sequence. The selected shRNAs 1 and 2 are specific for *rep78*/68 mRNA and shRNAs 3 and 4 also target *rep52*/*40* mRNA (**Figure 4.1A**). A scrambled shRNA (shRNAscr), with no known targets in human cells or viral transcripts was also generated and served as a negative control. A homology search of all five used shRNAs was performed using BLAST tools to avoid off-target effects. The designed shRNAs were synthesized in the form of two complementary ss oligos and then annealed. The integrity of the resulting ds oligos was confirmed by agarose gel electrophoresis (**Figure 4.1B**).

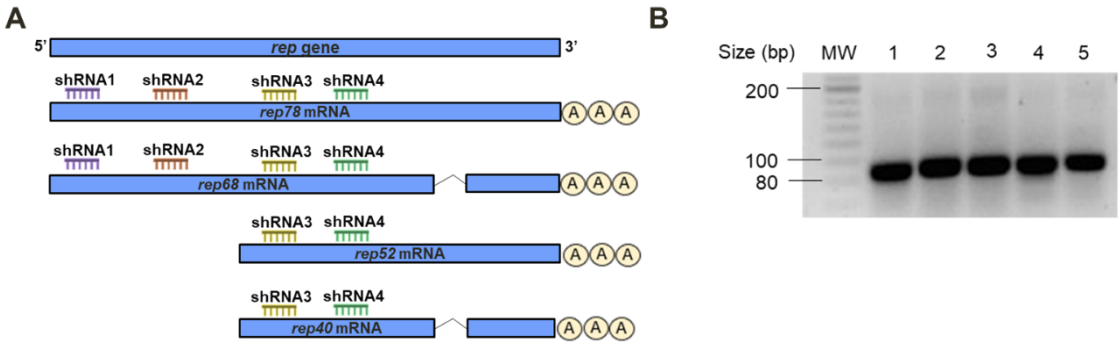

Figure 4.1: *rep*-specific shRNA binding sites and annealing. (A) Schematic representation of shRNA targeting locations on each *rep* mRNA (created with BioRender). shRNA1 and shRNA2 bind to *rep78*/68 mRNA in position nt 119-140 and nt 388-409, respectively. shRNA3 and shRNA4 have affinity for all *rep* transcripts through binding to a common sequence. shRNA3 binds to *rep*78/68 in position 801-822 nt and to *rep*52/*40* in position 129-150 nt, whereas shRNA4 binds to position nt 929-950 nt in the *rep*78/68 transcripts and position 257-278 nt in the *rep*52/40 transcript; **(B)** The integrity of each annealed ds oligos was confirmed by electrophoresis in a 3% agarose gel, which revealed the presence of bands in the expected size region (89 bp). Lanes 1 - 5 correspond to the dsDNA sequence coding for shRNA1, 2, 3, 4 and scr, respectively. The MW lane correspond to NZYDNA Ladder IV (NZYtech, Lisboa, Portugal), with molecular weights in base pairs (bp).

4.2 Development of AAV2 *rep*-specific shRNA packaging plasmids

The AAV2 *rep*-specific shRNA packaging plasmids were constructed starting from the same backbone, pRC (**Figure 4.2A**), which contains the AAV2 *rep* and *cap* genes under the control of their native promoters (p5, p19 and p40) and a transcription fusion GFP-P2A-BSD, under the dependence of a hPGK promoter. Co-expression of the *GFP* reporter gene and the BSD S-resistance gene facilitates the monitoring of cell transfection efficiency and cell selection, respectively. The five generated ds oligos were cloned into the plasmid backbone pRC under the dependence of a U6 promoter and flanked by loxP sites (**Figure 4.2A** – pRCsh1-4 and pRC-shscr), to allow the recognition and excision by Cre recombinase. As a control, a plasmid without the *rep* gene nor shRNA was also generated (**Figure 4.2A**

- pΔRepC). The successful cloning of the resulting constructions was confirmed by restriction pattern analysis (Figure **4.2B** and **C**) and DNA sequencing (data not shown).

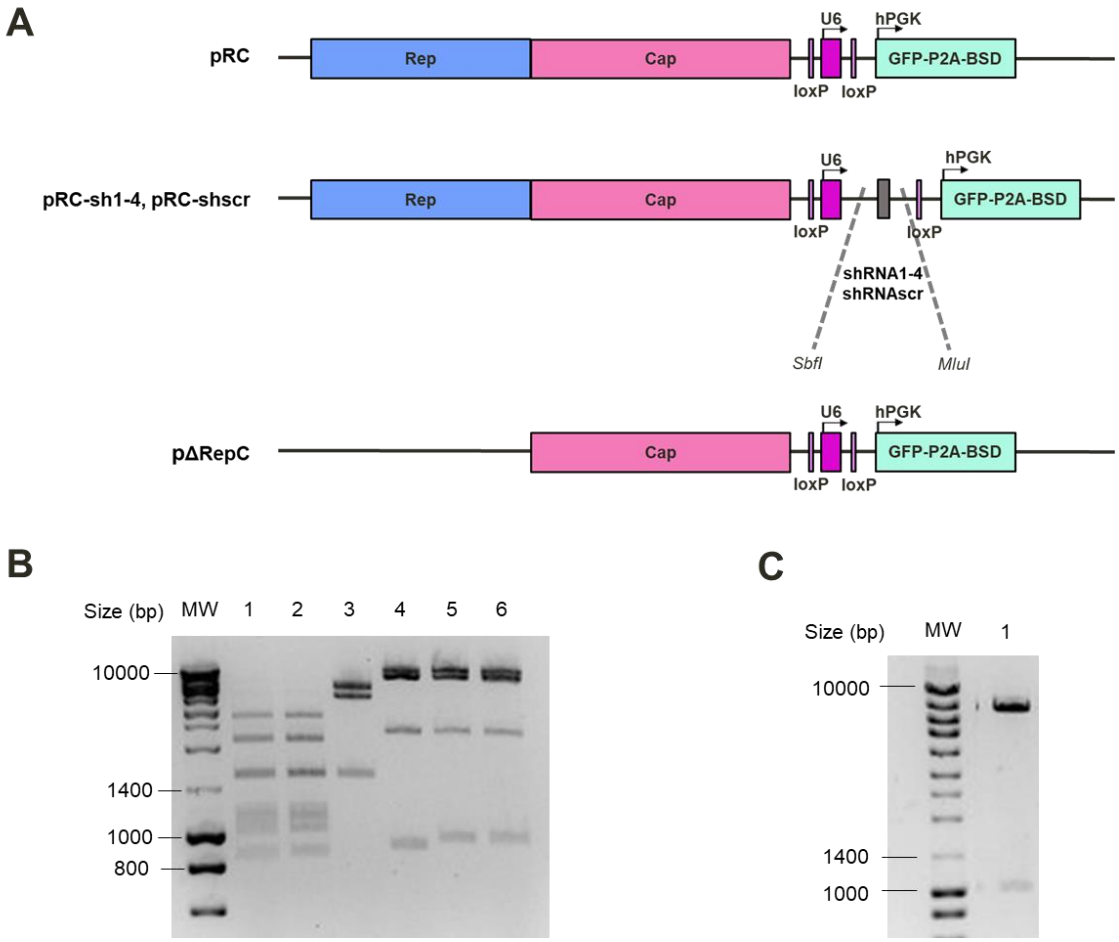

Figure 4.2: Construction of the *rep*-specific shRNA packaging plasmids. (A) Schematic representation of the plasmids constructed for this work. pRC is the plasmid control expressing AAV2 *rep* and *cap* genes and the vector backbone, from which the other plasmids were constructed. pRC-sh1-4 and pRC-shscr were generated through the digestion of the plasmid backbone with *Sbf*I and *Mlu*I and posterior cloning of the shRNA-coding sequence. pΔRepC is a control plasmid that does not contain the *rep* gene; **(B)** Confirmation of plasmid sequence; Lanes 1 and 2 show the *BpU*EI restriction pattern of plasmids pRC-sh1 and pRC-sh4, respectively, with expected bands of 2690, 2080 and 1529 bp. Lane 3 contains plasmid pRC-sh2 digested with *Xmn*I with expected bands of 4768, 3801 and 1519 bp. Lanes 4, 5 and 6 consist of plasmids pRC, pRC-sh3 and pRC-shscr, digested with *Mlu*I and *Nru*I, respectively, with expected bands of 6886, 2261 and 941/899 bp; **(C)** Confirmation of plasmid sequence; Lane 1 shows the restriction pattern of plasmid pΔRepC through the digestion with *SalI* and *MscI* with expected bands of 7503 and 1008 bp. The MW lane correspond to NZYDNA Ladder IV (NZYtech, Lisboa, Portugal), with molecular weights in bp.

4.3 Establishment of stable AAV2 *rep*-specific shRNA packaging populations

The AAV packaging populations based on 293 cells were established through the transfection with plasmids pRC, pΔRepC, pRC-sh1-4 and pRC-scr (RepCap, ΔRep, RC-sh1–4, RC-shscr, respectively; **Table 3.3**) using 5 µg DNA/10^6 cells and PEIpro in a 1:1 (w/w) DNA:PEI ratio. As evident from **Figure 4.3A**, 48 hpt all transfected cells presented a remarkable impact in cell survival and morphology. As this was also observed in ΔRep population, unable to express the *rep* gene, it might

indicate a phenomenon of PEIpro-induced cytoxicity. GFP expression was confirmed by fluorescence microscopy (data not shown) and flow cytometry (FC). The latter revealed different transfection efficiencies, ranging from 8% to 27% (**Figure 4.3B**). Interestingly, the highest percentage was achieved in cells harbouring the control plasmid without the *rep* gene (ΔRep) and the lowest was observed in cells transfected with the scrambled shRNA control (RC-shscr).

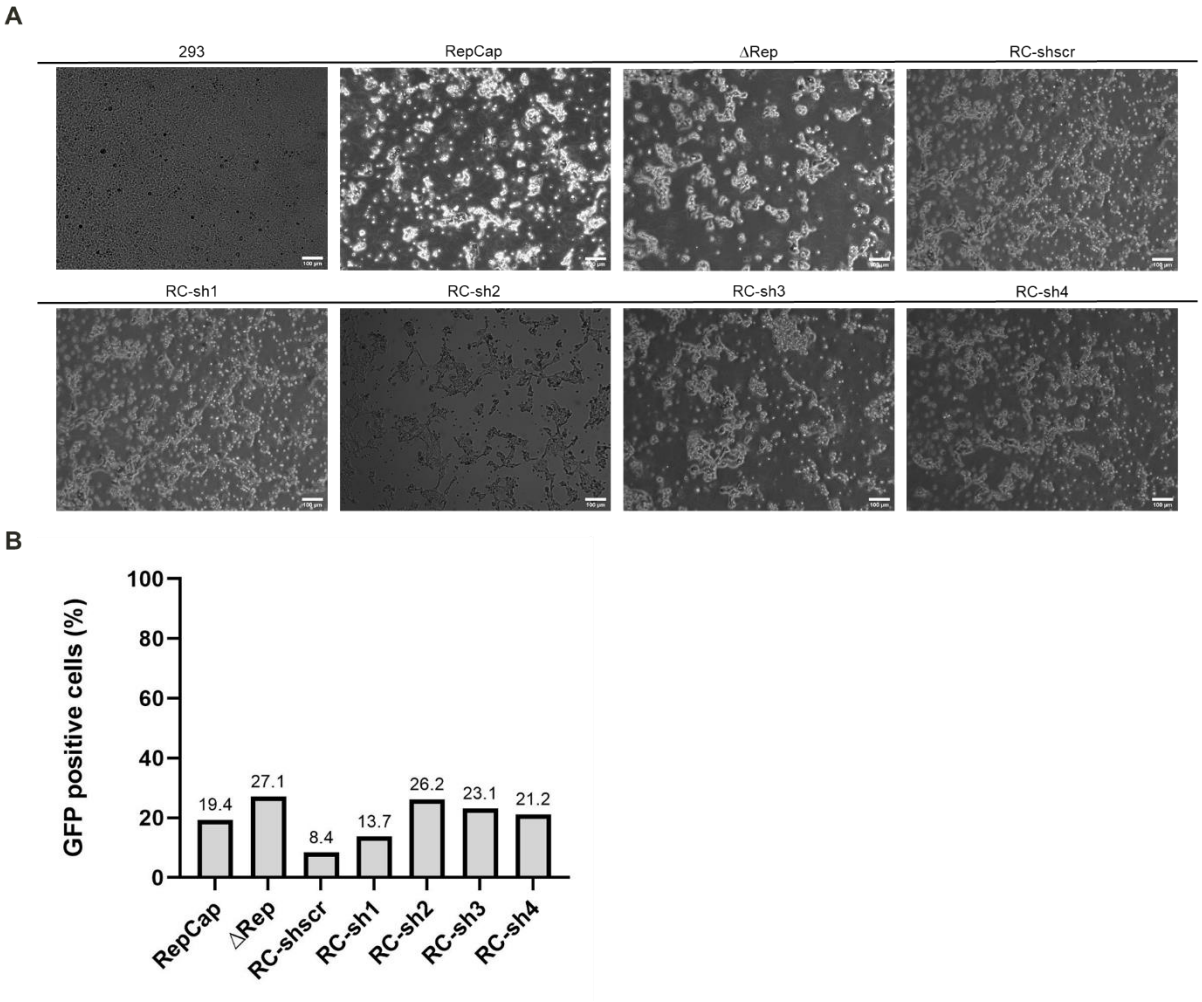

Figure 4.3: Evaluation of cell confluency and transfection efficiency for the establishment of AAV2 *rep*-specific shRNA packaging populations. 293 cells were transfected with different plasmids at **5** µg/10^6 cells at a DNA:PEIpro ratio of 1:1 (w/w) and collected 48 hpt for analysis by **(A)** phase contrast microscopy and **(B)** flow cytometry (n=1). The scale bar corresponds to 100 µm.

After transfection, the cells were grown in the presence of blasticidin for cell selection and monitored by FC. The selection proceeded for a period of almost nine weeks, until populations presented more than 90% of GFP positive cells. Due to some unforeseen events, after four weeks of cell selection, a master cell bank had to be performed for all populations, which may have compromised cell viability and the selection process. Compared to other stable populations, RepCap took the longest time to recover and achieve confluences of approximately 80%. All the populations expressing shRNAs, including the scrambled control, were selected almost at the same pace, alongside ΔRep. After selection, all populations presented the same growth and proliferation profile as parental 293 cells, determined by cell confluency observation.

4.4 Optimization of transfection conditions

To increase cell survival while maintaining or increasing transfection efficiency, transfections using different DNA concentrations were performed. 293 cells were transfected with 2, 3, 4 and 5 µg pRC/10^6 cells using in-house PEI at a DNA:PEI ratio of 1:1.5 (w/w). In parallel, the same conditions were mimicked using a control plasmid, expressing GFP (pGFP). **Figure 4.4A** shows that an increased concentration of DNA:PEI complexes inhibits cells growth, with both plasmids. However, in general, the transfection with pRC resulted in decreased cell confluency for all tested conditions, when compared to pGFP. For the same amount of DNA (5 µg DNA/10^6 cells) transfection of plasmid pRC complexed with PEIpro (**Figure 4.3A** - RepCap) was more toxic to cells than with in-house PEI (**Figure 4.4A** – pRC, 5 µg). In cells transfected with pGFP, the percentage of GFP positive cells increases as the concentration of DNA increases as well. For pRC, the transfection efficiency peaks when using 3 µg DNA/10^6 cells (**Figure 4.4B**).

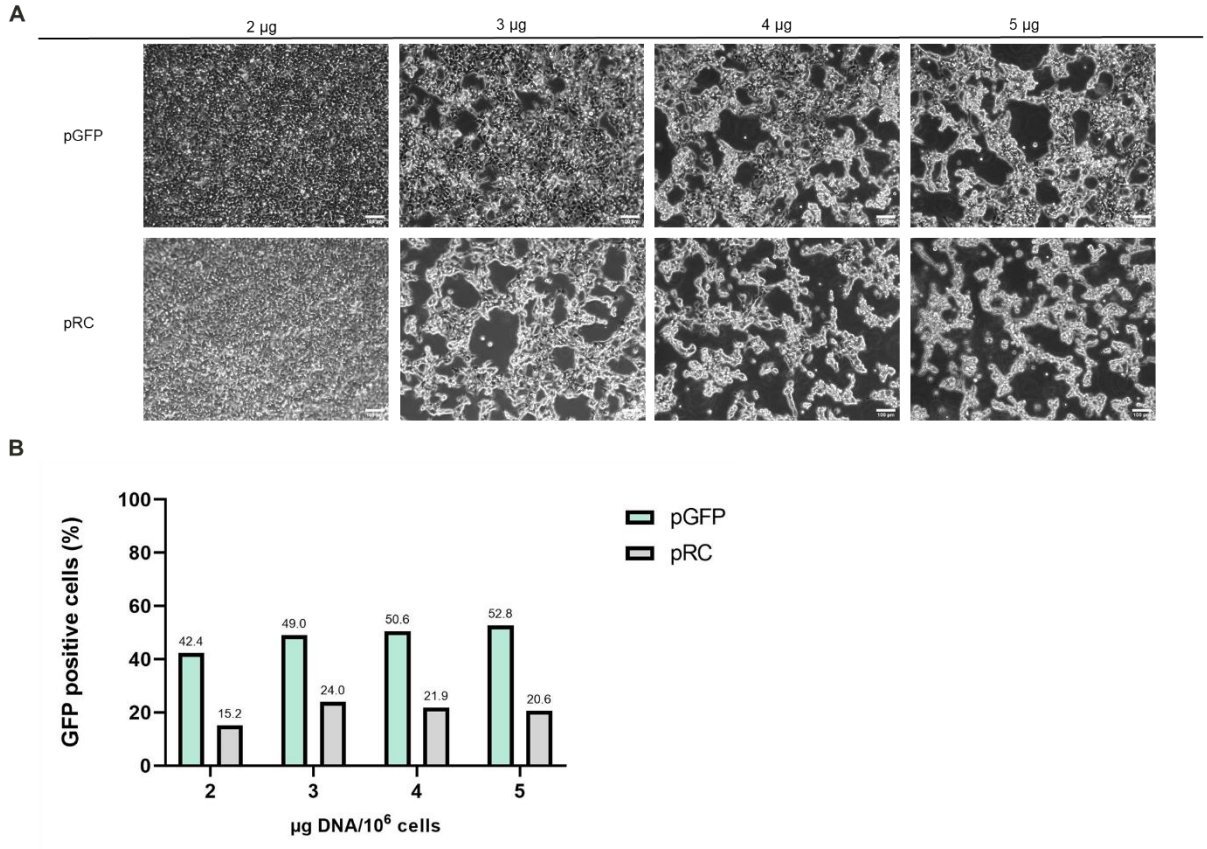

Figure 4.4: Effect of transfection conditions on 293 cell growth and transfection efficiency. 293 cells were transfected with pGFP or pRC at 2, 3, 4 and 5 µg DNA/10^6 cells with 1.5 x in-house PEI and collected 48 hpt for analysis by **(A)** phase contrast microscopy and **(B)** flow cytometry (n=1). The scale bar corresponds to 100 µm.

To study the knockdown of different *rep*-specific shRNAs in transiently transfected 293 cells, the best condition identified was applied (3 µg DNA/10^6 cells) using in-house PEI in a DNA:PEI ratio of 1:1.5 (w/w) (**Figure 4.4**). Transfection efficiencies remained below 30% (**Figure 4.5B**). Regarding phase contrast microscopy (**Figure 4.5A**), cell death is still predominant in almost every transfection, except for cells transfected with pRC-sh4 and scr, which also have the lowest transfection efficiency (**Figure**

4.5B). Again, when comparing phase contrast microscopy images of cells transfected in this assay (**Figure 4.5A**) with the images of the establishment of stable populations (**Figure 4.3A**), cells have an overall better morphology in the first one, which means that DNA ratio alongside the used PEI type in the population establishment might be causing increased cytotoxicity.

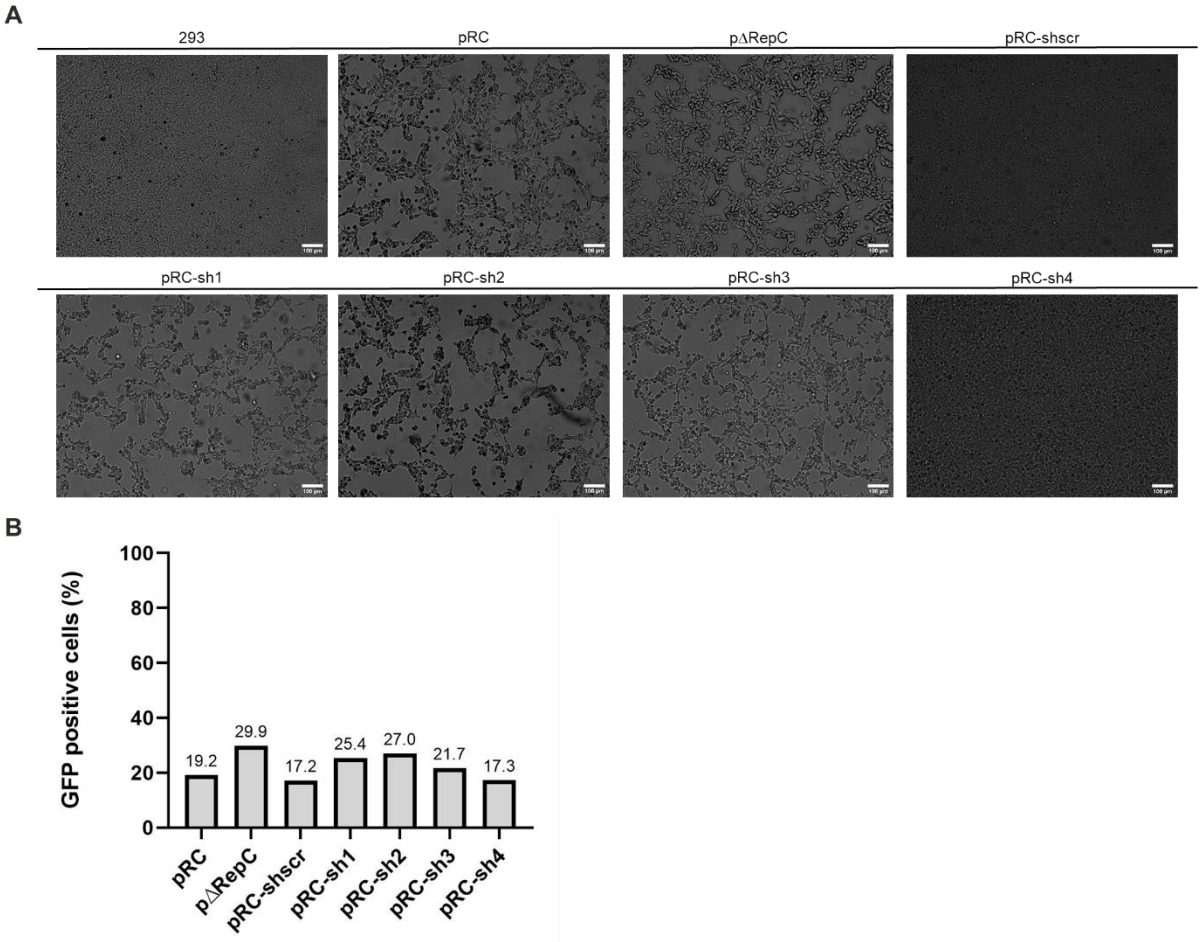

Figure 4.5: Evaluation of cell confluency and transfection efficiency in cells transiently transfected with the AAV2 *rep*-specific shRNA packaging plasmids. 293 cells were transfected with different plasmids at **3** µg/10^6 cells at DNA:PEI ratio of 1:1.5 (w/w) and collected 48 hpt for analysis by **(A)** phase contrast microscopy and **(B)** flow cytometry (n=1). The scale bar corresponds to 100 µm.

4.5 Gene expression analysis

First, a method validation was carried out to assess whether the target and reference gene PCR amplification efficiencies were approximately equal, as described in Livak and Schmittgen *(*2001*)* [187]. Graphics in **Figure 4.6** show the results of this experiment validation where a log of cDNA diluted over a 3-fold range was plotted against the ΔC_T (C_T target gene – C_T RG). As the absolute slopes were below 0.1, the assumption where target and RG amplification efficiencies are similar can be taken and the $\Delta\Delta C_T$ method was considered valid to be used.

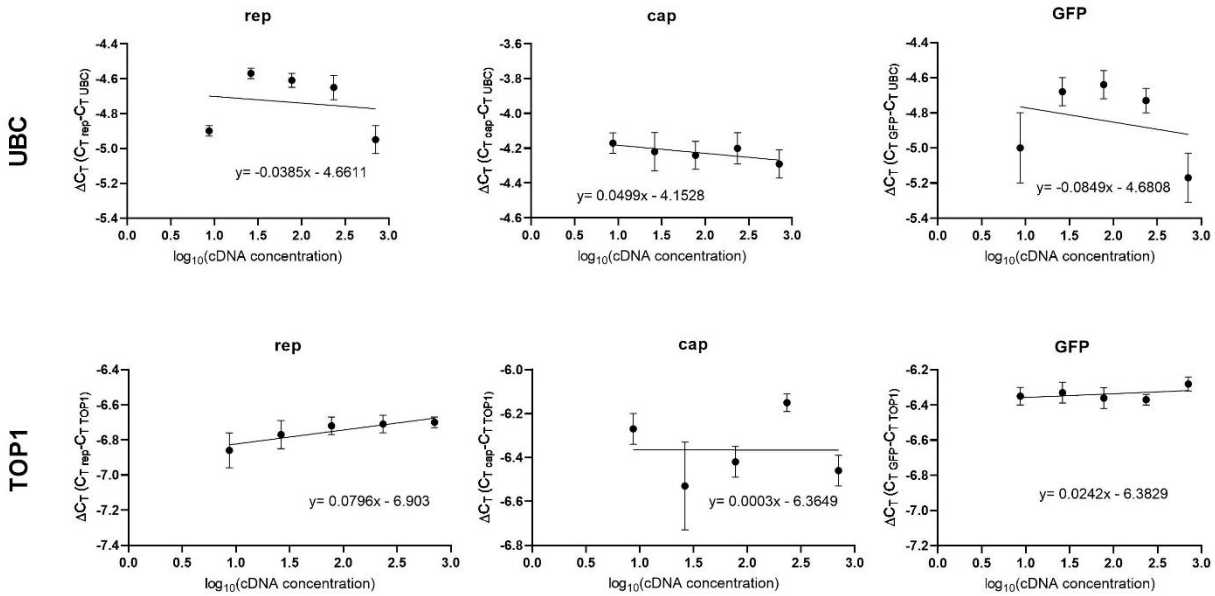

Figure 4.6: Validation of the ΔΔC$_T$ method. The amplification efficiency of the target genes (*rep*, *cap* and *GFP*) and reference genes (*TOP1* and *UBC*) was examined by RT-qPCR using specific primer/probe sets (**Tables 3.4** and **3.5**). cDNA was synthesized from 2 µg of total RNA extracted from 293 cells transfected with pRC then serially diluted 3-fold. The ΔC$_T$ (C$_{T\ rep,\ cap\ or\ GFP}$ – C$_{T\ UBC\ or\ TOP1}$) was calculated for each dilution. The data was plotted using linear regression analysis (n=2).

Expression of AAV genes as well as *GFP* was analysed 48 hpt and in the established stable populations by RT-qPCR, in the absence of helper factors. As depicted in **Figure 4.7A**, *rep*, *cap* and *GFP* were expressed 48 hpt and as expected, at higher levels in transient than in stable populations (**Figure 4.7C**). No *rep* gene silencing potential was observed with the four designed shRNAs in transiently transfected cells (pRC-sh1 – 4) since their *rep* levels were similar to pRC transfection (Figure **4.7A** and **B**).

In stable, *rep* mRNA levels in populations RC-sh1 and RC-sh3 were slightly higher (below 2-fold) compared to RepCap population, which might serve as an indicator of shRNA1 and 3's inefficiency in silencing *rep* (**Figure 4.7D**). The *rep* C$_T$ in RC-sh2 and RC-sh4 populations was below level of detection, what could indicate a *rep* repression phenomenon (or absence of the *rep* gene), probably not related with shRNA, as this was also observed for RC-shscr control population (**Fig. 4.7C**).

It is well known that c*ap* gene expression is regulated by Rep proteins [188], [189]. Consistent with this, in transient transfection, *cap* mRNA levels were in average 5-fold higher than *rep* levels, in most populations (**Figure 4.7A**). In the absence of *rep* (pΔRepC), the levels of *cap* mRNA were the lowest (**Figure 4.7A**), being 6-fold inferior when compared to pRC (**Figure 4.7B**). Stable packaging populations showed a decreased level of *cap*, which seems not to be related with *rep* levels (**Figure 4.7C**).

GFP amplification was detected in all tested populations, in higher levels in transient cells than in stable populations (**Figures 4.7A** and **C**, respectively). In transient transfection, the highest amount of GFP transcription was observed in cells transfected with pΔRepC and the lowest in cells transfected with pRC-sh2 and scrambled control (**Figure 4.7A**). In stable, the *GFP* mRNA is the most abundant transcript (compared to *rep-cap*) and similarly expressed in all established populations, except for pRC-sh2 whose expression is reduced only slightly (less than 2-fold) compared to RepCap (**Figure 4.7C**).

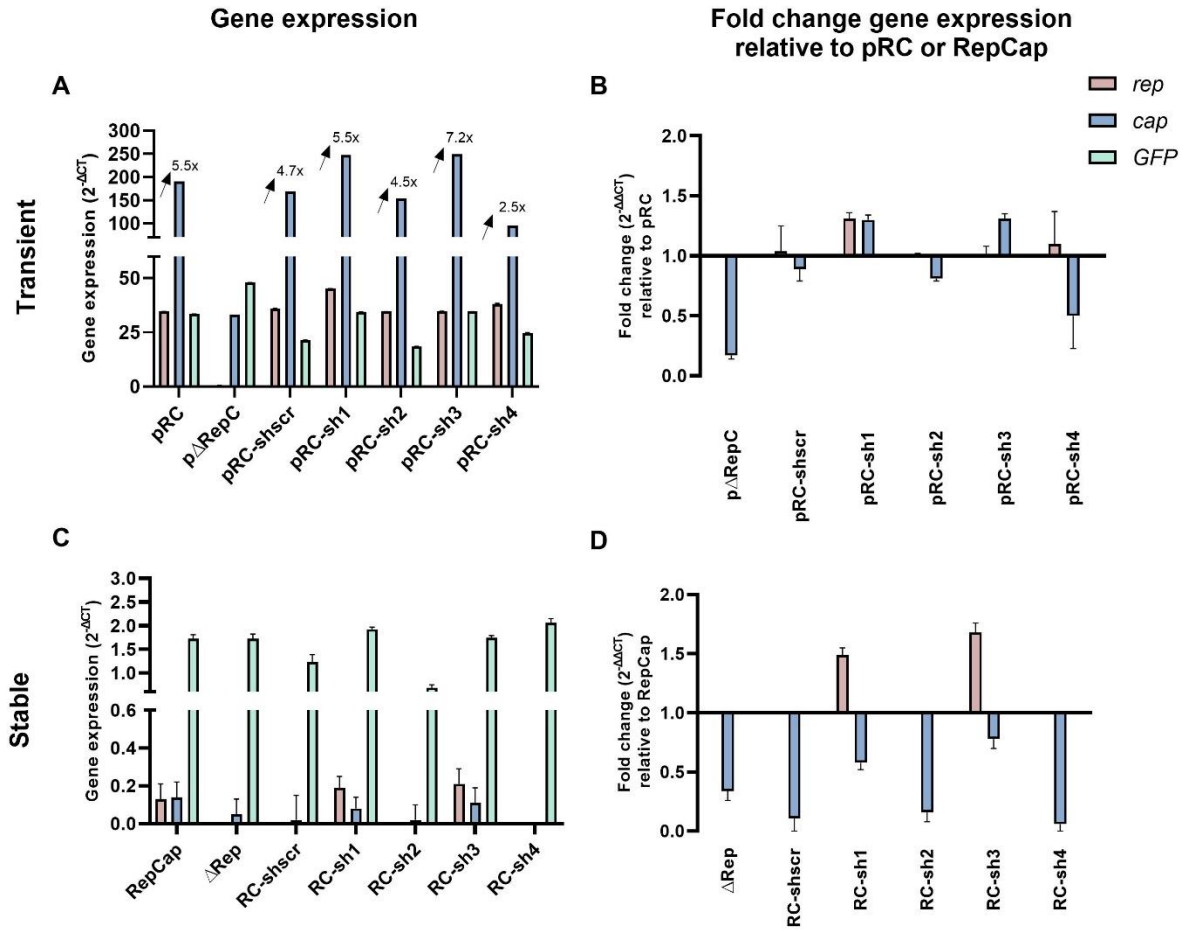

Figure 4.7: Relative gene expression analysis of *rep*, *cap* and *GFP* in transiently transfected cells, 48 hpt (A and B) and stable populations (C and D). cDNA was synthesized from 2 µg of total RNA extracted. Gene expression was assessed by RT-qPCR normalized against TOP1 and UBC reference genes within the same sample and are shown as gene expression ($2^{-\Delta CT}$) **(A and C)** or fold change relative to the respective levels in control cells harbouring the pRC plasmid ($2^{-\Delta\Delta CT}$) **(B and D)**. **(A)** Arrows indicate the **cap* expression ratio vs *rep* expression in the same sample. Data is shown by mean ± standard deviation (A and B n= 1; C and D n= 3).

4.6 Integrated plasmid copy number

The integrated plasmid copy number was calculated by qPCR, targeting *rep*, *cap* and *GFP* in the established stable populations. Firstly, to increase method throughput, a dual-colour detection protocol was implemented, in which rep, cap and GFP probes were labelled with FAM while the ALB probe was conjugated with HEX. Primer/probe validation of rep, cap and ALB was carried out in singleplex and multiplex qPCR. **Figure 4.8** shows similar amplification efficiencies (between 95-100%) amid singleplex and multiplex qPCR in all sets used, therefore, dual-colour qPCR can be carried out. The detection of GFP was performed in singleplex with an efficiency of 98.5%.

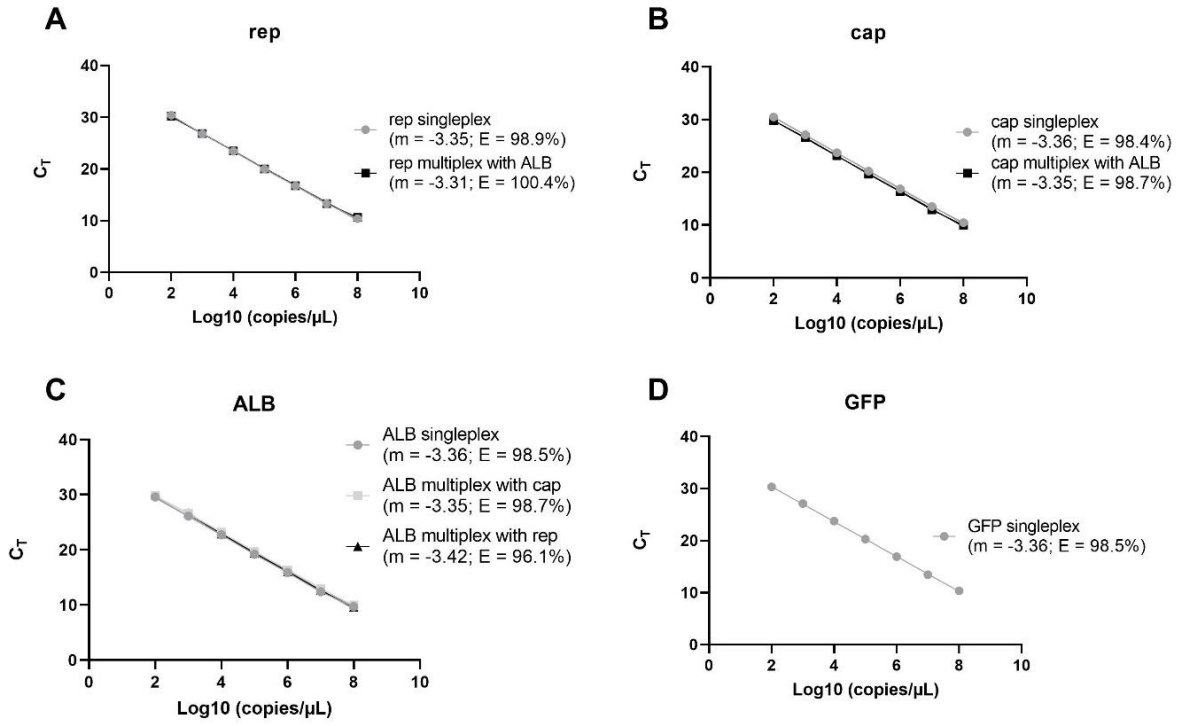

Figure 4.8: Primers/probe validation for rep, cap and ALB for multiplex qPCR and GFP for singleplex qPCR. (A, B, C) Amplification efficiency for rep, cap and ALB in singleplex and multiplex qPCR; **(D)** GFP singleplex qPCR amplification efficiency. The calibration curves were established with pSTD dilutions ranging from 10^8 to 10^2 copies/µL (C_T- crossing threshold).

As shown in **Table 4.1**, the integrated plasmid copy number varied between 0 and 1 in all cell populations, for all tested genes. Furthermore, the populations which do not express *rep* (RC-sh2, 4 and scr – **Figure 4.7C**) do not have any *rep* integrated copies. The inconsistency in amplified copy number (**Table 3.1**) and mRNA levels (**Figure 4.7C**) in populations RC-sh1 detecting 0 *rep* copies and a gene expression of 0.19, and populations RC-shscr, 2, 3 and 4 detecting 0 copies of *GFP* but having a gene expression of 1.23, 0.69, 1.74 and 2.06, respectively, is likely attributed to the heterogeneity of stable populations, since most of the cells may have 0 – 1 copies, limitations of qPCR protocol and/or poor cellular DNA extraction.

Table 4.1: Analysis of integrated plasmid copy number. qPCR analysis of *rep*, *cap* and *GFP* plasmid sequences was carried out using primers/probe specific sets (Table 3.4). Copy number calculation was performed through the normalization to ALB gene copies, with an assumed number of 2. The data is shown by mean ± standard deviation (n=3).

	Copy number		
Cell population	***rep***	***cap***	***GFP***
293	0.00 ± 0.01	0.00 ± 0.01	0.00 ± 0.00
RepCap	1.00 ± 0.12	1.00 ± 0.30	1.00 ± 0.32
ΔRep	0.00 ± 0.02	0.00 ± 0.10	1.00 ± 0.19
RC-shscr	0.00 ± 0.00	0.00 ± 0.02	0.00 ± 0.11
RC-sh1	0.00 ± 0.26	1.00 ± 0.30	1.00 ± 0.30
RC-sh2	0.00 ± 0.00	1.00 ± 0.19	0.00± 0.26
RC-sh3	1.00 ± 0.10	1.00 ± 0.07	0.00 ± 0.12
RC-sh4	0.00 ± 0.04	0.00 ± 0.09	0.00 ± 0.29

4.7 Rep protein detection

AAV2 Rep protein expression was assessed in the established stable populations. As shown in **Figure 4.9A**, no Rep protein was detected in samples by this technique. Since no Rep protein was visualized by traditional western blot methodology, preliminary testing was carried out in another western blot equipment named Jess. Samples with different whole protein concentrations as well as several target protein amounts were analysed. The first sample to be tested (**Figure 4.9B** – p1) consisted in cells transiently transfected with plasmid pRC, which had higher *rep* expression (assessed by RT-qPCR) although lower whole protein concentration. The second sample (**Figure 4.9B** – p2) is a concentrated protein extract from stable population RC-sh3, with low Rep protein expression. Results show the detection of two protein bands around 50 kDa in both samples. The band with higher size can be assumed to be Rep52 and the one bellow, Rep40 or non-specific detection. However, Rep78 was not detected in neither of the samples. More testing in this equipment and with other anti-Rep antibodies must be carried to allow the specific detection of all Rep proteins. The addition of a positive control sample which expresses Rep78 is of great interest as well.

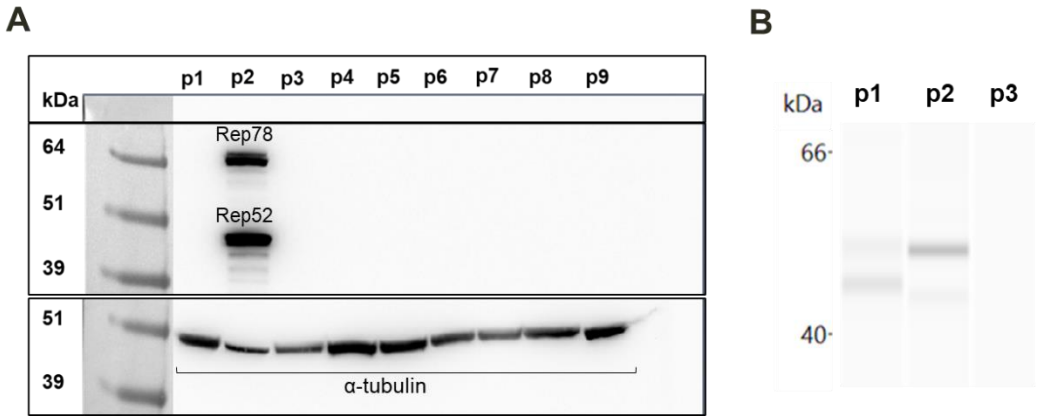

Figure 4.9: Assessment of AAV2 Rep protein expression in AAV2 *rep*-specific shRNA packaging stable populations. **(A)** Immunoblotting of protein extracts of 293 cells (p1), positive control (p2) and stable populations RepCap (p3), ΔRep (p4), RC-sh1 (p5), RC-sh2 (p6), RC-sh3 (7), RC-sh4 (p8) and RC-shscr (p9) for the detection of AAV2 Rep and α-tubulin. The indicated molecular weights in the figure correspond to bands of SeeBlue Plus2 Pre-Stained Protein Standard (Invitrogen, California, United States); **(B)** Jess immunoblotting of protein extracts from cells transiently transfected with pRC (p1) and from stable population RC-sh3 (p2).

4.8 Characterization of AAV2 *rep*-specific shRNA packaging cell populations after AdV-Cre infection

To assess the effects of helper virus infection on the amplification of AAV viral genes and *GFP*, stable populations were infected with two different AdVs. In the scope of this project, an AdV coding for Cre-recombinase (AdV-Cre) was produced and its infectious titer was determined by $TCID_{50}$ as $1.1x10^{10} \pm 0.4x10^{10}$ IP/mL (n=3). The expression of Rep and Cap was determined after the infection of established stable populations, RepCap, ΔRep, RC-sh1 and RC-sh3, with AdV-Cre and as control, with another AdV (without Cre recombinase – AdV-Control) in a MOI of 5.

24 hours post-infection, all cell populations and control exhibited cytopathic effects typical of adenoviral infection: loss of cell adhesion and cell rounding (data not shown). 42 hours post-infection, *rep*, *cap* and *GFP* levels were analysed by qPCR and RT-qPCR. Overall, both adenovirus infections did not show increased DNA copy number, apart for the RepCap population, that increased from 1 to 2 *rep* copies when infected with AdV-Control (**Table 4.2**).

Table 4.2: Analysis of copy number amplification before and after AdV infection. qPCR analysis of *rep*, *cap* and *GFP* plasmid sequences was carried out using primers/probe specific sets (Table 3.4). Copy number calculation was performed through the normalization to Albumin gene copies, with an assumed number of 2 (n=1). The data is shown by mean ± standard deviation of technical replicates (n=1).

	***rep* copy number**			***cap* copy number**		
Cell population	**No infection**	**AdV-Control**	**AdV-Cre**	**No infection**	**AdV-Control**	**AdV-Cre**
293	0.00 ± 0.03	0.00 ± 0.08	0.00 ± 0.05	0.00 ± 0.01	0.00 ± 0.03	0.00 ± 0.05
RepCap	1.00 ± 0.03	**2.00 ± 0.02**	1.00 ± 0.01	1.00 ± 0.06	1.00 ± 0.04	1.00 ± 0.06
∆Rep	0.00 ± 0.10	0.00 ± 0.06	0.00 ± 0.01	0.00 ± 0.03	0.00 ± 0.14	0.00 ± 0.13
RC-sh1	0.00 ± 0.04	0.00 ± 0.03	0.00 ± 0.07	0.00 ± 0.02	0.00 ± 0.10	0.00 ± 0.14
RC-sh3	1.00 ± 0.02	1.00 ± 0.06	1.00 ± 0.19	1.00 ± 0.02	1.00 ± 0.06	1.00 ± 0.03

	***GFP* copy number**		
Cell population	**No infection**	**AdV-Control**	**AdV-Cre**
293	0.00 ± 0.06	0.00 ± 0.06	0.00± 0.05
RepCap	1.00 ± 0.05	1.00 ± 0.03	1.00 ± 0.02
∆Rep	1.00 ± 0.02	1.00 ± 0.07	1.00 ± 0.01
RC-sh1	1.00 ± 0.07	1.00 ± 0.02	1.00 ± 0.03
RC-sh3	0.00 ± 0.02	0.00 ± 0.07	0.00 ± 0.06

Both adenoviral infections altered expression levels of UBC and TOP1, as shown in **Table 4.3**, which does not allow to normalize the infected samples to the non-infected.

Table 4.3: Impact of adenoviral infection on *UBC* and *TOP1* reference gene expression. Adenovirus infection altered the expression of the two chosen reference genes: *UBC* and *TOP1*.

	UBC C_T			**TOP1 C_T**		
Cell population	**No AdV**	**AdV-Control**	**AdV-Cre**	**No AdV**	**AdV-Control**	**AdV-Cre**
293	23.10	27.63	26.13	25.47	28.66	28.08
RepCap	22.54	26.30	25.10	25.20	28.38	28.32
∆Rep	22.72	26.44	25.15	24.92	27.55	27.89
RC-sh1	22.96	25.81	24.96	25.06	27.51	28.13
RC-sh3	23.29	24.51	23.85	25.39	26.58	26.63

rep expression was only slightly amplified in RepCap population, upon AdV infection (below 2-fold) (**Figure 4.10A**), which is coherent with *rep* DNA amplification regarding AdV-Control infection (**Table 4.2**). Among the *rep*-silencing populations, only RC-sh1 suffered a slight rep amplification (less

than 2-fold) when infected with AdV-Control (**Figure 4.10A**). Furthermore, there is no *rep* expression amplification of RC-sh1 and 3, relative to RepCap after AdV-Cre infection (**Figure 4.11B**). *cap* gene expression appeared to have increased very slightly with levels below 0.1 in population RC-sh1 and increased around 3-fold and 0.5-fold in populations RepCap and RC-sh3, respectively, upon AdV infection (**Figure 4.10B**). Still, *cap* mRNA amplification was not accompanied by *cap* DNA increase (**Table 4.2**). As expected, *cap* levels were the lowest in the population deleted for the *rep* gene (ΔRep) (**Figure 4.11B**). Again, *GFP* copy number of RC-sh3 (~0), *cap* copy number of ΔRep (~0) and *rep* and *cap* copy number of RC-sh1 (~0) are not coherent with mRNA levels shown in all tested conditions (**Figure 4.10A**, **B** and **C**). To confirm gene expression tendencies, more biological replicates need to be performed.

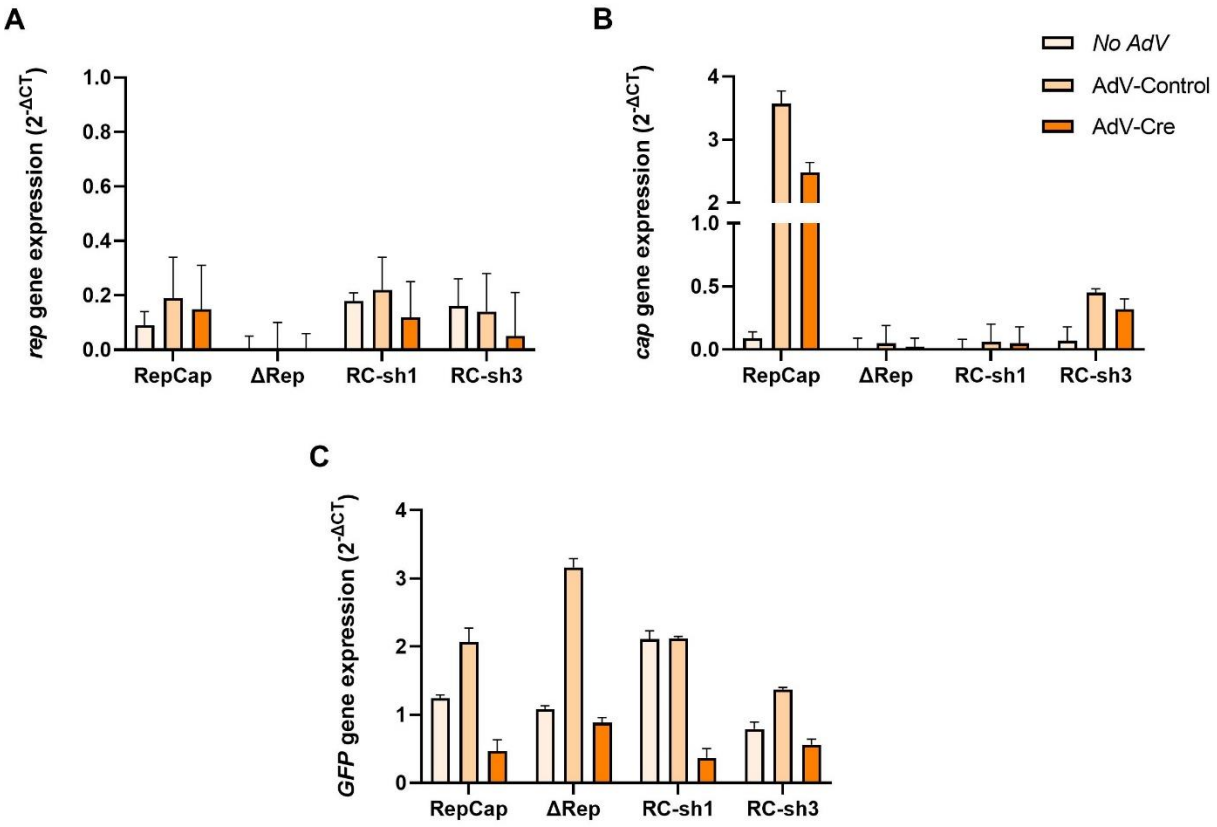

Figure 4.10: Gene expression analysis of *rep* (A), *cap* (B) and *GFP* (C) of RepCap, ΔRep, RC-sh1 and RC-sh3 stable populations, non-infected and infected with AdV-Control and AdV-Cre (42 hours post-infection). cDNA was synthesized from 2 µg of total RNA extracted. Gene expression was assessed by RT-qPCR normalized against TOP1 and UBC reference genes within the same sample and are shown as gene expression ($2^{-\Delta CT}$). Data is shown by mean ± standard deviation of technical replicates (n=1).

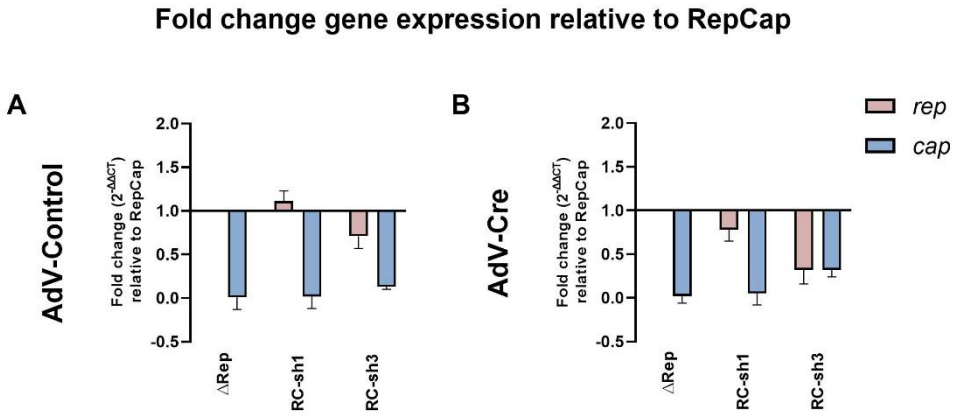

Figure 4.11: Fold change of *rep* and *cap* gene expression relative to RepCap population of ΔRep, RC-sh1 and RC-sh3 stable populations infected with AdV-Control (A) and AdV-Cre (B) (42 hours post-infection). cDNA was synthesized from 2 µg of total RNA extracted. Gene expression was assessed by RT-qPCR normalized against TOP1 and UBC reference genes within the same sample and are shown as fold change relative to the respective levels in control cells harbouring the pRC plasmid - RepCap ($2^{-\Delta\Delta CT}$). Data is shown by mean ± standard deviation of technical replicates (n=1).

5 Discussion and conclusions

There has been an increasing demand for AAV based viral vectors. An effective production method able to deliver a reproducible product in high amounts during extended culture time periods is the one based on the AAV production through packaging stable cell lines [121], [123]. 293 cells are very well characterized and receptive to transfection and infection with non-pathogenic AdV, due to the integration of adenoviral genes *E1a/b* [123]. However, these genes are able to support basal constitutive expression of Rep proteins, with known cytostatic and cytotoxic effects through time [136]–[138]. So, the main goal of this thesis was the development of 293 based AAV packaging cell lines harbouring a Cre/loxP shRNA-dependent system to control the expression of the *rep* gene.

The first reported attempts to control AAV Rep-induced cytotoxicity in 293 cells focused on the replacement of *rep* gene promoter p5 with heterologous inducible promoters [190]. However, after induction, the levels of Rep52/40, essential for AAV assembly, were too low to allow rAAV production [190]. Much of the published data highlights the importance of keeping the AAV native promoters for a more effective rAAV production in stable cells [191]–[193]. Later strategies were then based solely on *rep* (and *cap*)-coding region disruption and restoration using the Cre/loxP system [124], [139], [140]. To the best of our knowledge, a *rep* silencing mechanism based on RNAi system was never attempted. Therefore, four different shRNAs, complementary to different regions of the *rep* mRNA were designed and individually cloned in the same backbone, containing AAV *rep-cap* genes under the dependence of AAV2 native promoters (pRC). All shRNAs sequences (shRNA1-4) are complementary to Rep78/68, the main responsible of cytotoxicity [29], [30], shRNA3 and 4 were designed to also target Rep52/40. The rational for this design was to ensure an approximate equivalence of *rep-cap* and shRNA components and the integration of both critical components within the same site in the host genome. Since *rep-cap* amplification and expression profile are different in transient transfections and packaging/producer stable cell lines [130], the *rep*-specific shRNA repression system was studied in both systems.

For clinical vector manufacturing, the generation of stable cell lines through clone selection and characterization involves a significant time and effort. So, for the sake of time, population establishment was performed first, with 5 µg/10^6 cells of each generated plasmid **(Table 3.3)** using a certified PEI (PEIpro Polyplus) at 1:1 (w/w) DNA:PEI ratio. 48 h after transfection cells were placed in selection medium. The transfection effects were first analysed. A decreased cell survival was observed in all transfected cells, including the ones that received the vector deleted for the *rep* gene (pΔRepC) (**Figure 4.3A**). Transfection efficiencies were variable, and the highest percentage was achieved with plasmid pΔRepC and the lowest with pRC-shscr (**Figure 4.3B**). We can hypothesize that the observed cytotoxicity can be derived from the expression of the *rep* gene, the amount of delivered DNA and/or the type of transfection reagent. To assess and surpass this, a transfection optimization assay was conducted, where 293 cells were transfected with plasmid pRC or pGFP (transfection control) using different amounts of DNA (2 - 5 µg/10^6 cells) complexed with in-house PEI (w/w ratio of 1:1.5). Phase contrast microscopy revealed that as DNA concentration increases, cell toxicity does as well, with both plasmids (**Figure 4.4A**). Additionally, cells transfected with pRC were less confluent than the ones

transfected with the control plasmid, indicating an increased cell death in this condition, for all tested concentrations. The transfection efficiencies were always higher with pGFP, above 40%, than with pRC (below 25%) (**Figure 4.4B**). The combined results seem to indicate that the delivery of higher amounts of DNA (4 and 5 µg/10^6 cells) was more toxic to cells, an effect that might had been accentuated by the presence of the *rep* gene, since we have less cell confluency at 3 µg/10^6 with pRC (**Figure 4.4A**). PEIpro might have also contributed for an increased cytoxicity, since when comparing images of cells transfected with pRC using in-house PEI (**Figure 4.4A** – 5 µg) and PEIpro (**Figure 4.3A** - RepCap) in the same transfection ratio (5 µg/10^6 cells), the latter seem less viable. Regarding transfection efficiency both provided similar results (**Figures 4.3B** and **4.4B**). Using optimized conditions, 293 cells were again transfected with the AAV2 shRNA *rep*-specific packaging plasmids and controls using in-house PEI. The observed cell confluency and transfection efficiencies (**Figures 4.5A** and **B**) were within expected based on the previous assays.

The results indicate that none of the used shRNAs were able to knockdown *rep* gene expression both in transiently transfected cells as well as in the selected packaging stable populations. In transient, analysis of *rep* gene expression, relative to control (pRC), revealed similar or slightly higher levels of *rep* mRNA in all transfected cells (**Figures 4.7A and B)**. This was a first evidence that the used shRNAs were not being effective in *rep* gene knockdown, mainly when some reports point that shRNA-mediated gene silencing can be effective 48 hpt [194], [195]. Interestingly, even in the absence of helper factors, when the *rep* gene is expressed, the *cap* expression levels were 2.5 to 7.2-fold higher than *rep*, being the most abundant transcript is most transfections (**Figure 4.7A**). Comparatively, in cells transfected with pΔRepC, levels of *cap* mRNA where 6-fold reduced compared to transfection with pRC (**Figures 4.7A and B**). The expression of Rep proteins, detected 48 h after transfection in the populations expressing *rep*, is probably acting as a positive regulator of the p40 promoter, leading to an increased expression of *cap* mRNA, an observation in line with published results [188]. Regarding GFP expression, it seems to be higher in cells deleted for the *rep* gene (pΔRepC) (**Figure 4.7A**). Accordingly, it has been documented that Rep is able to downregulate expression from heterologous promoters [129], [196].

To confirm the shRNA properties as well as to characterize the selected populations, *rep-cap* gene expression and amplification were quantified by qPCR, before and after AdV infection. In the absence of helper factors, *rep* expression was not detected in RC-sh2, RC-sh4 and RC-shscr populations while RC-sh1 and RC-sh3 had a slight increase compared to control, RepCap (below 2-fold) (**Figures 4.7C** and **D**). The overall low *rep* gene expression results were further corroborated through traditional western blot analysis, since no AAV2 Rep proteins were detected in any of the populations (**Figure 4.9A**). Through a more sensitive western blot methodology (Jess), low Rep expression was confirmed (**Figure 4.9B**), although further tests are needed. As expected, *cap* mRNA levels were detected in levels below of what was observed for transient transfections (**Figures 4.7C** and **A**, respectively). To investigate whether the absent/low expression of *rep* (and consequently *cap*) could be due to a downregulation driven by shRNA, the integrated plasmid copy number of *rep*, *cap* and *GFP* was also assessed in these populations. At the beginning of work, it was hypothesized that if the shRNAs were efficient in silencing *rep* expression, then clones with higher integrated copy number could have endured. Populations RepCap and RC-sh3 have an average number of 1 copy of *rep* while RC-sh1 did

not reach 1 (**Table 4.1**). Populations RC-shscr, RC-sh2 and RC-sh4 do not have any *rep* integrated copies, which can explain the lack of *rep* gene expression (**Table 4.1** and **Figure 4.7C**). For other genes, the range was also between 0 and 1 (**Table 4.1**). It is important to point out that since these samples are populations, there is cell heterogeneity, meaning that the copy numbers obtained reflect only an average and do not represent each individual cell. Additionally, since these cells were transfected with a circular plasmid, that can be randomly linearized within the cell, there is an increased probability of generating clones that do not integrate essential genes [197]. It has been shown that the number of stable colonies can be increased through vector linearization, since foreign DNA integration into the chromosome likely occurs during nuclear replication, when linear DNA can be randomly copied into chromosomes [197]. It can also be hypothesized that despite the presence of Rep proteins, the lack of AAV ITRs in the constructions might have had a negative impact on integration. It has been described higher integration efficacy when using ITRs due to higher homology to the chromosome 19 sequence [198]. In contrast, it has been documented that ITRs are not required for integration and that the presence of a *cis* element, named AAV integration efficiency element (P5IEE) in the p5 promoter, alongside Rep proteins, is sufficient for this phenomenon. Thus, it has also been reported similar integration efficiencies between ITR-containing and ITR-deleted constructs [199]. Additionally, the severe cytotoxicity upon transfection during the establishment of stable populations may have compromised the survival of clones with a higher integrated plasmid copy number.

Stable cell lines tend to mimic post-adenoviral infection wt AAV life cycle through the amplification of *rep* and *cap* genes [130]. Hence, successful rAAV production is dependent on an efficient *rep* and *cap* amplification, that is driven by the presence of adenoviral helper factors [123], [127], [129], [130]. Thus, RepCap, ΔRep, RC-sh1 and RC-sh3 stable populations were infected with two AdV: one expressing Cre (AdV-Cre) and other not (AdV-Control) to assess if there is any *rep* gene amplification and if the shRNAs are indeed exerting a silencing effect on *rep*. Unfortunately, since RG *UBC* and *TOP1* suffered expression changes due to AdV infection, in some samples of 3 C_T (approximately 10-fold difference), the infected samples cannot be normalized to the non-infected ones (**Table 4.3**). Reports show that DNA topoisomerases are involved in AdV replication, transcription and packaging [200] and the ubiquitin system has a role in AdV disassembly and trafficking [201], which might explain gene expression changes. Nevertheless, a trend can be observed in the results depicted in **Figure 4.10**. For RepCap population, a slight increase in *rep* is observed (below 2-fold), after both AdV infection (**Figures 4.10A**). For RC-sh1 and RC-sh3 populations, there was no *rep* expression amplification after AdV-Cre infection when compared to RepCap (**Figure 4.11B**), which further reinforces the hypothesis that shRNA1 and 3 do not repress *rep*. Contrarily of what was expected, especially for the RC-sh3 population, *cap* expression seems to have been amplified after AdV infection, interestingly, the result was observed with both used AdVs (**Figure 4.10B**). *cap* gene expression is in fact amplified during AdV infection, however, it relies on Rep78-mediated transactivation of the p40 promoter [16], [189] and *rep* was not amplified upon AdV infection in population RC-sh3 (**Figure 4.10A**). In the future, a relative quantification with a standard curve should be employed to understand if this reported result is real or an artefact, related with the normalization using abnormally expressed UBC and TOP1. Regarding plasmid integrated copy number in stable cell lines, some reports attribute no

clear relation with rAAV productivity [123], while others still consider that possibility [129]. After infection, only RepCap population showed an increase of *rep* gene amplification from 1 to 2 copies, upon AdV-Control (**Table 4.2**), which aligns with the slight increase in *rep* mRNA levels, and consequently *cap* expression (**Figure 4.10A** and **B**). The combined results of this work point that only 1 copy of *rep-cap* per cell is not enough to trigger the desirable levels of *rep-cap* amplification required for an increased rAAV production. In line with our results, Chadeuf *et al.* (2000) [131] developed a 293 based AAV stable cell line with 1-2 *rep* integrated copies which ended up yielding 27-fold less AAV vectors than control 293 cells. Successful 293 based AAV producer cell lines have between 10 to 50 *rep* integrated copies and can reach up to 20-fold of *rep-cap* amplification upon AdV infection [123], [124].

Although, no AAV2 packaging cell line harbouring a *rep*-silencing mechanism based on shRNA was established, this work gave useful insights regarding transfection and *rep*-mediated cytoxicity, shRNA design and delivery, which will shape future assays. Moreover, the implementation and validation of several qPCR methods are definitely valuable for upcoming work. For the time being, functional assays for the validation of gene silencing mediated by shRNA and loxP-site excision by AdV-Cre are being performed. In the future, to improve the strategy herein presented and increase the chances of success of this work, new approaches should be employed. To guarantee *rep* silencing, new *rep*-specific shRNAs should be designed and, for example, delivered first in a separate plasmid (without the AAV2 *rep* and *cap* genes) combining different shRNAs sequences. Weng *et al.* (2017) [195] designed a multi-shRNA vector with the capacity for cloning 3 shRNAs, under the dependence of U6 promoters. The effectiveness of this vector was assayed in exogenously and endogenously expressed genes. Results shown that multi-site shRNA vector could maintain the silencing effect for longer periods of time, when compared to single-site and double-site shRNA vectors. Moreover, combinations of up to 6 shRNAs in a head-to-tail tandem array using H6 promoters have already been tested and validated [194]. Regarding vector delivery, one of the most used mechanisms are lentiviral vectors, since it allows high levels of target gene suppression [202]–[204]. Satkunanathan and colleagues [204] established a 293T based YB1 knockdown AAV producer cells through the delivery of a shRNA using lentiviral vectors. It was shown that this cellular endogenous gene was silenced for more than 80 days in culture. Still, the use of viral vectors can be avoided through the use other not PEI-based methods with reduced cell cytotoxicity, such as Lipofectamine [195], [205], [206] which may increase the overall transfection efficiency and recovery of a high producer clone.

The development of a screening method for high producer clones, which relates integrated copy number, gene expression and/or protein production with rAAV productivity, as preliminarily explored in this work, is quite useful and should be further investigated. In addition to find a high producer AAV packaging stable cell line, it would be of interest to develop a mother cell that could allow the production of different rAAVs through the transfection with different transgenes, and ideally, with interchangeable *cap* gene cassettes permitting serotype versatility.

6 References

[1] R. W. Atchison, B. C. Casto, and W. M. Hammon, “Adenovirus-Associated Defective Virus Particles,” *Science (80-.).*, vol. 149, no. 3685, pp. 754–755, Aug. 1965, doi: 10.1126/science.149.3685.754.

[2] N. R. Blacklow, M. D. Hoggan, and W. P. Rowe, “Isolation of adenovirus-associated viruses from man.,” *Proc. Natl. Acad. Sci. U. S. A.*, vol. 58, no. 4, pp. 1410–1415, 1967, doi: 10.1073/pnas.58.4.1410.

[3] International Committee on Taxonomy of Viruses (ICTV), “Taxonomy of viruses.” [Online]. Available: https://talk.ictvonline.org/taxonomy/. [Accessed: 07-Apr-2020].

[4] B. T. Kurien and R. H. Scofield, *Adeno-associated Virus: Methods and Protocols*. Humana Press, 2011.

[5] M. Salganik, M. Hirsch, and R. Samulski, “Adeno-associated Virus as a Mammalian DNA Vector,” *Microbiol. Spectr.*, 2015, doi: 10.1128/microbiolspec.MDNA3-0052-2014. Adeno-associated.

[6] D. Hüser, D. Khalid, T. Lutter, E.-M. Hammer, S. Weger, M. Heßler, U. Kalus, Y. Tauchmann, K. Hensel-Wiegel, D. Lassner, and R. Heilbronn, “High Prevalence of Infectious Adeno-associated Virus (AAV) in Human Peripheral Blood Mononuclear Cells Indicative of T Lymphocytes as Sites of AAV Persistence,” *J. Virol.*, vol. 91, no. 4, pp. 2137–2153, 2017, doi: 10.1128/jvi.02137-16.

[7] R. M. Kotin, M. Siniscalco, R. J. Samulski, X. D. Zhu, L. Hunter, C. A. Laughlin, S. McLaughlin, N. Muzyczka, M. Rocchi, and K. I. Berns, “Site-specific integration by adeno-associated virus.,” 1990.

[8] B. C. Schnepp, R. L. Jensen, C.-L. Chen, P. R. Johnson, and K. R. Clark, “Characterization of Adeno-Associated Virus Genomes Isolated from Human Tissues,” *J. Virol.*, vol. 79, no. 23, pp. 14793–14803, 2005, doi: 10.1128/jvi.79.23.14793-14803.2005.

[9] K. I. Berns, T. C. Pinkerton, G. F. Thomas, and M. D. Hoggan, “Detection of adeno-associated virus (AAV)-specific nucleotide sequences in DNA isolated from latently infected Detroit 6 cells,” *Virology*, vol. 68, no. 2, pp. 556–560, 1975, doi: 10.1016/0042-6822(75)90298-6.

[10] A. K. Cheung, M. D. Hoggan, W. W. Hauswirth, and K. I. Berns, “Integration of the adeno-associated virus genome into cellular DNA in latently infected human Detroit 6 cells.,” *J. Virol.*, vol. 33, no. 2, pp. 739–48, Feb. 1980.

[11] B. Balakrishnan and G. Jayandharan, “Basic Biology of Adeno-Associated Virus (AAV) Vectors Used in Gene Therapy,” *Curr. Gene Ther.*, vol. 14, no. 2, pp. 86–100, 2014, doi: 10.2174/1566523214666140302193709.

[12] M. Penaud-Budloo, C. Le Guiner, A. Nowrouzi, A. Toromanoff, Y. Cherel, P. Chenuaud, M. Schmidt, C. von Kalle, F. Rolling, P. Moullier, and R. O. Snyder, “Adeno-Associated Virus Vector Genomes Persist as Episomal Chromatin in Primate Muscle,” *J. Virol.*, vol. 82, no. 16, pp. 7875–7885, 2008, doi: 10.1128/jvi.00649-08.

[13] A. Nowrouzi, M. Penaud-Budloo, C. Kaeppel, U. Appelt, C. Le Guiner, P. Moullier, C. Von Kalle, R. O. Snyder, and M. Schmidt, “Integration frequency and intermolecular recombination of rAAV

vectors in non-human primate skeletal muscle and liver," *Mol. Ther.*, vol. 20, no. 6, pp. 1177–1186, 2012, doi: 10.1038/mt.2012.47.

[14] D. R. Deyle and D. W. Russell, "Adeno-associated virus vector integration," *Current Opinion in Molecular Therapeutics*, vol. 11, no. 4. pp. 442–447, 2009.

[15] L. M. Drouin and M. Agbandje-Mckenna, "Adeno-associated virus structural biology as a tool in vector development," *Future Virol.*, vol. 8, no. 12, pp. 1183–1199, 2013, doi: 10.2217/fvl.13.112.

[16] Q. Yang, A. Kadam, and J. P. Trempe, "Mutational analysis of the adeno-associated virus rep gene.," *J. Virol.*, vol. 66, no. 10, pp. 6058–6069, 1992, doi: 10.1128/jvi.66.10.6058-6069.1992.

[17] P. L. Hermonat, M. A. Labow, R. Wright, K. I. Berns, and N. Muzyczka, "Genetics of adeno-associated virus: isolation and preliminary characterization of adeno-associated virus type 2 mutants.," *J. Virol.*, vol. 51, no. 2, pp. 329–339, 1984, doi: 10.1128/jvi.51.2.329-339.1984.

[18] P. Ward, P. Elias, and R. M. Linden, "Rescue of the Adeno-Associated Virus Genome from a Plasmid Vector: Evidence for Rescue by Replication," *J. Virol.*, vol. 77, no. 21, pp. 11480–11490, 2003, doi: 10.1128/JVI.77.21.11480-11490.2003.

[19] D. J. Pereira, D. M. McCarty, and N. Muzyczka, "The adeno-associated virus (AAV) Rep protein acts as both a repressor and an activator to regulate AAV transcription during a productive infection.," *J. Virol.*, vol. 71, no. 2, pp. 1079–1088, 1997, doi: 10.1128/jvi.71.2.1079-1088.1997.

[20] J. A. King, R. Dubielzig, D. Grimm, and J. A. Kleinschmidt, "DNA helicase-mediated packaging of adeno-associated virus type 2 genomes into preformed capsids," 2001.

[21] R. F. Collaco, V. Kalman-Maltese, A. D. Smith, J. D. Dignam, and J. P. Trempe, "A Biochemical Characterization of the Adeno-associated Virus Rep40 Helicase," *J. Biol. Chem.*, vol. 278, no. 36, pp. 34011–34017, 2003, doi: 10.1074/jbc.M301537200.

[22] A. Beaton, P. Palumbo, and K. I. Berns, "Expression from the adeno-associated virus p5 and p19 promoters is negatively regulated in trans by the rep protein.," *J. Virol.*, vol. 63, no. 10, pp. 4450–4, 1989.

[23] S. R. M. Kyostio, R. S. Wonderling, and R. A. Owens, "Negative regulation of the adeno-associated virus (AAV) P5promoter involves both the P5Rep binding site and the consensus ATP-binding motif of the AAV Rep68 protein," *J. Virol.*, vol. 69, no. 11, pp. 6787–6796, 1995.

[24] P. L. Hermonat, "Down-regulation of the human c-fos and c-myc proto-oncogene promoters by adeno-associated virus Rep78," *Cancer Lett.*, vol. 81, no. 2, pp. 129–136, Jun. 1994, doi: 10.1016/0304-3835(94)90193-7.

[25] M. Horer, S. Weger, K. Butz, F. Hoppe-Seyler, C. Geisen, and J. A. Kleinschmidt, "Mutational analysis of adeno-associated virus Rep protein-mediated inhibition of heterologous and homologous promoters," *J. Virol.*, vol. 69, no. 9, pp. 5485–5496, 1995.

[26] Y. Shi, E. Seto, L. S. Chang, and T. Shenk, "Transcriptional repression by YY1, a human GLI-Krüppel-related protein, and relief of repression by adenovirus E1A protein," *Cell*, vol. 67, no. 2, pp. 377–388, Oct. 1991, doi: 10.1016/0092-8674(91)90189-6.

[27] C. A. Laughlin, N. Jones, and B. J. Carter, "Effect of deletions in adenovirus early region 1 genes upon replication of adeno-associated virus," *J. Virol.*, vol. 41, no. 3, pp. 868–876, Mar. 1982.

[28] M. A. Labow, P. L. Hermonat, and K. I. Berns, "Positive and negative autoregulation of the adeno-

associated virus type 2 genome.," *J. Virol.*, vol. 60, no. 1, pp. 251–8, 1986.

[29] M. Schmidt, S. Afione, and R. M. Kotin, "Adeno-Associated Virus Type 2 Rep78 Induces Apoptosis through Caspase Activation Independently of p53," *J. Virol.*, vol. 74, no. 20, pp. 9441–9450, Oct. 2000, doi: 10.1128/jvi.74.20.9441-9450.2000.

[30] P. Saudan, J. Vlach, and P. Beard, "Inhibition of S-phase progression by adenoassociated virus Rep78 protein is mediated by hypophosphorylated pRb," *EMBO J.*, vol. 19, no. 16, pp. 4351–4361, Aug. 2000, doi: 10.1093/emboj/19.16.4351.

[31] S. P. Becerra, F. Koczot, P. Fabisch, and J. A. Rose, "Synthesis of Adeno-Associated Virus Structural Proteins Requires Both Alternative mRNA Splicing and Alternative Initiations from a Single Transcript," 1988.

[32] K. M. Van Vliet, V. Blouin, N. Brument, M. Agbandje-McKenna, and R. O. Snyder, "The role of the adeno-associated virus capsid in gene transfer," *Methods Mol. Biol.*, vol. 437, pp. 51–91, 2008, doi: 10.1007/978-1-59745-210-6_2.

[33] A. Girod, C. E. Wobus, Z. Zádori, M. Ried, K. Leike, P. Tijssen, J. A. Kleinschmidt, and M. Hallek, "The VP1 capsid protein of adeno-associated virus type 2 is carrying a phospholipase A2 domain required for virus infectivity," *J. Gen. Virol.*, vol. 83, no. 5, pp. 973–978, 2002, doi: 10.1099/0022-1317-83-5-973.

[34] S. Stahnke, K. Lux, S. Uhrig, F. Kreppel, M. Hösel, O. Coutelle, M. Ogris, M. Hallek, and H. Büning, "Intrinsic phospholipase A2 activity of adeno-associated virus is involved in endosomal escape of incoming particles," *Virology*, vol. 409, no. 1, pp. 77–83, Jan. 2011, doi: 10.1016/j.virol.2010.09.025.

[35] K. H. Warrington, O. S. Gorbatyuk, J. K. Harrison, S. R. Opie, S. Zolotukhin, and N. Muzyczka, "Adeno-Associated Virus Type 2 VP2 Capsid Protein Is Nonessential and Can Tolerate Large Peptide Insertions at Its N Terminus," *J. Virol.*, vol. 78, no. 12, pp. 6595–6609, 2004, doi: 10.1128/jvi.78.12.6595-6609.2004.

[36] M. Hoque, K. Ishizu, A. Matsumoto, S. I. Han, F. Arisaka, M. Takayama, K. Suzuki, K. Kato, T. Kanda, H. Watanabe, and H. Handa, "Nuclear transport of the major capsid protein is essential for adeno-associated virus capsid formation.," *J. Virol.*, vol. 73, no. 9, pp. 7912–5, Sep. 1999.

[37] Q. Xie, W. Bu, S. Bhatia, J. Hare, T. Somasundaram, A. Azzi, and M. S. Chapman, "The atomic structure of adeno-associated virus (AAV-2), a vector for human gene therapy," *Proc. Natl. Acad. Sci. U. S. A.*, vol. 99, no. 16, pp. 10405–10410, 2002, doi: 10.1073/pnas.162250899.

[38] F. Sonntag, K. Schmidt, and J. A. Kleinschmidt, "A viral assembly factor promotes AAV2 capsid formation in the nucleolus," *Proc. Natl. Acad. Sci. U. S. A.*, vol. 107, no. 22, pp. 10220–10225, 2010, doi: 10.1073/pnas.1001673107.

[39] A. Maurer, S. Pacouret, A. Diaz, J. Blake, E. Andres-Mateos, and L. Vandenberghe, "The Assembly-Activating Protein Promotes Stability and Interactions between AAV's Viral Proteins to Nucleate Capsid Assembly," *Cell Rep.*, vol. 23, no. 6, pp. 1817–1830, 2018, doi: 10.1016/j.physbeh.2017.03.040.

[40] P. L. Hermonat, A. D. Santin, J. De Greve, M. De Rijcke, B. M. Bishop, L. Han, M. Mane, and N. Kokorina, "Chromosomal latency and expression at map unit 96 of a wild-type plus adeno-

associated virus (AAV)/Neo vector and identification of p81, a new AAV transcriptional promoter.," *J. Hum. Virol.*, vol. 2, no. 6, pp. 359–68, 1999.

[41] A. Srivastava, E. W. Lusby, and K. I. Berns, "Nucleotide sequence and organization of the adeno-associated virus 2 genome.," *J. Virol.*, vol. 45, no. 2, pp. 555–564, 1983, doi: 10.1128/jvi.45.2.555-564.1983.

[42] M. Cao, H. You, and P. L. Hermonat, "The X gene of Adeno-Associated Virus 2 (AAV2) is involved in viral DNA replication," *PLoS One*, vol. 9, no. 8, 2014, doi: 10.1371/journal.pone.0104596.

[43] P. J. Ogden, E. D. Kelsic, S. Sinai, and G. M. Church, "Comprehensive AAV capsid fitness landscape reveals a viral gene and enables machine-guided design," *Science (80-.).*, vol. 1143, no. November, pp. 1139–1143, 2019.

[44] B. L. Gurda, M. A. DiMattia, E. B. Miller, A. Bennett, R. McKenna, W. S. Weichert, C. D. Nelson, W. -j. Chen, N. Muzyczka, N. H. Olson, R. S. Sinkovits, J. A. Chiorini, S. Zolotutkhin, O. G. Kozyreva, R. J. Samulski, T. S. Baker, C. R. Parrish, and M. Agbandje-McKenna, "Capsid Antibodies to Different Adeno-Associated Virus Serotypes Bind Common Regions," *J. Virol.*, vol. 87, no. 16, pp. 9111–9124, 2013, doi: 10.1128/jvi.00622-13.

[45] L. M. Drouin, B. Lins, M. Janssen, A. Bennett, P. Chipman, R. McKenna, W. Chen, N. Muzyczka, G. Cardone, T. S. Baker, and M. Agbandje-McKenna, "Cryo-electron Microscopy Reconstruction and Stability Studies of the Wild Type and the R432A Variant of Adeno-associated Virus Type 2 Reveal that Capsid Structural Stability Is a Major Factor in Genome Packaging," *J. Virol.*, vol. 90, no. 19, pp. 8542–8551, 2016, doi: 10.1128/jvi.00575-16.

[46] A. Srivastava, "In vivo tissue-tropism of adeno-associated viral vectors," *Curr. Opin. Virol.*, vol. 21, pp. 75–80, 2016, doi: 10.1016/j.physbeh.2017.03.040.

[47] M. Schmidt, L. Govindasamy, S. Afione, N. Kaludov, M. Agbandje-Mckenna, and J. A. Chiorini, "Molecular Characterization of the Heparin-Dependent Transduction Domain on the Capsid of a Novel Adeno-Associated Virus Isolate, AAV(VR-942)," *J. Virol.*, vol. 82, no. 17, pp. 8911–8916, 2008, doi: 10.1128/JVI.00672-08.

[48] Z. Wu, A. Asokan, and R. J. Samulski, "Adeno-associated Virus Serotypes: Vector Toolkit for Human Gene Therapy," *Molecular Therapy*, vol. 14, no. 3. pp. 316–327, 2006, doi: 10.1016/j.ymthe.2006.05.009.

[49] I. Kwon and D. V. Schaffer, "Designer gene delivery vectors: Molecular engineering and evolution of adeno-associated viral vectors for enhanced gene transfer," *Pharmaceutical Research*, vol. 25, no. 3. pp. 489–499, Mar-2008, doi: 10.1007/s11095-007-9431-0.

[50] C. Burger, O. S. Gorbatyuk, M. J. Velardo, C. S. Peden, P. Williams, S. Zolotukhin, P. J. Reier, R. J. Mandel, and N. Muzyczka, "Recombinant AAV viral vectors pseudotyped with viral capsids from serotypes 1, 2, and 5 display differential efficiency and cell tropism after delivery to different regions of the central nervous system," *Mol. Ther.*, vol. 10, no. 2, pp. 302–317, Aug. 2004, doi: 10.1016/j.ymthe.2004.05.024.

[51] D. Grimm and M. Kay, "From Virus Evolution to Vector Revolution: Use of Naturally Occurring Serotypes of Adeno-associated Virus (AAV) as Novel Vectors for Human Gene Therapy," *Curr.*

Gene Ther., vol. 3, no. 4, pp. 281–304, Jul. 2005, doi: 10.2174/1566523034578285.

[52] S. Pillay, N. L. Meyer, A. S. Puschnik, O. Davulcu, J. Diep, Y. Ishikawa, L. T. Jae, J. E. Wosen, C. M. Nagamine, M. S. Chapman, and J. E. Carette, “An essential receptor for adeno-associated virus infection,” *Nature*, vol. 530, no. 7588, pp. 108–112, 2016, doi: 10.1038/nature16465.

[53] J. Rabinowitz, Y. K. Chan, and R. J. Samulski, “Adeno-associated Virus (AAV) versus immune response,” *Viruses*, vol. 11, no. 2, 2019, doi: 10.3390/v11020102.

[54] R. Calcedo, L. H. Vandenberghe, G. Gao, J. Lin, and J. M. Wilson, “Worldwide Epidemiology of Neutralizing Antibodies to Adeno-Associated Viruses,” *J. Infect. Dis.*, vol. 199, no. 3, pp. 381–390, Feb. 2009, doi: 10.1086/595830.

[55] D. Wang, P. W. L. Tai, and G. Gao, “Adeno-associated virus vector as a platform for gene therapy delivery,” *Nat. Rev. Drug Discov.*, vol. 18, no. 5, pp. 358–378, 2019, doi: 10.1038/s41573-019-0012-9.

[56] J. S. Bartlett, R. Wilcher, and R. J. Samulski, “Infectious Entry Pathway of Adeno-Associated Virus and Adeno-Associated Virus Vectors,” *J. Virol.*, vol. 74, no. 6, pp. 2777–2785, 2000, doi: 10.1128/jvi.74.6.2777-2785.2000.

[57] J. Hansen, K. Qing, and A. Srivastava, “Adeno-Associated Virus Type 2-Mediated Gene Transfer: Altered Endocytic Processing Enhances Transduction Efficiency in Murine Fibroblasts,” *J. Virol.*, vol. 75, no. 9, pp. 4080–4090, 2001, doi: 10.1128/jvi.75.9.4080-4090.2001.

[58] F. Sonntag, S. Bleker, B. Leuchs, R. Fischer, and J. A. Kleinschmidt, “Adeno-Associated Virus Type 2 Capsids with Externalized VP1/VP2 Trafficking Domains Are Generated prior to Passage through the Cytoplasm and Are Maintained until Uncoating Occurs in the Nucleus,” *J. Virol.*, vol. 80, no. 22, pp. 11040–11054, Nov. 2006, doi: 10.1128/jvi.01056-06.

[59] K. Pajusola, M. Gruchala, H. Joch, T. F. Lüscher, S. Ylä-Herttuala, H. Büeler, and A. I. Virtanen, “Cell-Type-Specific Characteristics Modulate the Transduction Efficiency of Adeno-Associated Virus Type 2 and Restrain Infection of Endothelial Cells,” *J. Virol.*, vol. 76, no. 22, pp. 11530–11540, 2002, doi: 10.1128/JVI.76.22.11530-11540.2002.

[60] S. Cohen, A. K. Marr, P. Garcin, and N. Panté, “Nuclear Envelope Disruption Involving Host Caspases Plays a Role in the Parvovirus Replication Cycle Downloaded from,” *J. Virol.*, vol. 85, no. 10, pp. 4863–4874, 2011, doi: 10.1128/JVI.01999-10.

[61] C. Li, Y. He, S. Nicolson, M. Hirsch, M. S. Weinberg, P. Zhang, T. Kafri, and R. J. Samulski, “Adeno-associated virus capsid antigen presentation is dependent on endosomal escape,” *J. Clin. Invest.*, vol. 123, 2013, doi: 10.1172/JCI66611.

[62] M. Mezzina and O. W. Merten, *Adeno-associated Virus*, vol. 737. 2011.

[63] K. Nash, W. Chen, W. F. Mcdonald, X. Zhou, and N. Muzyczka, “Purification of Host Cell Enzymes Involved in Adeno-Associated Virus DNA Replication,” *J. Virol.*, vol. 81, no. 11, pp. 5777–5787, 2007, doi: 10.1128/JVI.02651-06.

[64] K. Nash, W. Chen, and N. Muzyczka, “Complete In Vitro Reconstitution of Adeno-Associated Virus DNA Replication Requires the Minichromosome Maintenance Complex Proteins,” *J. Virol.*, vol. 82, no. 3, pp. 1458–1464, Feb. 2008, doi: 10.1128/jvi.01968-07.

[65] K. Nash, W. Chen, M. Salganik, and N. Muzyczka, “Identification of Cellular Proteins That

Interact with the Adeno-Associated Virus Rep Protein Downloaded from," *J. Virol.*, vol. 83, no. 1, pp. 454–469, 2009, doi: 10.1128/JVI.01939-08.

[66] R. J. Samulski and N. Muzyczka, "AAV-Mediated Gene Therapy for Research and Therapeutic Purposes," *Annu. Rev. Virol.*, vol. 1, no. 1, pp. 427–451, Nov. 2014, doi: 10.1146/annurev-virology-031413-085355.

[67] M. D. Weitzman and M. Linden, "Adeno-Associated Virus Biology," in *Gene Therapy*, vol. 807, 2011, pp. 119–140.

[68] J. R. Brister and N. Muzyczka, "Mechanism of Rep-Mediated Adeno-Associated Virus Origin Nicking," *J. Virol.*, vol. 74, no. 17, pp. 7762–7771, 2000, doi: 10.1128/jvi.74.17.7762-7771.2000.

[69] M. W. Myers and B. J. Carter, "Assembly of adeno-associated virus," *Virology*, vol. 102, no. 1, pp. 71–82, Apr. 1980, doi: 10.1016/0042-6822(80)90071-9.

[70] S. Bleker, M. Pawlita, and J. A. Kleinschmidt, "Impact of Capsid Conformation and Rep-Capsid Interactions on Adeno-Associated Virus Type 2 Genome Packaging," *J. Virol.*, vol. 80, no. 2, pp. 810–820, 2006, doi: 10.1128/jvi.80.2.810-820.2006.

[71] C. Meyers, M. Mane, N. Kokorina, S. Alam, and P. L. Hermonat, "Ubiquitous human adeno-associated virus type 2 autonomously replicates in differentiating keratinocytes of a normal skin model," *Virology*, vol. 272, no. 2, pp. 338–346, 2000, doi: 10.1006/viro.2000.0385.

[72] J. Hansen, K. Qing, and A. Srivastava, "Infection of purified nuclei by adeno-associated virus 2," *Mol. Ther.*, vol. 4, no. 4, pp. 289–296, 2001, doi: 10.1006/mthe.2001.0457.

[73] M. A. F. V. Gonçalves, "Adeno-associated virus: From defective virus to effective vector," *Virology Journal*, vol. 2, no. February 2005. 2005, doi: 10.1186/1743-422X-2-43.

[74] L. S. Chang, Y. Shi, and T. Shenk, "Adeno-associated virus P5 promoter contains an adenovirus E1A-inducible element and a binding site for the major late transcription factor.," *J. Virol.*, vol. 63, no. 8, pp. 3479–88, 1989.

[75] J. D. Tratschin, M. H. West, T. Sandbank, and B. J. Carter, "A human parvovirus, adeno-associated virus, as a eucaryotic vector: transient expression and encapsidation of the procaryotic gene for chloramphenicol acetyltransferase.," *Mol. Cell. Biol.*, vol. 4, no. 10, pp. 2072–2081, Oct. 1984, doi: 10.1128/mcb.4.10.2072.

[76] R. J. Samulski and T. Shenk, "Adenovirus EBB 55-Mr Polypeptide Facilitates Timely Cytoplasmic Accumulation of Adeno-Associated Virus mRNAs," 1988.

[77] T. B. Lentz and R. J. Samulski, "Insight into the Mechanism of Inhibition of Adeno-Associated Virus by the Mre11/Rad50/Nbs1 Complex," *J. Virol.*, vol. 89, no. 1, pp. 181–194, 2015, doi: 10.1128/jvi.01990-14.

[78] M. D. Weitzman, K. J. Fisher, and J. M. Wilson, "Recruitment of wild-type and recombinant adeno-associated virus into adenovirus replication centers.," *J. Virol.*, vol. 70, no. 3, pp. 1845–54, 1996.

[79] M. H. West, J. P. Trempe, J. D. Tratschin, and B. J. Carter, "Gene expression in adeno-associated virus vectors: the effects of chimeric mRNA structure, helper virus, and adenovirus VA1 RNA.," *Virology*, vol. 160, no. 1, pp. 38–47, Sep. 1987, doi: 10.1016/0042-6822(87)90041-9.

[80] R. Nayak and D. J. Pintel, “Adeno-Associated Viruses Can Induce Phosphorylation of eIF2 via PKR Activation, Which Can Be Overcome by Helper Adenovirus Type 5 Virus-Associated RNA,” *J. Virol.*, vol. 81, no. 21, pp. 11908–11916, 2007, doi: 10.1128/JVI.01132-07.

[81] F. W. Weindler and R. Heilbronn, “A subset of herpes simplex virus replication genes provides helper functions for productive adeno-associated virus replication.,” *J. Virol.*, vol. 65, no. 5, pp. 2476–2483, 1991, doi: 10.1128/jvi.65.5.2476-2483.1991.

[82] R. Heilbronn, M. Engstler, S. Weger, A. Krahn, C. Schetter, and M. Boshart, “ssDNA-dependent colocalization of adeno-associated virus Rep and herpes simplex virus ICP8 in nuclear replication domains,” *Nucleic Acids Res.*, vol. 31, no. 21, pp. 6206–6213, 2003, doi: 10.1093/nar/gkg827.

[83] H. Slanina, S. Weger, N. D. Stow, A. Kuhrs, and R. Heilbronn, “Role of the Herpes Simplex Virus Helicase-Primase Complex during Adeno-Associated Virus DNA Replication,” *J. Virol.*, vol. 80, no. 11, pp. 5241–5250, 2006, doi: 10.1128/JVI.02718-05.

[84] M.-C. Geoffroy, A. L. Epstein, E. Toublanc, P. Moullier, A. Salvetti, and B. Jean Monnet, “Herpes Simplex Virus Type 1 ICP0 Protein Mediates Activation of Adeno-Associated Virus Type 2 rep Gene Expression from a Latent Integrated Form,” *J. Virol.*, vol. 78, no. 20, pp. 10977–10986, 2004, doi: 10.1128/JVI.78.20.10977-10986.2004.

[85] N. Alazard-Dany, N. A. Ploquin, A. Strasser, and R. Greco, “Definition of Herpes Simplex Virus Type 1 Helper Activities for Adeno-Associated Virus Early Replication Events,” *PLoS Pathog*, vol. 5, no. 3, p. 1000340, 2009, doi: 10.1371/journal.ppat.1000340.

[86] Official Journal of the European Union, “Amending Directive 2001/83/EC of the European Parliament and of the Council on the Community code relating to medicinal products for human use as regards advanced therapy medicinal products,” 2009.

[87] J. Y. Sun, V. Anand-Jawa, S. Chatterjee, and K. K. Wong, “Immune responses to adeno-associated virus and its recombinant vectors,” *Gene Ther.*, vol. 10, no. 11 SPEC., pp. 964–976, 2003, doi: 10.1038/sj.gt.3302039.

[88] D. Stone, Y. Liu, Z.-Y. Li, R. Strauss, E. E. Finn, J. M. Allen, J. S. Chamberlain, and A. Lieber, “Biodistribution and Safety Profile of Recombinant Adeno-Associated Virus Serotype 6 Vectors following Intravenous Delivery,” *J. Virol.*, vol. 82, no. 15, pp. 7711–7715, 2008, doi: 10.1128/jvi.00542-08.

[89] S. G. Jacobson, A. V. Cideciyan, R. Ratnakaram, E. Heon, S. B. Schwartz, A. J. Roman, M. C. Peden, T. S. Aleman, S. L. Boye, A. Sumaroka, T. J. Conlon, R. Calcedo, J. J. Pang, K. E. Erger, M. B. Olivares, C. L. Mullins, M. Swider, S. Kaushal, W. J. Feuer, A. Iannaccone, G. A. Fishman, E. M. Stone, B. J. Byrne, and W. W. Hauswirth, “Gene therapy for leber congenital amaurosis caused by RPE65 mutations: Safety and efficacy in 15 children and adults followed up to 3 years,” *Arch. Ophthalmol.*, vol. 130, no. 1, pp. 9–24, Jan. 2012, doi: 10.1001/archophthalmol.2011.298.

[90] V. Ferreira, H. Petry, and F. Salmon, “Immune responses to AAV-vectors, The Glybera example from bench to bedside,” *Front. Immunol.*, vol. 5, no. MAR, 2014, doi: 10.3389/fimmu.2014.00082.

[91] M. A. Vance, A. Mitchell, and R. J. Samulski, “AAV Biology, Infectivity and Therapeutic Use from

Bench to Clinic," in *Gene Therapy - Principles and Challenges*, InTech, 2015.

[92] C. Zincarelli, S. Soltys, G. Rengo, and J. E. Rabinowitz, "Analysis of AAV serotypes 1-9 mediated gene expression and tropism in mice after systemic injection," *Mol. Ther.*, vol. 16, no. 6, pp. 1073–1080, 2008, doi: 10.1038/mt.2008.76.

[93] Z. Wu, H. Yang, and P. Colosi, "Effect of genome size on AAV vector packaging," *Mol. Ther.*, vol. 18, no. 1, pp. 80–86, 2010, doi: 10.1038/mt.2009.255.

[94] J. C. Nault, S. Datta, S. Imbeaud, A. Franconi, M. Mallet, G. Couchy, E. Letouzé, C. Pilati, B. Verret, J. F. Blanc, C. Balabaud, J. Calderaro, A. Laurent, M. Letexier, P. Bioulac-Sage, F. Calvo, and J. Zucman-Rossi, "Recurrent AAV2-related insertional mutagenesis in human hepatocellular carcinomas," *Nat. Genet.*, vol. 47, no. 10, pp. 1187–1193, Sep. 2015, doi: 10.1038/ng.3389.

[95] R. J. Samulski, K. I. Berns, M. Tan, and N. Muzyczka, "Cloning of adeno-associated virus into pBR322: Rescue of intact virus from the recombinant plasmid in human cells," 1982.

[96] S. K. McLaughlin, P. Collis, P. L. Hermonat, and N. Muzyczka, "Adeno-associated virus general transduction vectors: analysis of proviral structures.," *J. Virol.*, vol. 62, no. 6, pp. 1963–1973, 1988, doi: 10.1128/jvi.62.6.1963-1973.1988.

[97] R. J. Samulski, L.-S. Chang, and T. Shenk2, "Helper-Free Stocks of Recombinant Adeno-Associated Viruses: Normal Integration Does Not Require Viral Gene Expression," 1989.

[98] R. J. Samulski and N. Muzyczka, "AAV-Mediated Gene Therapy for Research and Therapeutic Purposes," *Annu. Rev. Virol.*, vol. 1, no. 1, pp. 427–451, Nov. 2014, doi: 10.1146/annurev-virology-031413-085355.

[99] A. Asokan, D. V Schaffer, and R. J. Samulski, "The AAV vector toolkit: Poised at the clinical crossroads," *Molecular Therapy*, vol. 20, no. 4. pp. 699–708, 2012, doi: 10.1038/mt.2011.287.

[100] T. Gaj, B. E. Epstein, and D. V Schaffer, "Genome engineering using Adeno-associated virus: Basic and clinical research applications," *Molecular Therapy*, vol. 24, no. 3. pp. 458–464, 2016, doi: 10.1038/mt.2015.151.

[101] F. Borel, M. A. Kay, and C. Mueller, "Recombinant AAV as a platform for translating the therapeutic potential of RNA interference.," *Molecular Therapy*, vol. 22, no. 4. pp. 692–701, 2014, doi: 10.1038/mt.2013.285.

[102] J. Labbadia and R. I. Morimoto, "Huntington's disease: Underlying molecular mechanisms and emerging concepts," *Trends in Biochemical Sciences*, vol. 38, no. 8. pp. 378–385, 2013, doi: 10.1016/j.tibs.2013.05.003.

[103] K. Chamberlain, J. M. Riyad, and T. Weber, "Expressing transgenes that exceed the packaging capacity of adeno-associated virus capsids," *Human Gene Therapy Methods*, vol. 27, no. 1. pp. 1–12, 2016, doi: 10.1089/hgtb.2015.140.

[104] F. K. Ferrari, T. Samulski, T. Shenk, and R. J. Samulski, "Second-strand synthesis is a rate-limiting step for efficient transduction by recombinant adeno-associated virus vectors.," *J. Virol.*, vol. 70, no. 5, pp. 3227–34, May 1996.

[105] D. M. McCarty, "Self-complementary AAV vectors; advances and applications," *Mol. Ther.*, vol. 16, no. 10, pp. 1648–1656, 2008, doi: 10.1038/mt.2008.171.

[106] G. Mittermeyer, C. W. Christine, K. H. Rosenbluth, S. L. Baker, P. Starr, P. Larson, P. L. Kaplan,

J. Forsayeth, M. J. Aminoff, and K. S. Bankiewicz, “Long-term evaluation of a phase 1 study of AADC gene therapy for parkinson’s disease,” *Hum. Gene Ther.*, vol. 23, no. 4, pp. 377–381, Dec. 2011, doi: 10.1089/hum.2011.220.

[107] R. E. MacLaren, M. Groppe, A. R. Barnard, C. L. Cottriall, T. Tolmachova, L. Seymour, K. Reed Clark, M. J. During, F. P. M. Cremers, G. C. M. Black, A. J. Lotery, S. M. Downes, A. R. Webster, and M. C. Seabra, “Retinal gene therapy in patients with choroideremia: Initial findings from a phase 1/2 clinical trial,” *Lancet*, vol. 383, no. 9923, pp. 1129–1137, 2014, doi: 10.1016/S0140-6736(13)62117-0.

[108] M. S. Rafii, T. L. Baumann, R. A. E. Bakay, J. M. Ostrove, J. Siffert, A. S. Fleisher, C. D. Herzog, D. Barba, M. Pay, D. P. Salmon, Y. Chu, J. H. Kordower, K. Bishop, D. Keator, S. Potkin, and R. T. Bartus, “A phase1 study of stereotactic gene delivery of AAV2-NGF for Alzheimer’s disease,” *Alzheimers. Dement.*, vol. 10, no. 5, pp. 571–581, Sep. 2014, doi: 10.1016/j.jalz.2013.09.004.

[109] J. R. Mendell, L. R. Rodino-Klapac, X. Rosales-Quintero, J. Kota, B. D. Coley, G. Galloway, J. M. Craenen, S. Lewis, V. Malik, C. Shilling, B. J. Byrne, T. Conlon, K. J. Campbell, W. G. Bremer, L. Viollet, C. M. Walker, Z. Sahenk, and K. R. Clark, “Limb-girdle muscular dystrophy type 2D gene therapy restores α-sarcoglycan and associated proteins,” *Ann. Neurol.*, vol. 66, no. 3, pp. 290–297, Sep. 2009, doi: 10.1002/ana.21732.

[110] S. Ylä-Herttuala, “Endgame: Glybera finally recommended for approval as the first gene therapy drug in the European union,” *Molecular Therapy*, vol. 20, no. 10. pp. 1831–1832, Oct-2012, doi: 10.1038/mt.2012.194.

[111] F. Simonelli, A. M. Maguire, F. Testa, E. A. Pierce, F. Mingozzi, J. L. Bennicelli, S. Rossi, K. Marshall, S. Banfi, E. M. Surace, J. Sun, T. M. Redmond, X. Zhu, K. S. Shindler, G. S. Ying, C. Ziviello, C. Acerra, J. F. Wright, J. W. McDonnell, K. A. High, J. Bennett, and A. Auricchio, “Gene therapy for leber’s congenital amaurosis is safe and effective through 1.5 years after vector administration,” *Mol. Ther.*, vol. 18, no. 3, pp. 643–650, Mar. 2010, doi: 10.1038/mt.2009.277.

[112] J. R. Mendell, S. Al-Zaidy, R. Shell, W. D. Arnold, L. R. Rodino-Klapac, T. W. Prior, L. Lowes, L. Alfano, K. Berry, K. Church, J. T. Kissel, S. Nagendran, J. L’Italien, D. M. Sproule, C. Wells, J. A. Cardenas, M. D. Heitzer, A. Kaspar, S. Corcoran, L. Braun, S. Likhite, C. Miranda, K. Meyer, K. D. Foust, A. H. M. Burghes, and B. K. Kaspar, “Single-dose gene-replacement therapy for spinal muscular atrophy,” *N. Engl. J. Med.*, vol. 377, no. 18, pp. 1713–1722, Nov. 2017, doi: 10.1056/NEJMoa1706198.

[113] N. Clément and J. C. Grieger, “Manufacturing of recombinant adeno-associated viral vectors for clinical trials,” *Mol. Ther. - Methods Clin. Dev.*, vol. 3, no. November 2015, p. 16002, 2016, doi: 10.1038/mtm.2016.2.

[114] A. C. Nathwani, E. G. Tuddenham, S. Rangarajan, C. Rosales, J. McIntosh, D. C. Linch, P. Chowdary, A. Riddell, A. J. Pie, C. Harrington, J. O’Beirne, K. Smith, J. Pasi, B. Glader, P. Rustagi, C. Y. Ng, M. A. Kay, J. Zhou, Y. Spence, C. L. Morton, J. Allay, J. Coleman, S. Sleep, J. M. Cunningham, D. Srivastava, E. Basner-Tschakarjan, F. Mingozzi, K. A. High, J. T. Gray, U. M. Reiss, A. W. Nienhuis, and A. M. Davidoff, “Adenovirus-associated virus vector-mediated gene transfer in hemophilia B,” *N. Engl. J. Med.*, vol. 365, no. 25, pp. 2357–2365, 2011, doi:

10.1056/NEJMoa1108046.

[115] M. Penaud-Budloo, A. François, N. Clément, and E. Ayuso, “Pharmacology of Recombinant Adeno-associated Virus Production,” *Mol. Ther. - Methods Clin. Dev.*, vol. 8, no. March, pp. 166–180, 2018, doi: 10.1016/j.omtm.2018.01.002.

[116] R. F. Collaco, X. Cao, and J. P. Trempe, “A helper virus-free packaging system for recombinant adeno-associated virus vectors,” *Gene*, vol. 238, no. 2, pp. 397–405, Oct. 1999, doi: 10.1016/S0378-1119(99)00347-9.

[117] J. F. Wright, “Transient transfection methods for clinical adeno-associated viral vector production.,” *Human gene therapy*, vol. 20, no. 7. pp. 698–706, 2009, doi: 10.1089/hum.2009.064.

[118] J. C. Grieger, S. M. Soltys, and R. J. Samulski, “Production of recombinant adeno-associated virus vectors using suspension HEK293 cells and continuous harvest of vector from the culture media for GMP FIX and FLT1 clinical vector,” *Mol. Ther.*, vol. 24, no. 2, pp. 287–297, Feb. 2016, doi: 10.1038/mt.2015.187.

[119] D. Blessing, G. Vachey, C. Pythoud, M. Rey, V. Padrun, F. M. Wurm, B. L. Schneider, and N. Déglon, “Scalable Production of AAV Vectors in Orbitally Shaken HEK293 Cells,” *Mol. Ther. - Methods Clin. Dev.*, vol. 13, no. June, pp. 14–26, 2019, doi: 10.1016/j.omtm.2018.11.004.

[120] D. Grimm and J. A. Kleinschmidt, “Progress in adeno-associated virus type 2 vector production: Promises and prospects for clinical use,” *Hum. Gene Ther.*, vol. 10, no. 15, pp. 2445–2450, 1999, doi: 10.1089/10430349950016799.

[121] J. C. M. van der Loo and J. F. Wright, “Progress and challenges in viral vector manufacturing,” *Human molecular genetics*, vol. 25, no. R1. pp. R42–R52, 2016, doi: 10.1093/hmg/ddv451.

[122] M. G. Moleirinho, R. J. S. Silva, P. M. Alves, M. J. T. Carrondo, and C. Peixoto, “Current challenges in biotherapeutic particles manufacturing,” *Expert Opinion on Biological Therapy*. 2019, doi: 10.1080/14712598.2020.1693541.

[123] Z. Yuan, C. Qiao, P. Hu, J. Li, and X. Xiao, “A versatile adeno-associated virus vector producer cell line method for scalable vector production of different serotypes,” *Hum. Gene Ther.*, vol. 22, no. 5, pp. 613–624, 2011, doi: 10.1089/hum.2010.241.

[124] C. Qiao, B. Wang, X. Zhu, J. Li, and X. Xiao, “A Novel Gene Expression Control System and Its Use in Stable, High-Titer 293 Cell-Based Adeno-Associated Virus Packaging Cell Lines,” *J. Virol.*, vol. 76, no. 24, pp. 13015–13027, 2002, doi: 10.1128/JVI.76.24.13015-13027.2002.

[125] K. R. Clark, F. Voulgaropoulou, D. M. Fraley, and P. R. Johnson, “Cell Lines for the Production of Recombinant Adeno-Associated Virus,” *Hum. Gene Ther.*, vol. 6, no. 10, pp. 1329–1341, Oct. 1995, doi: 10.1089/hum.1995.6.10-1329.

[126] G. P. Gao, G. Qu, L. Z. Faust, R. K. Engdahl, W. Xiao, J. V. Hughes, P. W. Zoltick, and J. M. Wilson, “High-titer adeno-associated viral vectors from a Rep/Cap cell line and hybrid shuttle virus,” *Hum. Gene Ther.*, vol. 9, no. 16, pp. 2353–2362, Nov. 1998, doi: 10.1089/hum.1998.9.16-2353.

[127] G. P. Gao, F. Lu, J. C. Sanmiguel, P. T. Tran, Z. Abbas, K. S. Lynd, J. Marsh, N. B. Spinner, and J. M. Wilson, “Rep/cap gene amplification and high-yield production of AAV in an A549 cell line

expressing rep/cap," *Mol. Ther.*, vol. 5, no. 5 I, pp. 644–649, 2002, doi: 10.1006/mthe.2001.0591.

[128] D. Farson, T. C. Harding, L. Tao, J. Liu, S. Powell, V. Vimal, S. Yendluri, K. Koprivnikar, K. Ho, C. Twitty, P. Husak, A. Lin, R. O. Snyder, and B. A. Donahue, "Development and characterization of a cell line for large-scale, serum-free production of recombinant adeno-associated viral vectors," *J. Gene Med.*, vol. 6, no. 12, pp. 1369–1381, 2004, doi: 10.1002/jgm.622.

[129] J. Martin, A. Frederick, Y. Luo, R. Jackson, M. Joubert, B. Sol, F. Poulin, E. Pastor, D. Armentano, S. Wadsworth, and K. Vincent, "Generation and characterization of adeno-associated virus producer cell lines for research and preclinical vector production," *Hum. Gene Ther. Methods*, vol. 24, no. 4, pp. 253–269, 2013, doi: 10.1089/hgtb.2013.046.

[130] X. Liu, F. Voulgaropoulou, R. Chen, P. R. Johnson, and K. R. Clark, "Selective Rep-Cap gene amplification as a mechanism for high-titer recombinant AAV production from stable cell lines," *Mol. Ther.*, vol. 2, no. 4, pp. 394–403, 2000, doi: 10.1006/mthe.2000.0132.

[131] G. Chadeuf, D. Favre, J. Tessier, N. Provost, P. Nony, J. Kleinschmidt, P. Moullier, and A. Salvetti, "Efficient recombinant adeno-associated virus production by a stable rep-cap HeLa cell line correlates with adenovirus-induced amplification of the integrated rep-cap genome," *J. Gene Med.*, vol. 2, no. 4, pp. 260–268, Jul. 2000, doi: 10.1002/1521-2254(200007/08)2:4<260::aid-jgm111>3.0.co;2-8.

[132] N. Inoue and D. W. Russell, "Packaging Cells Based on Inducible Gene Amplification for the Production of Adeno-Associated Virus Vectors," *J. Virol.*, vol. 72, no. 9, pp. 7024–7031, 1998, doi: 10.1128/jvi.72.9.7024-7031.1998.

[133] T. Flotte, B. Carter, C. Conrad, W. Guggino, T. Reynolds, B. Rosenstein, G. Taylor, S. Walden, and R. Wetzel, "A phase I study of an adeno-associated Virus-CFTR gene vector in adult CF patients with mild lung disease," *Human Gene Therapy*, vol. 7, no. 9. Mary Ann Liebert Inc., pp. 1145–1159, 10-Jun-1996, doi: 10.1089/hum.1996.7.9-1145.

[134] B. A. Thorne, R. K. Takeya, and R. W. Peluso, "Manufacturing recombinant adeno-associated viral vectors from producer cell clones.," *Human gene therapy*, vol. 20, no. 7. pp. 707–714, Jul-2009, doi: 10.1089/hum.2009.070.

[135] N. Office of Technology Transfer, "A549 Cells: Lung Carcinoma Cell Line for Adenovirus," 2018. [Online]. Available: https://www.ott.nih.gov/technology/e-129-2009. [Accessed: 21-Apr-2020].

[136] C. Berthet, K. Raj, P. Saudan, and P. Beard, "How adeno-associated virus Rep78 protein arrests cells completely in S phase," *Proc. Natl. Acad. Sci. U. S. A.*, vol. 102, no. 38, pp. 13634–13639, Sep. 2005, doi: 10.1073/pnas.0504583102.

[137] Z. Li, J. R. Brister, D. S. Im, and N. Muzyczka, "Characterization of the adenoassociated virus Rep protein complex formed on the viral origin of DNA replication," *Virology*, vol. 313, no. 2, pp. 364–376, Sep. 2003, doi: 10.1016/S0042-6822(03)00340-4.

[138] Q. Yang, F. Chen, and J. P. Trempe, "Characterization of cell lines that inducibly express the adeno-associated virus Rep proteins.," *J. Virol.*, vol. 68, no. 8, pp. 4847–4856, 1994, doi: 10.1128/jvi.68.8.4847-4856.1994.

[139] T. Okada, H. Mizukami, M. Urabe, T. Nomoto, T. Matsushita, Y. Hanazono, A. Kume, K. Tobita, and K. Ozawa, "Development and characterization of an antisense-mediated prepackaging cell

line for adeno-associated virus vector production," *Biochem. Biophys. Res. Commun.*, vol. 288, no. 1, pp. 62–68, Oct. 2001, doi: 10.1006/bbrc.2001.5730.

[140] H. Mizukami, T. Okada, Y. Ogasawara, T. Matsushita, M. Urabe, A. Kume, and K. Ozawa, "Separate control of rep and cap expression using mutant and wild-type loxP sequences and improved packaging system for adeno-associated virus vector production," *Appl. Biochem. Biotechnol. - Part B Mol. Biotechnol.*, vol. 27, no. 1, pp. 7–14, 2004, doi: 10.1385/mb:27:1:07.

[141] H. Chen, "Intron splicing-mediated expression of AAV rep and cap genes and production of AAV vectors in insect cells," *Mol. Ther.*, vol. 16, no. 5, pp. 924–930, 2008, doi: 10.1038/mt.2008.35.

[142] M. Urabe, C. Ding, and R. M. Kotin, "Insect cells as a factory to produce adeno-associated virus type 2 vectors," *Hum. Gene Ther.*, vol. 13, no. 16, pp. 1935–1943, 2002, doi: 10.1089/10430340260355347.

[143] R. H. Smith, J. R. Levy, and R. M. Kotin, "A simplified baculovirus-AAV expression vector system coupled with one-step affinity purification yields high-titer rAAV stocks from insect cells," *Mol. Ther.*, vol. 17, no. 11, pp. 1888–1896, 2009, doi: 10.1038/mt.2009.128.

[144] H. Chen, "Intron splicing-mediated expression of AAV rep and cap genes and production of AAV vectors in insect cells," *Mol. Ther.*, vol. 16, no. 5, pp. 924–930, 2008, doi: 10.1038/mt.2008.35.

[145] G. Aslanidi, K. Lamb, and S. Zolotukhin, "An inducible system for highly efficient production of recombinant adeno-associated virus (rAAV) vectors in insect Sf9 cells," *Proc. Natl. Acad. Sci. U. S. A.*, vol. 106, no. 13, pp. 5059–5064, 2009, doi: 10.1073/pnas.0810614106.

[146] M. Mietzsch, S. Grasse, C. Zurawski, S. Weger, A. Bennett, M. Agbandje-Mckenna, N. Muzyczka, S. Zolotukhin, and R. Heilbronn, "OneBac: Platform for scalable and high-titer production of adeno-associated virus serotype 1-12 vectors for gene therapy," *Hum. Gene Ther.*, vol. 25, no. 3, pp. 212–222, 2014, doi: 10.1089/hum.2013.184.

[147] Y. Wu, T. Mei, L. Jiang, Z. Han, R. Dong, T. Yang, and F. Xu, "Development of versatile and flexible sf9 packaging cell line-dependent onebac system for large-scale recombinant adeno-associated virus production," *Hum. Gene Ther. Methods*, vol. 30, no. 5, pp. 172–183, 2019, doi: 10.1089/hgtb.2019.123.

[148] E. Kohlbrenner, G. Aslanidi, K. Nash, S. Shklyaev, M. Campbell-Thompson, B. J. Byrne, R. O. Snyder, N. Muzyczka, K. H. Warrington, and S. Zolotukhin, "Successful production of pseudotyped rAAV vectors using a modified baculovirus expression system," *Mol. Ther.*, vol. 12, no. 6, pp. 1217–1225, 2005, doi: 10.1016/j.ymthe.2005.08.018.

[149] J. E. Conway, C. M. J. Ap Rhys, I. Zolotukhin, S. Zolotukhin, N. Muzyczka, G. S. Hayward, and B. J. Byrne, "High-titer recombinant adeno-associated virus production utilizing a recombinant herpes simplex virus type I vector expressing AAV-2 rep and cap," *Gene Ther.*, vol. 6, no. 6, pp. 986–993, 1999, doi: 10.1038/sj.gt.3300937.

[150] D. L. Thomas, L. Wang, J. Niamke, J. Liu, W. Kang, M. M. Scotti, G. J. Ye, G. Veres, and D. R. Knop, "Scalable recombinant adeno-associated virus production using recombinant herpes simplex virus type 1 coinfection of suspension-adapted mammalian cells," *Hum. Gene Ther.*, vol. 20, no. 8, pp. 861–870, Aug. 2009, doi: 10.1089/hum.2009.004.

[151] L. Adamson-Small, M. Potter, D. J. Falk, B. Cleaver, B. J. Byrne, and N. Clément, "A scalable

method for the production of high-titer and high-quality adeno-associated type 9 vectors using the HSV platform," *Mol. Ther. - Methods Clin. Dev.*, vol. 3, p. 16031, Mar. 2016, doi: 10.1038/mtm.2016.31.

[152] G. Ye, M. M. Scotti, D. L. Thomas, L. Wang, D. R. Knop, and J. D. Chulay, "Herpes Simplex Virus Clearance During Purification of a Recombinant Adeno-Associated Virus Serotype 1 Vector," *Hum. Gene Ther. Clin. Dev.*, vol. 25, no. 4, pp. 212–217, Dec. 2014, doi: 10.1089/humc.2014.060.

[153] J. F. Wright, "Manufacturing and characterizing AAV-based vectors for use in clinical studies," *Gene Therapy*, vol. 15, no. 11. pp. 840–848, Jun-2008, doi: 10.1038/gt.2008.65.

[154] A. M. Gruntman, L. Su, Q. Su, G. Gao, C. Mueller, and T. R. Flotte, "Stability and Compatibility of Recombinant Adeno-Associated Virus Under Conditions Commonly Encountered in Human Gene Therapy Trials," *Hum. Gene Ther. Methods*, vol. 26, no. 2, pp. 71–76, Apr. 2015, doi: 10.1089/hgtb.2015.040.

[155] M. Hebben, "Downstream bioprocessing of AAV vectors: industrial challenges & regulatory requirements," *Cell Gene Ther. Insights*, vol. 4, no. 2, pp. 131–146, Mar. 2018, doi: 10.18609/cgti.2018.016.

[156] G. Dias Florencio, G. Precigout, C. Beley, P. O. Buclez, L. Garcia, and R. Benchaouir, "Simple downstream process based on detergent treatment improves yield and in vivo transduction efficacy of adeno-associated virus vectors," *Mol. Ther. - Methods Clin. Dev.*, vol. 2, p. 15024, Apr. 2015, doi: 10.1038/mtm.2015.24.

[157] E. Ayuso, F. Mingozzi, J. Montane, X. Leon, X. M. Anguela, V. Haurigot, S. A. Edmonson, L. Africa, S. Zhou, K. A. High, F. Bosch, and J. F. Wright, "High AAV vector purity results in serotype- and tissue-independent enhancement of transduction efficiency," *Gene Ther.*, vol. 17, no. 4, pp. 503–510, Apr. 2010, doi: 10.1038/gt.2009.157.

[158] S. Zolotukhin, B. J. Byrne, E. Mason, I. Zolotukhin, M. Potter, K. Chesnut, C. Summerford, R. J. Samulski, and N. Muzyczka, "Recombinant adeno-associated virus purification using novel methods improves infectious titer and yield," *Gene Ther.*, vol. 6, no. 6, pp. 973–985, Jun. 1999, doi: 10.1038/sj.gt.3300938.

[159] B. Strobel, F. D. Miller, W. Rist, and T. Lamla, "Comparative Analysis of Cesium Chloride- and Iodixanol-Based Purification of Recombinant Adeno-Associated Viral Vectors for Preclinical Applications," *Hum. Gene Ther. Methods*, vol. 26, no. 4, pp. 147–157, Aug. 2015, doi: 10.1089/hgtb.2015.051.

[160] T. Okada, M. Nonaka-Sarukawa, R. Uchibori, K. Kinoshita, H. Hayashita-Kinoh, Y. Nitahara-Kasahara, S. Takeda, and K. Ozawa, "Scalable purification of adeno-associated virus serotype 1 (AAV1) and AAV8 vectors, using dual ion-exchange adsorptive membranes," *Hum. Gene Ther.*, vol. 20, no. 9, pp. 1013–1021, Sep. 2009, doi: 10.1089/hum.2009.006.

[161] B. Venkatakrishnan, J. Yarbrough, J. Domsic, A. Bennett, B. Bothner, O. G. Kozyreva, R. J. Samulski, N. Muzyczka, R. McKenna, and M. Agbandje-McKenna, "Structure and Dynamics of Adeno-Associated Virus Serotype 1 VP1-Unique N-Terminal Domain and Its Role in Capsid Trafficking," *J. Virol.*, vol. 87, no. 9, pp. 4974–4984, 2013, doi: 10.1128/jvi.02524-12.

[162] J. N. Leonard, P. Ferstl, A. Delgado, and D. V. Schaffer, “Enhanced preparation of adeno-associated viral vectors by using high hydrostatic pressure to selectively inactivate helper adenovirus,” *Biotechnol. Bioeng.*, vol. 97, no. 5, pp. 1170–1179, Aug. 2007, doi: 10.1002/bit.21355.

[163] P. Rueda, J. Fominaya, J. P. Langeveld, C. Bruschke, C. Vela, and J. I. Casal, “Effect of different baculovirus inactivation procedures on the integrity and immunogenicity of porcine parvovirus-like particles.,” *Vaccine*, vol. 19, no. 7–8, pp. 726–34, Nov. 2000, doi: 10.1016/s0264-410x(00)00259-0.

[164] D. Grimm, A. Kern, M. Pawlita, F. K. Ferrari, R. J. Samulski, and J. A. Kleinschmidt, “Titration of AAV-2 particles via a novel capsid ELISA: Packaging of genomes can limit production of recombinant AAV-2,” *Gene Ther.*, vol. 6, no. 7, pp. 1322–1330, Jul. 1999, doi: 10.1038/sj.gt.3300946.

[165] A. Wistuba, A. Kern, S. Weger, D. Grimm, and J. A. Kleinschmidt, “Subcellular compartmentalization of adeno-associated virus type 2 assembly.,” *J. Virol.*, vol. 71, no. 2, pp. 1341–1352, 1997, doi: 10.1128/jvi.71.2.1341-1352.1997.

[166] D. Dobnik, P. Kogovšek, T. Jakomin, N. Košir, M. T. Žnidarič, M. Leskovec, S. M. Kaminsky, J. Mostrom, H. Lee, and M. Ravnikar, “Accurate quantification and characterization of adeno-associated viral vectors,” *Front. Microbiol.*, vol. 10, no. JULY, 2019, doi: 10.3389/fmicb.2019.01570.

[167] J. M. Sommer, P. H. Smith, S. Parthasarathy, J. Isaacs, S. Vijay, J. Kieran, S. K. Powell, A. McClelland, and F. Wright, “Quantification of adeno-associated virus particles and empty capsids by optical density measurement,” *Mol. Ther.*, vol. 7, no. 1, pp. 122–128, Jan. 2003, doi: 10.1016/S1525-0016(02)00019-9.

[168] R. J. Samulski, L. S. Chang, and T. Shenk, “Helper-free stocks of recombinant adeno-associated viruses: normal integration does not require viral gene expression.,” *J. Virol.*, vol. 63, no. 9, pp. 3822–3828, 1989, doi: 10.1128/jvi.63.9.3822-3828.1989.

[169] S. D’Costa, V. Blouin, F. Broucque, M. Penaud-Budloo, A. Fçranois, I. C. Perez, C. Le Bec, P. Moullier, R. O. Snyder, and E. Ayuso, “Practical utilization of recombinant AAV vector reference standards: focus on vector genomes titration by free ITR qPCR,” *Mol. Ther. - Methods Clin. Dev.*, vol. 3, p. 16019, Mar. 2016, doi: 10.1038/mtm.2016.19.

[170] B. Furuta-Hanawa, T. Yamaguchi, and E. Uchida, “Two-Dimensional Droplet Digital PCR as a Tool for Titration and Integrity Evaluation of Recombinant Adeno-Associated Viral Vectors,” *Hum. Gene Ther. Methods*, vol. 30, no. 4, pp. 127–136, 2019, doi: 10.1089/hgtb.2019.031.

[171] J. C. Grieger, V. W. Choi, and R. J. Samulski, “Production and characterization of adeno-associated viral vectors,” *Nat. Protoc.*, vol. 1, no. 3, pp. 1412–1428, 2006, doi: 10.1038/nprot.2006.207.

[172] B. Burnham, S. Nass, E. Kong, M. E. Mattingly, D. Woodcock, A. Song, S. Wadsworth, S. H. Cheng, A. Scaria, and C. R. O’Riordan, “Analytical Ultracentrifugation as an Approach to Characterize Recombinant Adeno-Associated Viral Vectors,” *Hum. Gene Ther. Methods*, vol. 26, no. 6, pp. 228–242, Dec. 2015, doi: 10.1089/hgtb.2015.048.

[173] F. Dorange and C. Le Bec, “Analytical approaches to characterize AAV vector production & purification: Advances and challenges,” *Cell Gene Ther. Insights*, vol. 4, no. 2, pp. 119–129, 2018, doi: 10.18609/cgti.2018.015.

[174] X. Fu, W. C. Chen, C. Argento, P. Clarner, V. Bhatt, R. Dickerson, G. Bou-Assaf, M. Bakhshayeshi, X. Lu, S. Bergelson, and J. Pieracci, “Analytical Strategies for Quantification of Adeno-Associated Virus Empty Capsids to Support Process Development,” *Hum. Gene Ther. Methods*, vol. 30, no. 4, pp. 144–152, 2019, doi: 10.1089/hgtb.2019.088.

[175] M. G. Aucoin, M. Perrier, and A. A. Kamen, “Critical assessment of current adeno-associated viral vector production and quantification methods,” *Biotechnol. Adv.*, vol. 26, no. 1, pp. 73–88, 2008, doi: 10.1016/j.biotechadv.2007.09.001.

[176] U. P. Rohr, M. A. Wulf, S. Stahn, U. Steidl, R. Haas, and R. Kronenwett, “Fast and reliable titration of recombinant adeno-associated virus type-2 using quantitative real-time PCR,” *J. Virol. Methods*, vol. 106, no. 1, pp. 81–88, 2002, doi: 10.1016/S0166-0934(02)00138-6.

[177] Z. Zhen, Y. Espinoza, T. Bleu, J. M. Sommer, and J. F. Wright, “Infectious titer assay for adeno-associated virus vectors with sensitivity sufficient to detect single infectious events,” *Hum. Gene Ther.*, vol. 15, no. 7, pp. 709–715, Jul. 2004, doi: 10.1089/1043034041361262.

[178] L. Drittanti, C. Jenny, K. Poulard, A. Samba, P. Manceau, N. Soria, N. Vincent, O. Danos, and M. Vega, “Optimised helper virus-free production of high-quality adeno-associated virus vectors,” *J. Gene Med.*, vol. 3, no. 1, pp. 59–71, Jan. 2001, doi: 10.1002/1521-2254(2000)9999:9999<::AID-JGM152>3.0.CO;2-U.

[179] J. A. Allay, S. Sleep, S. Long, D. M. Tillman, R. Clark, G. Carney, P. Fagone, J. H. McIntosh, A. W. Nienhuis, A. M. Davidoff, A. C. Nathwani, and J. T. Gray, “Good manufacturing practice production of self-complementary serotype 8 adeno-associated viral vector for a hemophilia B clinical trial,” *Hum. Gene Ther.*, vol. 22, no. 5, pp. 595–604, 2011, doi: 10.1089/hum.2010.202.

[180] S. L. Semple-Rowland, W. E. Coggin, M. Geesey, K. S. Eccles, L. Abraham, K. Pachigar, R. Ludlow, S. C. Khani, and W. C. Smith, “Expression characteristics of dual-promoter lentiviral vectors targeting retinal photoreceptors and müller cells,” *Mol. Vis.*, vol. 16, pp. 916–934, 2010.

[181] Broad Institute, “GPP Web Portal - Design Hairpins to Target a Transcript Sequence,” 2020. [Online]. Available: https://portals.broadinstitute.org/gpp/public/seq/search. [Accessed: 18-Apr-2020].

[182] GenScript, “siRNA Target Finder,” 2020. [Online]. Available: https://www.genscript.com/tools/sirna-target-finder. [Accessed: 18-Apr-2020].

[183] J. H. Kim, S. R. Lee, L. H. Li, H. J. Park, J. H. Park, K. Y. Lee, M. K. Kim, B. A. Shin, and S. Y. Choi, “High cleavage efficiency of a 2A peptide derived from porcine teschovirus-1 in human cell lines, zebrafish and mice,” *PLoS One*, vol. 6, no. 4, p. e18556, 2011, doi: 10.1371/journal.pone.0018556.

[184] M. Kimura, A. Takatsuki, and I. Yamaguchi, “Blasticidin S deaminase gene from Aspergillus terreus (BSD): a new drug resistance gene for transfection of mammalian cells,” *BBA - Gene Struct. Expr.*, vol. 1219, no. 3, pp. 653–659, Nov. 1994, doi: 10.1016/0167-4781(94)90224-0.

[185] E. Pasmant, I. Laurendeau, D. Héron, M. Vidaud, D. Vidaud, and I. Bièche, “Characterization of

a germ-line deletion, including the entire INK4/ARF locus, in a melanoma-neural system tumor family: Identification of ANRIL, an antisense noncoding RNA whose expression coclusters with ARF," *Cancer Res.*, vol. 67, no. 8, pp. 3963–3969, Apr. 2007, doi: 10.1158/0008-5472.CAN-06-2004.

[186] T. D. Schmittgen and K. J. Livak, "Analyzing real-time PCR data by the comparative CT method," *Nat. Protoc.*, vol. 3, no. 6, pp. 1101–1108, 2008, doi: 10.1038/nprot.2008.73.

[187] K. J. Livak and T. D. Schmittgen, "Analysis of relative gene expression data using real-time quantitative PCR and the 2-ΔΔCT method," *Methods*, vol. 25, no. 4, pp. 402–408, 2001, doi: 10.1006/meth.2001.1262.

[188] J. P. Trempe and B. J. Carter, "Regulation of Adeno-Associated Virus Gene Expression in 293 Cells: Control of mRNA Abundance and Translation," 1988.

[189] S. Weger, A. Wistuba, D. Grimm, J. Ju¨, and J. A. Kleinschmidt, "Control of Adeno-Associated Virus Type 2 Cap Gene Expression: Relative Influence of Helper Virus, Terminal Repeats, and Rep Proteins," 1997.

[190] Q. Yang, F. Chen, and J. P. Trempe, "Characterization of cell lines that inducibly express the adeno-associated virus Rep proteins.," *J. Virol.*, vol. 68, no. 8, pp. 4847–4856, 1994, doi: 10.1128/jvi.68.8.4847-4856.1994.

[191] K. A. Vincent, S. T. Piraino, and S. C. Wadsworth, "Analysis of Recombinant Adeno-Associated Virus Packaging and Requirements for rep and cap Gene Products," 1997.

[192] Y. Ogasawara, M. Urabe, and K. Ozawa, "The use of heterologous promoters for adeno-associated virus (AAV) protein expression in aav vector production," *Microbiol. Immunol.*, vol. 42, no. 3, pp. 177–185, Mar. 1998, doi: 10.1111/j.1348-0421.1998.tb02269.x.

[193] Y. Ogasawara, H. Mizukami, M. Urabe, A. Kume, Y. Kanegae, I. Saito, J. Monahan, and K. Ozawa, "Highly regulated expression of adeno-associated virus large Rep proteins in stable 293 cell lines using the Cre/loxP switching system," *J. Gen. Virol.*, vol. 80, no. 9, pp. 2477–2480, 1999, doi: 10.1099/0022-1317-80-9-2477.

[194] T. L. Cheng, C. F. Teng, W. H. Tsai, C. W. Yeh, M. P. Wu, H. C. Hsu, C. F. Hung, and W. T. Chang, "Multitarget therapy of malignant cancers by the head-to-tail tandem array multiple shRNAs expression system," *Cancer Gene Ther.*, vol. 16, no. 6, pp. 516–531, 2009, doi: 10.1038/cgt.2008.102.

[195] Y. Weng, Y. Shi, X. Xia, W. Zhou, H. Wang, and C. Wang, "A multi-shRNA vector enhances the silencing efficiency of exogenous and endogenous genes in human cells," *Oncol. Lett.*, vol. 13, no. 3, pp. 1553–1562, Mar. 2017, doi: 10.3892/ol.2017.5672.

[196] M. Hörer, S. Weger, K. Butz, F. Hoppe-Seyler, C. Geisen, and J. A. Kleinschmidt, "Mutational analysis of adeno-associated virus Rep protein-mediated inhibition of heterologous and homologous promoters.," *J. Virol.*, vol. 69, no. 9, pp. 5485–5496, 1995, doi: 10.1128/jvi.69.9.5485-5496.1995.

[197] G. Stuchbury and G. Münch, "Optimizing the generation of stable neuronal cell lines via pre-transfection restriction enzyme digestion of plasmid DNA," *Cytotechnology*, vol. 62, no. 3, pp. 189–194, 2010, doi: 10.1007/s10616-010-9273-1.

[198] D. M. Feng, J. Z. Chen, Y. B. Yue, H. Z. Zhu, J. L. Xue, and W. W. G. Jia, “A 16 bp Rep binding element is sufficient for mediating Rep-dependent integration into AAVS1,” *J. Mol. Biol.*, vol. 358, no. 1, pp. 38–45, 2006, doi: 10.1016/j.jmb.2006.01.029.

[199] N. J. Philpott, J. Gomos, K. I. Berns, and E. Falck-Pedersen, “A p5 integration efficiency element mediates Rep-dependent integration into AAVS1 at chromosome 19,” *Proc. Natl. Acad. Sci. U. S. A.*, vol. 99, no. 19, pp. 12381–12385, 2002, doi: 10.1073/pnas.182430299.

[200] B. Saha, C. M. Wong, and R. J. Parks, “The Adenovirus Genome Contributes to the Structural Stability of the Virion,” *Viruses*, vol. 6, pp. 3563–3583, 2014, doi: 10.3390/v6093563.

[201] H. Wodrich, D. Henaff, B. Jammart, C. Segura-Morales, S. Seelmeir, O. Coux, Z. Ruzsics, C. M. Wiethoff, and E. J. Kremer, “A capsid-encoded PPxY-motif facilitates adenovirus entry,” *PLoS Pathog.*, vol. 6, no. 3, p. 1000808, 2010, doi: 10.1371/journal.ppat.1000808.

[202] S. A. Stewart, D. M. Dykxhoorn, D. Palliser, H. Mizuno, E. Y. Yu, D. S. An, D. M. Sabatini, I. S. Y. Chen, W. C. Hahn, P. A. Sharp, R. A. Weinberg, and C. D. Novina, “Lentivirus-delivered stable gene silencing by RNAi in primary cells,” 2003, doi: 10.1261/rna.2192803.

[203] Y.-H. Wang, Z.-X. Wang, Y. Qiu, J. Xiong, Y.-X. Chen, D.-S. Miao, and W. De, “Lentivirus-mediated RNAi knockdown of insulin-like growth factor-1 receptor inhibits growth, reduces invasion, and enhances radiosensitivity in human osteosarcoma cells,” *Mol. Cell. Biochem.*, vol. 327, no. 1–2, pp. 257–266, Jul. 2009, doi: 10.1007/s11010-009-0064-y.

[204] S. Satkunanathan, J. Wheeler, R. Thorpe, and Y. Zhao, “Establishment of a novel cell line for the enhanced production of recombinant adeno-associated virus vectors for gene therapy,” *Hum. Gene Ther.*, vol. 25, no. 11, pp. 929–941, Nov. 2014, doi: 10.1089/hum.2014.041.

[205] J. Song, A. Giang, Y. Lu, S. Pang, and R. Chiu, “Multiple shRNA expressing vector enhances efficiency of gene silencing,” *J. Biochem. Mol. Biol.*, vol. 41, no. 5, pp. 358–362, 2008, doi: 10.5483/bmbrep.2008.41.5.358.

[206] D. Weng, X. Song, H. Xing, X. Ma, X. Xia, Y. Weng, J. Zhou, G. Xu, L. Meng, T. Zhu, S. Wang, and D. Ma, “Implication of the Akt2/survivin pathway as a critical target in paclitaxel treatment in human ovarian cancer cells,” *Cancer Lett.*, vol. 273, no. 2, pp. 257–265, 2009, doi: 10.1016/j.canlet.2008.08.027.